5-20-2011

Kinetics of the electrocoagulation of oil and grease

Guillermo Rincon
University of New Orleans

Kinetics of the electrocoagulation of oil and grease

A Thesis

Submitted to the Graduate Faculty of the
University of New Orleans
in partial fulfillment of the
requirements for the degree of

Master of Science
in
Environmental Engineering

by

Guillermo J. Rincón

B.S., Chemical Engineering
Universidad del Zulia
Maracaibo, Venezuela, 2000

May, 2011

Disclaimer

All the laboratory equipment and instruments, including the proprietary bench-scale reactor, mentioned in this document, are property of the University of New Orleans and where purchased by this institution prior to the conception of this research. It is not the author's intention to support, advertise, criticize or disqualify the design, performance and/or use of any of these equipment and instruments.

Acknowledgements

My special thanks go to my advisor, Dr. Enrique J. La Motta, Ph.D., for his invaluable guidance throughout this endeavor.

Thanks to the Graduate School Office at the University of New Orleans for its recognition and support through the Doctoral Diversity Fellowship.

I am also grateful to the Faculty and Staff of the Department of Civil and Environmental Engineering of the University of New Orleans.

I would also like to thank Mr. Blake Mickler for his valuable assistance during the experimental phase of this research.

This research was partially founded by SPAWAR through eVenture Technologies (Task Order 0099).

Table of Contents

List of Symbols and Abbreviations

A : electrode active surface area, m^2
A_e : electrode volumetric surface area, $m^2\ m^{-3}$
A_E : effective electrode area, m^2
A_F : reactor's cross-sectional area, m^2
C^* : concentration of electroactive species in bulk electrolyte, kg m^{-3}
C_0 : reactant initial concentration, kg m^{-3}
C_L : reactant concentration at distant L inside the reactor, kg m^{-3}
CSTR : continuous stirred-tank reactor
D : dispersion coefficient, $m^2\ s^{-1}$
Da : Damkohler number, dimensionless
e : number of electrons
EC : electrocoagulation
$E(t)$: exit-age distribution function, s
$E(\Theta)$: dimensionless exit-age distribution function
η_{AP} : applied overpotential, V
η_{IR} : solution resistance overpotential, V
η_{k} : kinetic overpotential, V
η_{Mt} : concentration overpotential, V
F : Faraday's constant, 96500 C mol^{-1}
F_A : molar feed rate, mol s^{-1}
$F(t)$: cumulative exit-age distribution function, s
HEM : hexane extractable materials
i : current density, Amp m^2
I : current, Amps
I_L : limiting current, Amps
k' : kinetic constant, s^{-1}
k_m : mass transport coefficient, m s^{-1}
L : length of reactor in direction of flow, m
M : molar mass, moles
MW : molecular weight, Kg mol^{-1}
n : number of tanks in series
n_{CELL} : number of cells corresponding to V_R
Pe : Peclet number, dimensionless
PFR : plug-flow reactor
Q : volumetric flow rate, m^3
r : reaction rate, mol $s^{-1}m^{-3}$
SE : synthetic emulsion

τ : constant density average residence time, s

σ^2 : variance, s^2

σ_Θ^2 : dimensionless variance

t : time, s

$\overline{t}$: average residence time, s

Θ : dimensionless time

TIS : Tanks-in-Series

U : superficial velocity, m s^{-1}

v : fluid's linear flow velocity, m s^{-1}

V : reactor volume, m^3

V_{CELL} : cell volume, m^3

V_e : electrode volume, m^3

V_R : reactor volume calculated from RTD data, m^3

w : mass of electrode material dissolved in reaction, Kg m^{-2}

W : cell width, m

x : fractional conversion, dimensionless

List of Figures

List of Tables

Abstract

Research on the electrocoagulation (EC) of hexane extractable materials (HEM) has been conducted at the University of New Orleans using a proprietary bench-scale EC reactor. The original reactor configuration forced the fluid to follow a vertical upward-downward path. An alternate electrode arrangement was introduced so that the path of flow became horizontal. Both configurations were evaluated by comparing the residence time distribution (RTD) data generated in each case. These data produced indication of internal recirculation and stagnant water when the fluid followed a vertical path. These anomalies were attenuated when the fluid flowed horizontally and at a velocity higher than 0.032 m s^{-1} .

A series of EC experiments were performed using a synthetic emulsion with a HEM concentration of approximately 700 mg l^{-1}. It was confirmed that EC of HEM follows first-order kinetics, and kinetic constants of 0.0441 s^{-1} and 0.0443 s^{-1} were obtained from applying both the dispersion and tanks-in-series (TIS) models, respectively. In both cases R^2 was 0.97. Also, the TIS model indicated that each cell of the EC behaves as an independent continuous-stirred-tank reactor.

Key words: Electrocoagulation, residence time distribution, bench-scale reactor, step-input tracer test, hexane extractable materials, first-order kinetics, dispersion model, tanks-in-series model, plug-flow reactor, aluminum electrode, non-ideal flow, wastewater treatment, oil and grease.

I. Introduction

Even though electrochemical treatment of wastewater has been used for over a hundred years as an effective mean for metal recovery, and removal of dyes, and oil and grease, among other applications, most of the progress on knowledge base development and large-scale use of this technology has been made in the last 20 years. An indication of this renewed interest on electrochemical treatment is the increasing number of publications found in scientific literature, and booming in commercial and industrial size equipment available from different sources and for a wide range of applications. Probably one of the most underexploited uses of this technology is the electrocoagulation (EC) of contaminants from wastewater due, in the author's opinion, to the "opposition" of chemical corporations whose business is largely benefited from the manufacturing and supply of chemical coagulants, polymer-based additives and related equipment to large treatment facilities around the world. However, even in such corporation-dominated environment, EC treatment has found its way through and has established as a convenient, efficient, economical and compact alternative to conventional chemical coagulation and other traditional methods of pollutants removal. Among the benefits of EC, and perhaps the most notorious, is the in-situ generation of coagulants by electrolytic oxidation of an appropriate anode material (e.g. iron or aluminum). Also, the entire process occurs inside a single stand-alone EC reactor that accommodates the dissolving metal electrodes in a compact frame. Such features make this technology especially attractive for use in facilities where space is limited or portability is desired.

Research on electrochemical treatment of hydrocarbon-contaminated bilge and sea water is currently taking place at the University of New Orleans using a bench-scale EC reactor that utilizes aluminum or iron electrodes as the source of coagulants. The extensive experimental work carried out using this reactor has so far confirmed the effectiveness of EC for oil and grease removal from conductive wastewater; however, very little had been done to establish the kinetics of the EC process. Moreover, the same laboratory work also yielded indications of possible flaws in the design of the bench-scale reactor, which affect the overall reactor efficiency.

The research presented herein aims to address both deficiencies. First, making use of tracer test techniques, the residence time distributions (RTD) for different experimental reactor configurations are obtained, allowing for identification and understanding of the causes and consequences of the non-ideal behavior of the bench-scale reactor. Next, a series of EC experiments were performed and the results

were combined with the RTD data in order to establish the kinetics of the EC process. Finally, the EC reactor was modeled by applying non-ideal flow correlations to the experimental results.

The results of this research are an important contribution to a better understanding of the nature of mass transport and kinetics of oil and grease removal from wastewater in an electrochemical cell; they also provide a possible explanation for the abnormal fluid behavior through the EC reactor. The effect of electrode plate arrangement and fluid velocity on reactor performance is analyzed, and finally, a model for optimization and design of an EC plug-flow reactor is presented.

II. Literature Review

In this chapter, the fundamentals of electrocoagulation and reactor modeling are introduced. The concepts and equations used for data analysis, results acquisition and interpretation are presented herein.

This section begins with a brief discussion of electrocoagulation principles, reactions and relevant operational parameters when using either aluminum or iron electrodes. This is followed by a discussion of the analysis and correlation of kinetic data, residence time distribution determination and reactor modeling by means of both the dispersion model and the tanks-in-series model.

1. Electrochemical Wastewater Treatment

As documented by Chen and Hung (2007), using electricity to treat water was first proposed in England in 1889. The application of electrolysis in mineral beneficiation was patented by Elmore in 1904. Electrocoagulation (EC) with aluminum and iron electrodes was patented in the United States in 1909. The EC of drinking water was first applied on a large scale in the United States in 1946. At that time, because of the relatively large capital investment and the expensive electricity supply, electrochemical water or wastewater technologies did not find wide application worldwide. However, in the United States and former USSR extensive research during the following half century has accumulated abundant amount of information. With the ever increasing standard of drinking water supply and the stringent environmental regulations regarding the wastewater discharge, electrochemical technologies have regained their importance worldwide during the past two decades and processes such as electrochemical metal recovery, EC, electroflotation (EF) and electro-oxidation (EO) can be regarded nowadays as established technologies.

1.1. Electrocoagulation

In the environmental field, electrocoagulation is one of the main applications of electrochemical reactor technology for the treatment of water and wastewater. EC is a complicated process that involves many chemical and physical phenomena using consumable electrodes (Fe/Al) to supply ions into the water stream. During the late nineteenth century, EC was applied in several large-scale water treatment plants in London (Matteson et al., 1995), while electrolytic sludge treatment plants were operated as early as 1911 in various parts of the United States (Vik et al. 1984).

Fe or Al is dissolved from the anode generating the respective metal ions, which immediately hydrolyze to polymeric iron or aluminum, and finally, generate the respective hydroxide. These polymeric hydroxides are excellent coagulating agents. The consumable (sacrificial) metal anodes are used to continuously produce polymeric hydroxides in the vicinity of the anode. Coagulation occurs when these metal cations combine with the negative colloidal particles carried toward the anode by electrophoretic motion. Contaminants present in the wastewater stream are treated either by chemical reactions and precipitation or by physical and chemical attachment to colloidal materials being generated by the electrode erosion. They are then removed by flotation, sedimentation and filtration. In conventional coagulation process, coagulant chemicals are added. By contrast, these coagulant agents are generated in situ in the EC process.

The destabilization mechanism of the contaminants, particulate suspension, and breaking of emulsions taking place in an EC reactor may be summarized as follows (Comninellis and Chen, 2010):

1) Compression of the diffuse double layer around the charged species by the interactions of ions generated by oxidation of the sacrificial anode;
2) Charge neutralization of the ionic species present in wastewater by counter ions produced by the electrochemical dissolution of the sacrificial anode. These counter ions reduce the electrostatic inter-particle repulsion to the extent that the van der Waals attraction predominates, thus causing coagulation. A zero net charge results in the process;
3) Floc formation: the floc formed as a result of coagulation creates a sludge blanket that entraps and bridges colloidal particles that are still remaining in the aqueous medium.

Water is also electrolyzed in a parallel reaction, producing small bubbles of oxygen at the anode and hydrogen at the cathode. These bubbles attach to the flocculated particles and make them float to the surface through natural buoyancy. In addition, the following physicochemical reactions may also take place in the EC cell (Paul, 1996):

1) Cathodic reduction of impurities present in wastewater;
2) Electrophoretic migration of the ions in solution;
3) Reduction of metal ions at the cathode; and
4) Other complex electrochemical reactions.

The simplest EC reactor is made up of one anode and one cathode. When a potential (usually of direct current) is applied from an external power source, the anode material undergoes oxidation,

while the cathode will be subjected to reduction or reductive deposition of elemental metals. The electrochemical reactions with metal M as anode may be summarized as follows:

At the anode:

$$\mathrm{M_{(s)} \rightarrow M_{(aq)}^{n+} + ne^-} \quad (1)$$

$$\mathrm{2H_2O_{(l)} \rightarrow 4H^+_{(aq)} + O_{2(g)} + 4e^-} \quad (2)$$

At the cathode:

$$\mathrm{M_{(aq)}^{n+} + ne^- \rightarrow M_{(s)}} \quad (3)$$

$$\mathrm{2H_2O_{(l)} + 2e^- \rightarrow 2H_{2(g)} + 2OH^-_{(aq)}} \quad (4)$$

If iron or aluminum electrodes are used, the generated $\mathrm{Fe_{(aq)}^{2+}}$ (thermodynamically favored), $\mathrm{Fe_{(aq)}^{3+}}$ or $\mathrm{Al_{(aq)}^{3+}}$ ions will immediately undergo further spontaneous reactions to produce corresponding hydroxides and/or polyhydroxides. These compounds have strong affinity for dispersed particles as well as counter ions to cause coagulation. The gasses evolved at the electrodes may impinge on and cause flotation of the coagulated materials (Jiang et al., 2002).

Although the above reactions suggest the evolution of oxygen at the anode, Moreno et al. (2007) presented experimental evidence that oxygen is not generated at the cathode, as claimed by reaction 2.

Upon oxidation in an electrolytic system, iron produces ferrous hydroxide, $\mathrm{Fe(OH)_2}$, or ferric hydroxide, $\mathrm{Fe(OH)_3}$, depending on the pH of the electrolyte. A mechanism has been proposed by Yousuf et al. (2001) for the production of iron hydroxide in the absence of oxygen

At the anode:

$$\mathrm{Fe_{(s)} \rightarrow Fe^{2+}_{(aq)} + 2e^-} \quad (5)$$

$$\mathrm{Fe^{2+}_{(aq)} + 2OH^-_{(aq)} \rightarrow Fe(OH)_{2(s)}} \quad (6)$$

At the cathode:

$$\mathrm{2H_2O_{(l)} + 2e^- \rightarrow H_{2(g)} + 2OH^-_{(aq)}} \quad (7)$$

Overall reaction:

$$\mathrm{Fe_{(s)} + 2H_2O_{(l)} \rightarrow Fe(OH)_{2(s)} + H_{2(g)}} \quad (8)$$

The iron hydroxide formed remains in the aqueous stream as a gelatinous suspension, which can remove the pollutants from wastewater either by complexation or by electrostatic attraction, followed by coagulation. In the surface complexation mode, the pollutant acts as a ligand (L) to chemically bind hydrous iron:

$$L-H_{(aq)}(OH)OFe_{(s)} \rightarrow L-OFe_{(s)} + H_2O_{(l)} \quad (9)$$

The pre-hydrolysis of Fe^{3+} cations also leads to the formation of reactive clusters for water treatment.

The H_2 produced as a result of the *redox* reaction may remove dissolved organics or any suspended materials by flotation. However, the Fe^{3+} ions may undergo hydration and depending on the pH of the solution, $Fe(OH)^{2+}$, $Fe(OH)_2^+$ and $Fe(OH)_3$ species may be present under acidic conditions. The reactions involved are:

$$Fe^{3+}{}_{(aq)} + H_2O_{(l)} \rightarrow Fe(OH)^{2+}{}_{(aq)} + 2H^+{}_{(aq)} \quad (10)$$

$$Fe^{3+}{}_{(aq)} + 2H_2O_{(l)} \rightarrow Fe(OH)^+_{2\,(aq)} + 2H^+{}_{(aq)} \quad (11)$$

$$Fe^{3+}{}_{(aq)} + 3H_2O_{(l)} \rightarrow Fe(OH)_3 + 3H^+{}_{(aq)} \quad (12)$$

Under alkaline conditions, $Fe(OH)_6^-$ and $Fe(OH)_4^-$ ions may also be present. It is, therefore, quite apparent that EC of both ionic and cationic species is possible by using an iron plate/rod as a sacrificial electrode.

When aluminum electrodes are used, the electrochemical reactions occurring are the following (Bensadok et al., 2008):

At the anode:

$$Al_{(s)} \rightarrow Al^{3+}_{(aq)} + 3e^- \quad (13)$$

At the cathode, depending on pH:

$$2H_2O_{(l)} + 2e^- \rightarrow H_{2(g)} + 2OH^-_{(aq)} \quad (14)$$

$$2H^+_{(aq)} + 2e^- \rightarrow H_{2(g)} \quad (15)$$

The generated $Al^{3+}_{(aq)}$ ions combine with water and hydroxyl ions to form corresponding hydroxides and/or polyhydroxides as follows:

- Monomeric species such as $Al(OH)^{2+}$, $Al(OH)_2^+$, and $Al(OH)_4^-$ by equations 16, 17 and 19.
- Polymeric species such as $Al_2(OH)_2{}^{4+}$ and $Al_2(OH)_5^+$,

- Amorphous and less soluble species such as $Al(OH)_3$ by equation 18 and Al_2O_3.

$$Al^{3+} + H_2O \rightarrow Al(OH)^{2+} + H^+ \quad (16)$$

$$Al(OH)^{2+} + H_2O \rightarrow Al(OH)_2^+ + H^+ \quad (17)$$

$$Al(OH)_2^+ + H_2O \rightarrow Al(OH)_3 + H^+ \quad (18)$$

$$Al(OH)_3 + H_2O \rightarrow Al(OH)_4^- + H^+ \quad (19)$$

Considering only mononuclear speciation, the concentration of the various Al forms present in solution was calculated by Holt et al. (2002) depending on pH. Figure 1 provides the speciation diagram obtained by the authors.

Al complexes acting as coagulants are adsorbed on oil the particles and thus neutralize the colloidal charges, resulting in destabilization of the emulsion. This phenomenon is similar to the action of chemical coagulants in the conventional chemical treatment. Hydrogen bubbles formed at the cathode can adsorb on the flocculated species and induce their flotation. The bubbles formed also reduce fouling of the cathode surface which could occur due the formation of deposits.

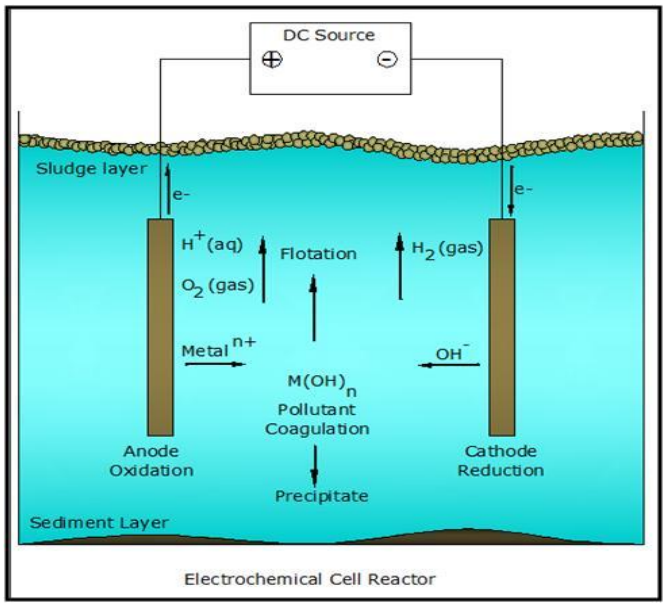

Figure 1. Interactions occurring within an electrochemical reactor (Mollah et al. 2004)

$NaCl$ is usually employed to increase the conductivity of the water or the wastewater to be treated. The presence of the chloride ion in solution has been reported to decrease passivation of the aluminum surface and thereby increase the efficiency of electrocoagulation processes. (Donini

et al., 1994; Jia qian, 1988). The chloride ion has been attributed a role in the pitting corrosion of the metal surface.

1.1.1. Factors affecting Electrocoagulation

1.1.1.1. Effect of Current Density or Charge Loading

Operating current density is very important in electrocoagulation because it is the only operational parameter that can be controlled directly. In this system, electrode spacing is fixed and current is a continuous supply. Current density directly determines both coagulant dosage and bubble generation rates and strongly influences both solution mixing and mass transfer at the electrodes.

In an EC reactor, the electrode or electrode assembly is usually connected to an external DC source. The amount of metal dissolved or deposited is dependent on the quantity of electricity passed through the electrolytic solution. A simple relationship between current density (A cm^{-2}) and the amount of substances (M) dissolved (g of M cm^{-2}) can be derived from Faraday's law:

$$w = \frac{itM}{eF} \tag{20}$$

where w is the quantity of electrode material dissolved (g of M cm^{-2}), i the current density (A cm^{-2}) defined as the current per unit electrode surface area (area of electrode perpendicular to the direction of electrons' flow), t the time in s; M the relative molar mass of the electrode concerned, e the number of electrons in the oxidation-reduction, and F is the Faraday's constant, 96500 $Cmol^{-1}$.

It is expected that there should be an agreement between the calculated amount of substances dissolved as a result of passing a definite quantity of electricity and the experimental amount determined. Usually a good agreement is obtained (Vik et al., 1984). One uncertainty is in the measurement of potential of the EC cell. The measured potential is the sum of three components:

$$\eta_{\mathrm{AP}} = \eta_{\mathrm{k}} + \eta_{\mathrm{Mt}} + \eta_{\mathrm{IR}} \tag{21}$$

where η_{AP} is the applied overpotential (V), η_{k} the kinetic overpotential (V), η_{Mt} the concentration overpotential (V), and η_{IR} is the overpotential caused by solution resistance or IR drop (V).

The IR drop is related to the distance (d in cm) between the electrodes, surface area (A in m^2) of the cathode undergoing electrochemical reduction, specific conductivity of the solution (k in mS m^{-1}), and the current (I in A). The IR drop can be easily minimized by decreasing the distance between the electrodes and increasing the surface area of the electrodes and the specific conductivity of the solution. Concentration overpotential (η_{Mt}, V), also known as mass-transfer or diffusion overpotential, is caused by the change in analytic concentration occurring in the proximity of the electrode surface due to electrode reaction; in other words, by the differences in electroactive species concentration between the bulk solution and the electrode surface. This condition occurs when the electrochemical reaction is sufficiently rapid to lower surface concentration of electroactive species below that of the bulk solution (Liu et al., 2010). The overpotential is small when the reaction rate constant is much smaller than the mass-transfer coefficient. The mass-transfer overpotential (η_{Mt}, V) can be reduced by increasing the mass of the metal ions transported from the anode surface to the bulk of the solution, which can be achieved by enhancing the solution turbulence. It can also be overcome by passing electrolyte solution from anode to cathode at a higher velocity by using some mechanical means. With the increase in the current, both kinetic and concentration overpotential increase.

The current density is the key operational parameter, affecting not only the system's response time but also strongly influencing the dominant pollutant separation mode. The highest allowable current density may not be the most efficient mode of running the reactor. It is well known that the optimal current density will invariably involve a trade-off between operational costs and efficient use of solution pH, temperature, flow rate, etc (Liu et al., 2010).

The current supply to the EC system determines the amount of Al^{3+} or Fe^{2+} ions released from the respective electrodes. For aluminum, the electrochemical equivalent mass is 335.6 mg A^{-1} h^{-1}. For iron, the value is 1041.0 mg A^{-1} h^{-1}. In order for the electrocoagulation system to operate for a long period of time without maintenance, its current density is suggested to be 20 – 25 A m^{-2} with the exception of measures taken for periodical cleaning of the surface of the electrodes. The current density selection should be made with other operating parameters such as pH,

temperature, as well as flow rate to ensure a high current efficiency (Chen and Hung, 2004). The current efficiency is defined as the ratio of current consumed in producing a target product to that of total consumed current. For aluminum electrodes can be 120 – 140%, while that for iron is around 100%. The overall 100% current efficiency for aluminum is aluminum is attributed to the pitting corrosion effect, especially when there are chlorine ions present in solution. The current efficiency depends on the current density as well as on the types of the anions. The operating current density, or charge loading, can be determined experimentally if there are not any reported values available. There is a critical charge loading required. Once the charge loading reaches the critical value, the effluent quality does not show any significant improvement upon further current increase (Chen et al., 2000).

1.1.1.2. Effect of Conductivity

When the electrolytic conductivity is low, the current efficiency will decrease, and high-applied bias potential is needed. This will lead to passivation of the electrode and increased treatment cost. Generally, $NaCl$ is added in order to increase the electrolytic conductivity. Active chloride will also produce the Cl^- electrolysis, which will contribute to water disinfection (Wong et al. 2002). The addition of Cl^- will also decrease the negative effect of CO_3^{2-} and SO_4^{2-}. The presence of CO_3^{2-} and SO_4^{2-} leads to the deposition of Ca^{2+} and Mg^{2+} and the formation formation of an oxide layer that will cause a rapid decrease in current efficiency. It is therefore recommended that the electrolyte contains at least 200 mg L^{-1} of Cl^- to ensure an efficient electrocoagulation in water treatment (Holt et al., 2005)

1.1.1.3. Effect of Temperature

The water temperature will also influence the electrocoagulation process. (Liu et al., 2010). Al anode dissolution was investigated in the water temperature range from 2 to 90 °C. The Al current efficiency increased rapidly when the water temperature increased from 2 to 30 °C. The temperature increase will speed up the destructive reaction of oxide membrane and increase the current efficiency. However, when the temperature was over 60 °C, the current efficiency began to

decrease. In this case, the volume of colloidal $Al(OH)_3$ will decrease and pores produced on the Al anode will be closed. The above factors will be responsible for the decreased current efficiency

1.1.1.4. Effect of pH

The pH of the solution plays an important role in electrochemical and chemical coagulation processes (Chen et al., 2000). Under certain conditions, various complex and polymer compounds can be formed via hydrolysis and polymerization reaction of electrochemically dissolved Al^{3+}. The formation of Al^{3+} single-core coordination compounds is described by equations 16 to 19.

With the extension of hydrolysis of Al^{3+}, multicore coordination compounds and $Al(OH)_3$ precipitate can be formed.

$$Al^{3+} \rightarrow Al(OH)_n^{3-n} \rightarrow Al_2^{4+} \rightarrow Al_{13}complex \rightarrow Al(OH)_3 \quad (22)$$

In the pH range of 4-9, $Al(OH)^{2+}$, $Al(OH)_2^{+}$, $Al_2(OH)_2^{4+}$, $Al(OH)_3$, and $Al_{13}(OH)_{32}^{7+}$ are formed. The surface of these compounds has large amounts of positive charge, which can lead to adsorption, electrochemical neutralization and net floc-forming reactions. At pH > 10, $Al(OH)_4^-$ is dominant, and the coagulation effect rapidly decreases. At low pH, Al^{3+} is dominant, which has no coagulation effect.

In chemical coagulation, pH has to be adjusted after it changes due to the addition of coagulants. In EC processes, the evolution of H_2 at the cathode will increase the OH^- concentration. Thus, pH in the aqueous solution will increase when the pH of original water is in the range of 4 – 9. However, when the pH of the original water is higher than 9, the pH of the treated water will decrease. Compared with the chemical coagulation, EC can neutralize the pH of the treated water to some extend via the following reactions.

$$Al + 3H^+ \rightarrow Al^{3+} \quad (23)$$

$$Al^{3+} + 3H_2O \rightarrow Al(OH)_3 + 3H^+ \quad (24)$$

$$Al(OH)_3 + OH^- \rightarrow Al(OH)_4^- \quad (25)$$

When there are chloride ions, the following chemical reaction take place:

$$2Cl^- - 2e^- \rightarrow Cl_2 \quad (26)$$

$$Cl_2 + H_2O \rightarrow HOCl + Cl^- + H^+ \quad (27)$$

$$HOCl \rightarrow OCl^- + H^+ \quad (28)$$

Hence, the increase of pH because of hydrogen evolution is more or less compensated by the H^+ release reactions earlier. For the increase in pH at acidic influent, the increase of pH is believed to be caused by the CO_2 release from hydrogen bubbling, because of the formation of precipitates of other anions with Al^{3+}, and because of the shift of equilibrium toward the products in H^+ releasing reactions. At high pH, reaction 24 occurs to the right easily, Ca^+ and Mg^+ can precipitate with $Al(OH)_3$. At higher pH, reaction 25 proceeds. These processes are responsible for the decrease of aqueous pH (Liu et al., 2010).

1.1.2. Advantages and disadvantages of Electrocoagulation

As explained by Rajeshwar and Ibanez (1997), electrocoagulation offers several advantages over traditional technologies, including the following:

- The smallest charged colloids can be treated, since they can move more easily than their larger counterparts within an electrical field; this facilitates coagulation. Furthermore, such motion avoids the need for mechanical agitation, which (if uncontrolled) may destroy precipitates as soon as they are formed.
- The amount of required chemicals is much lower (on the order of 1/10). For example, in conventional lime-neutralization processes, water hardness is increased.
- A smaller amount of sludge is produced, due to the higher content of dry solids. For example, conventional addition of ferric chloride followed by lime or sodium hydroxide produces up to 30 liters of sludge for every liter of removed oil. In addition, the sludge produced by the electrochemical treatment is more hydrophobic, which leads to more compact residues; this also leads to shorter decantation times.
- No mixing of chemicals is required.
- The durability of the electrodes translates to low “down times” for maintenance or replacement.

- Organic matter removal (including nonbiodegradable organics) is more effective; this facilitates subsequent biological treatment.
- Coagulant dosing as well as required overpotential can be easily calculated and controlled.
- Often, pH control is not necessary, unless this parameter acquires extreme values; this facilitates process design and operation.
- High current efficiencies (~90%) can be achieved in well-designed systems.
- Short contact times are required.
- Operating costs are much lower when compared with most of the conventional technologies.

The major challenges for these processes are:

- The production of H_2 at the cathode may prevent precipitated matter from settling properly.
- The concentration of aluminum or iron ions in the effluent will most likely be increased (for example, in oil removal, up to 550 mg l^{-1} of dissolved solids can be added by this process; nevertheless, by comparison, chemical coagulation methods generally add 2000-3000 mg l^{-1} of dissolved solids). Careful pH control would be needed if Al or Fe contents are outside of the regulatory limits.
- The produced insoluble hydroxides may agglomerate between the electrodes, hampering their further production.
- These direct current processes are frequently accompanied by anode passivation and sludge deposition on the electrodes; to prevent this, alternating current with controlled reverse pulses (and with the addition of anode activating ions such as chlorides) has been found to substantially lower the required anodic polarization and facilitate continuous renewal of the electrode surface by redeposition of the metal oxidized in the forward pulse. This procedure has the added benefit of doubling the time required for electrode replacement.
- Investment costs are relatively high, although operating cost tend to be smaller than with other techniques.

2. Analysis and Correlation of Kinetic Data

2.1. Ideal Reactors

In an ideal reactor the conditions of mixing and fluid flow are defined very precisely.

In the continuous stirred-tank reactor (CSTR), mixing is so intense that the species concentrations and the temperature are the same at every point in the reactor. Moreover, mixing is complete down to a molecular scale. Every molecule that enters the reactor is immediately mixed with molecules that have been in the reactor for a longer time. There is no tendency for molecules that entered the reactor at the same time to remain associated.

In the plug-flow reactor (PFR) there is no mixing in the direction of flow. All the molecules that enter the reactor at the same time stay together as they flow through the reactor, and they all leave the reactor at the same time. Moreover, there are no gradients of either concentration or temperature normal to the direction of flow.

These two continuous, ideal reactors represent limiting cases of fluid mixing. The behavior of a real reactor will often approximate either one of these ideal reactors. However, this is not always the case.

2.1.1. Stirred-Tank Reactors (CSTRs)

In ideal CSTRs there are no spatial variations of concentration or temperature, and the rate is the same at every point inside the reactor.

The design equation for an ideal CSTR can be written as follows (Roberts, 2009)

$$-r_A = \frac{x_A F_{A0}}{V} = \frac{x_A C_{A0} Q}{V\ MW} \tag{29}$$

where $F_{A0} = C_{A0} Q / MW_A$. This equation shows that the reaction rate, r_A, can be obtained directly in a CSTR if the fractional conversion x_A is measured, and if the molar feed rate F_{A0} and the reactor volume V are known. C_{A0} is the concentration of specie A, MW_A its molecular weight, and Q is the volumetric flow rate.

In order to obtain data useful for testing the assumed rate equation, the composition in the CSTR must be varied over a wide range in order to determine how the reaction rate, $-r_A$, behaves as a result of changes in the various species concentrations. This can be achieved by varying the composition of the inlet stream and by varying the space time τ (V / Q).

The major advantage of using a CSTR to study the kinetics of a reaction is that values of the reaction rate $-r_A$ can be obtained directly from the data via equation 29, which simplifies the analysis.

2.1.2. Plug-Flow Reactors (PFRs)

2.1.2.1. Differential Plug-Flow Reactors

Differential plug-flow reactors operate at very low (differential) conversion and, therefore, are widely used in kinetic studies of heterogeneous catalytic reactions. The design equation for an ideal PFR in differential form is (Roberts, 2009)

$$\frac{\mathrm{d}V}{F_{A0}} = \frac{\mathrm{d}x_A}{-r_A} \tag{30}$$

Assuming that the PFR operates at a very small fractional conversion x_A, of the order of a few percent, and that the reactor is isothermal, then the reaction rate will not vary substantially between the reactor inlet and the reactor outlet. Equation 30 can be integrated by assuming that $-r_A$ is constant at some average value, $-\bar{r}_A$. Thus,

$$\frac{V}{F_{A0}} = \frac{x_A}{-\bar{r}_A} \tag{31}$$

or

$$-\bar{r}_A = x_A F_{A0} / V \tag{32}$$

A value of the average reaction rate can be calculated from the measured outlet conversion x_A using equation 31. The concentrations that are associated with this value of $-\bar{r}_A$ usually are taken to be the average of the inlet and outlet concentrations.

2.1.2.2. Integral Plug-Flow Reactors

In an integral PFR, the reactant conversion is significant; therefore, the assumption that the reaction rate is constant in the direction of flow is not valid. If an ideal, isothermal PFR is operated with a constant feed composition at several different values of V / F_{A0}, and the fractional conversion, x_A, is measured at each value of V / F_{A0}. The resulting data will have the form shown in the following figure.

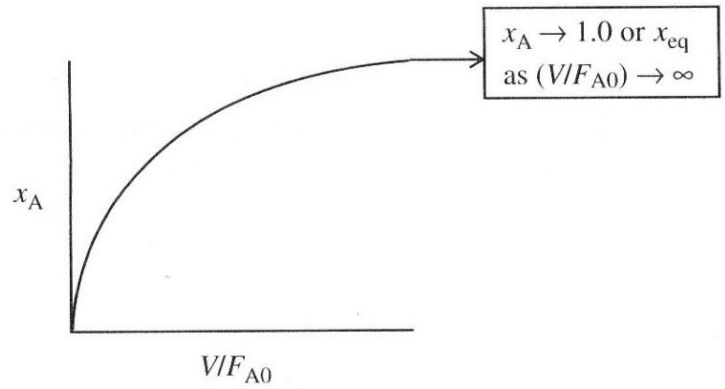

Figure 2. Fractional conversion vs reactor volume to molar feed ratio in an integral PFR. (Roberts, 2009)

It is possible to calculate values of the reaction rate $-r_A$ at various values of x_A. The integral form of the PFR design equation (Roberts, 2009)

$$\frac{V}{F_{A0}} = \int_0^{x_A} \frac{\mathrm{d}x_A}{-r_A} \tag{33}$$

can be differentiated to give

$$-r_A = \frac{\mathrm{d}x_A}{\mathrm{d}(V / F_{A0})} \tag{34}$$

Equation 34 shows that the reaction rate at any value of x_A is equal to the slope of the curve in the figure above, taken at the specific value of x_A. This relationship is represented in the following figure.

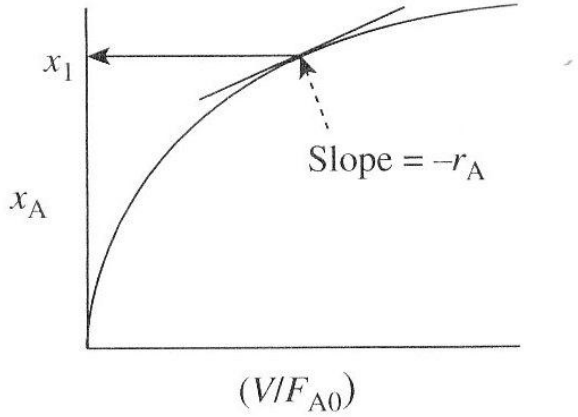

Figure 3. Reaction rate determination in an integral PFR. (Roberts, 2009)

Therefore, a value of the reaction rate at x_1 can be obtained by taking the derivative of the x_A vs. V / F_{A0} curve at x_1 according to equation 34.

2.1.2.3. Electrochemical (Plug-Flow) Reactors

Many electrochemical reactors operate under limiting current conditions when the overall rate of reaction is restricted by the rate of convective-diffusion of species towards the electrode surface. This mode of operation is found when the *overpotential* at the electrode is high and the rate of the process then depends on the rate at which the reactant reaches the electrode. The interconversion of an oxidized (O) and reduced (R) species of a redox couple O / R

$$O + ze^- \rightarrow R \tag{35}$$

can be considered. The cathodic reaction may be explained through a three step mechanism:

a) Mass transport of reactant towards the electrode:

$$O_{bulk} \rightarrow O_{surface} \tag{35a}$$

b) Electron (or charge) transfer at the surface:

$$O_{surface} + ze^- \rightarrow R_{surface} \tag{35b}$$

c) Mass transport of product away from the electrode:

$$R_{surface} \rightarrow R_{bulk} \tag{35c}$$

For the case of the electrochemical reaction (35), in which the overpotential is sufficiently high, the rate of reaction becomes dependent only on the rate at which the reactant is supplied to the electrode. The limiting current conditions have then been achieved. In this case the process becomes completely mass transport controlled, i.e., reaction 35a becomes the rate controlling step, and the production rate becomes highly dependent of the fluid flow conditions in the reactor.

In reactor analysis, it is necessary to set up a material balance in order to determine the reactor design equations. The material balance is based in the principle of the conservation of matter and in the case of the component O in reaction, equation 35 can be written as:

$$\begin{aligned}&\text{Rate of mass input - Rate of mass output}\\ &\text{- Rate of loss = Rate of accumulation}\end{aligned} \tag{36}$$

For the case of PFRs, there is no accumulation of materials and we can write for component O:

$$\text{Rate of mass input-Rate of mass output} = \text{Rate of mass disappearance} \tag{37}$$

In an electrochemical reaction the rate of mass disappearance of O (i.e. $d[O]/dt$) is given by the expression:

$$\frac{I}{eF} = -\frac{\mathrm{d}\,[O]}{\mathrm{d}t} \tag{38}$$

where I is the cell current in Amps. The quantity I/eF is the rate of material flow and has units of mol s^{-1}.

Here, the reaction is considered to take place under mass transport control and the value of I is the limiting current, I_L, given by:

$$I_L = eFk_m AC^* \tag{39}$$

where k_m is the mass transport coefficient (a type of heterogeneous rate constant) in m s^{-1}, A is the reactive electrode surface area in m^2 and C^* is the concentration of the electroactive species in the bulk electrolyte. For a given reaction and a given reactant level, the product $k_m A$ must be as large as possible. As explained by Rajeshwar and Ibanez (1997), one strategy to accomplish this is by using three-dimensional electrodes. In such case, the active electrode area per unit volume is

$$A_e = \frac{A}{V_e} \tag{40}$$

where A_e is the electrode's volumetric surface area in m^2/m^3 and V_e is the electrode volume. If a volumetric mass transport coefficient is defined as the kinetic constant for this type of reaction, $k' = k_m A_e = k_m A/V$, then, equation 39 can be rearranged for a two-dimensional electrode as

$$k' = \frac{I_L}{eFC^*V} \tag{41}$$

with k' in s^{-1} and V being the reactor volume in m^3.

Combining equations 38 and 41 yields

$$\frac{\mathrm{d}[O]}{\mathrm{d}t} = \frac{I_L}{eF} = k'C^*V \tag{42}$$

which can be rewritten, for a plug-flow reactor, by dividing by both V and the linear flow velocity of the fluid, v in m/s, to give

$$\frac{\mathrm{d}C_L}{\mathrm{d}L} = -\frac{k'}{v}C_L \tag{43}$$

where C_L is the reactant concentration at a distance L into the reactor. This equation is equivalent to equations 34 or 44 and indicates that the reactor performance, in terms of conversion, depends strongly upon the product of the volumetric mass transport coefficient. The value of k_m depends upon reactor geometry, the type of flow and volumetric flow rate.

Equation 43 can be integrated and rearranged in terms of fractional conversion

$$\ln\left(\frac{C_{AL}}{C_{A0}}\right) = \ln\left(1-x_A\right) = -\left(\frac{k'}{v}\right)L \tag{44}$$

or

$$x_A = 1-\exp\left[-\left(\frac{k'}{v}\right)L\right] \tag{45}$$

This is equivalent to

$$\ln\left(\frac{C_{A,E}}{C_{A,0}}\right) = \ln\left(1-x_A\right) = -k'\left(\frac{Q}{V}\right) \tag{46}$$

Equation 46 indicates that the reactor's average detention time $\tau = Q/V$.

Therefore, equation 46 results in

$$\ln\left(\frac{C_{A,E}}{C_{A,0}}\right) = \ln\left(1-x_A\right) = -k'\tau \tag{47}$$

It is very important to calculate the value of k', since this is the factor determining the overall reactor performance.

2.2. The Integral Method of Data Analysis

The integral method of analysis can be used when available data are in the form of concentration (or fractional conversion) versus time or space time. This kind of data is obtained when an ideal batch reactor or an ideal plug-flow reactor is used. Therefore, use of the integral method avoids the need for numerical or graphical differentiation.

As explained by Roberts (2009), the steps in the integral method are:

1. A rate equation is assumed.
2. The appropriate design equation is integrated to generate a relationship between concentration (or conversion) and time (or space time).
3. The relationship is linearized.
4. The data are plotted so as to test the linearized equation.
5. If the equation fits the data, the values of the slope and the intercept are used to estimate the unknown parameters in the rate equation.

For example, if a first-order rate equation is to be assumed, then equation 34 can be rewritten as

$$-r_A = -\frac{\mathrm{d}C_A}{\mathrm{d}t} = kC_A \tag{48}$$

which after integrating becomes

$$\ln\frac{C_A}{C_{A0}} = -kt \tag{49}$$

In terms of conversion, the rate equation 44 is

$$\frac{\mathrm{d}x_A}{\mathrm{d}t} = k(1-x_A) \tag{50}$$

This equation can be rearranged and integrated so that a linearized expression results

$$\ln\left(1-x_A\right) = -kt \tag{51}$$

If the experimental data corresponds to this form of rate of equation, plotting $\ln\left(1-x_A\right)$ or $\ln\left(C_A / C_{A0}\right)$ vs. t will give a straight line through the origin.

3. Diagnose and Characterization of Reactor Flow

In a real reactor, every molecule may not spend exactly the same time in the vessel. If there were mixing in the direction of flow, some of the molecules that entered the vessel at time $t = 0$, might catch up to molecules that entered at an earlier time, say $t = -\delta$. Similarly, some of the molecules that

entered at $t = 0$ might be overtaken by ones that that entered at a later time, say $t = \delta$. In general, individual molecules will spend different amounts of time in the vessel.

Given a fluid flowing through a vessel at steady state and assuming that there is no change in density, the time each molecule of fluid spends in the reactor or *distribution* of times can be calculated experimentally by means of *tracer injection techniques.*

The use of a tracer to study the flow of a fluid through a vessel is known as a *tracer response* technique. A known amount of tracer is injected in a known pattern (such as an instantaneous pulse), and the response of the tracer to the flow conditions that exist in the vessel is measured. The use of tracer response techniques is common in medicine, as well as in chemical and environmental engineering.

Selection of a suitable tracer can be a challenging task. Since the tracer must move through the vessel exactly like the bulk fluid, the tracer cannot settle, phase separate, react, adsorb on the vessel walls or on any internal components such as an agitator or baffle or on a solid catalyst, diffuse relative to the bulk fluid, or influence the flow of the bulk fluid in any way.

The tracer concentration must also be easy to measure. Some commonly used measurement techniques are radioactivity, electrical conductivity, absorptivity and refractive index.

3.1. Tracer Response Curves for Ideal Reactors

3.1.1. Ideal Plug-Flow Reactor

In an Ideal PFR, elements of fluid pass through the reactor in single file. There is no fluid mixing in the direction of flow. Each element of fluid spends exactly the same time in the vessel. Therefore, every molecule of an ideal tracer will spend exactly that time in the vessel. At the vessel exit, the entire quantity of injected tracer will be detected at the same time.

The tracer response curve will resemble the one shown below.

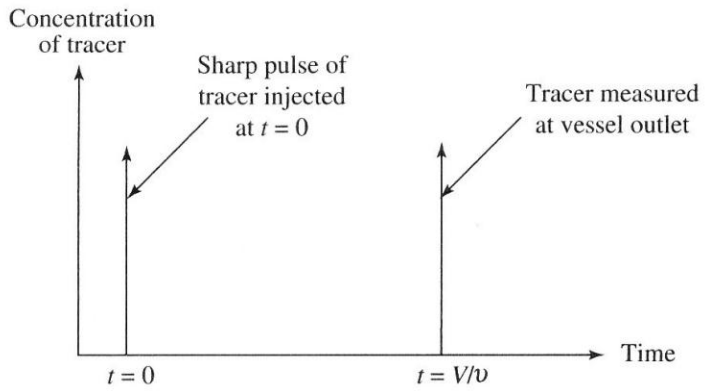

Figure 4. Tracer response in an ideal plug-flow reactor (Roberts, G. 2009)

The time that the tracer spends in an ideal PFR is $t = \tau = V/Q$ (Eq. 60). This is easy to see if the reactor has a constant cross section A in the direction of flow. In this case, the velocity of the fluid in the direction of flow is Q/A at every point in the reactor. If the length of the vessel in the direction of flow is L, the time required to traverse the vessel is $L/(Q/A) = V/Q$ (Roberts, 2009).

If there were a slight amount of mixing in the direction of flow, all of the tracer would not emerge at exactly the same time. A small amount might mix with fluid elements that were injected somewhat earlier, and a small amount might mix with elements that were injected somewhat later. This mixing would cause "spreading" of the response curve, as shown below,

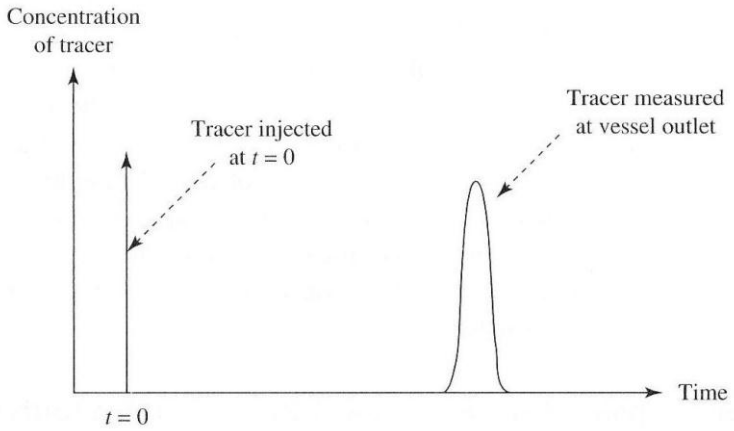

Figure 5. Tracer response in a plug-flow reactor with a slight amount of mixing in the direction of flow. (Roberts, G. 2009)

3.1.2. Ideal Continuous Stirred-Tank Reactor

In an ideal CSTR, the feed mixes instantaneously into the contents of the reactor, and the composition of the effluent stream is exactly the same as the composition of the fluid in the reactor. If a pulse of tracer is injected at $t = 0$, it will mix instantaneously with the fluid in the reactor. The concentration of tracer in the reactor at $t = 0$ is as high as it ever will be. This is because the fluid that enters the reactor at later times does not contain any tracer, and because the tracer begins to leave the reactor as soon as it is injected, since the composition of the effluent stream is the same as the composition of the fluid in the reactor.

The concentration of tracer in the stream leaving the CSTR has a maximum at $t = 0$, and it declines continuously thereafter. The tracer response curve for an ideal CSTR will resemble the one shown below (Roberts, 2009).

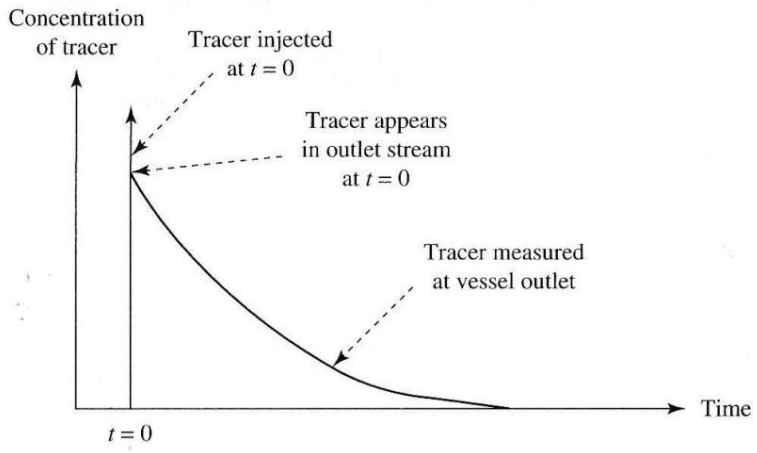

Figure 6. Tracer response in an ideal continuous stirred-tank reactor (Roberts, G. 2009)

3.2. Non-Ideal Reactors and the Residence Time Distributions

Real equipment always deviate from the ideal flow patterns, plug flow and mixed flow. In order to account for these deviations from ideality, some interrelated factors like the residence time distribution (RTD), the state of aggregation and the earliness and lateness of mixing of material flowing through the vessel, may yield an approximate picture of the real/non-ideal flow pattern.

Deviation from the two ideal flow patterns can be caused by channeling of fluid, by recycling of fluid, or by creation of stagnant regions in the vessel.

Residence time distribution or RTD functions provide a quantitative way to describe how much time a flowing fluid spends in a reactor and can be obtained from a *stimulus-response experiment* like the previously discussed *tracer injection technique*.

3.2.1. The Exit-Age Distribution Function, $E(t)$

If we consider a vessel with a constant density fluid flowing through it at steady state and the fluid crosses the boundaries of the vessel only by convection (there is no diffusion across the system boundaries, i.e*., closed vessel*), then, the *exit-age distribution function*, $E(t)$, is defined as

$$E(t)\mathrm{d}t \equiv \text{fraction of fluid leaving the vessel at time } t \text{ that was in the vessel, for a time between } t \text{ and } t+\mathrm{d}t$$

The exit-age distribution function is also known as the *external-age* distribution function and can be represented graphically in the following figure

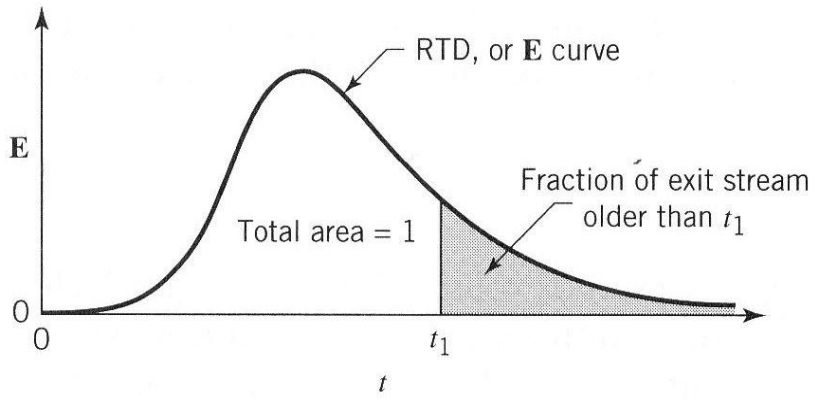

Figure 7. The exit-age distribution curve E or RTD for fluid flowing through a vessel (Levenspiel, O. 1999)

By definition,

$$\int_0^\infty E(t)\mathrm{d}t = 1 \tag{52}$$

The fraction of fluid in the effluent stream that was in the vessel for a time between $t = 0$ and $t = t$ is given by

$$\int_0^t E(t)\mathrm{d}t = \left\{\begin{matrix}\text{fraction of fluid in the exit stream that} \\ \text{was in the vessel for a time less than } t\end{matrix}\right\}$$

Similarly, the fraction of fluid in the effluent stream that was in the vessel for a time t or longer is given by

$$\int_{t}^{\infty} E(t)\mathrm{d}t = \left\{\begin{matrix}\text{fraction of fluid in exit stream that was}\\ \text{in the vessel for a time greater than } t\end{matrix}\right\}$$

Now, consider a pulse of tracer is injected right at the inlet of a closed vessel at a time $t = 0$, then

$$\left\{\begin{matrix}\text{fraction of tracer in the effluent stream that was}\\ \text{in the vessel for a time between } t \text{ and } t+\mathrm{d}t\end{matrix}\right\}$$

$$= \left\{\begin{matrix}\text{fraction of fluid in the effluent stream that was}\\ \text{in the vessel for a time between } t \text{ and } t+\mathrm{d}t\end{matrix}\right\} = E(t)\mathrm{d}t$$

The fraction of fluid that was in the vessel for a time between t and $(t+\mathrm{d}t)$ is just $E(t)\mathrm{d}t$. Since all the tracer was injected exactly at $t = 0$, the fraction of tracer that was in the vessel for a time between t and $t+\mathrm{d}t$ is

$$\left\{\begin{matrix}\text{fraction of tracer in the effluent stream that was}\\ \text{in the vessel for a time between } t \text{ and } t+\mathrm{d}t\end{matrix}\right\} = \frac{QC(t)\mathrm{d}t}{Q\int_{0}^{\infty} C(t)\mathrm{d}t}$$

where Q is the volumetric flow rate through the vessel in m^3/s and $C(t)$ is the concentration of tracer in the exit stream at any time t.

This leads to

$$E(t) = \frac{C(t)}{\int_{0}^{\infty} C(t)\mathrm{d}t} \tag{53}$$

Equation 53 allows calculating the exit-age distribution function $E(t)$ from the tracer response data that is obtained after a *pulse experiment.*

3.2.2. The Cumulative Exit-Age Distribution Function, $F(t)$

An alternative approach to the pulse experiment is a *step input* of tracer. Consider again a vessel with a constant density fluid flowing at steady state. There is no tracer in the influent fluid. Then, at time $t = 0$ the concentration of tracer in the feed is abruptly changed to a value C_0 and is maintained at this concentration.

The concentration of tracer in the effluent stream is measured continuously. Eventually, the effluent tracer concentration will become C_0. This type of *step input* experiment is illustrated in the following figure.

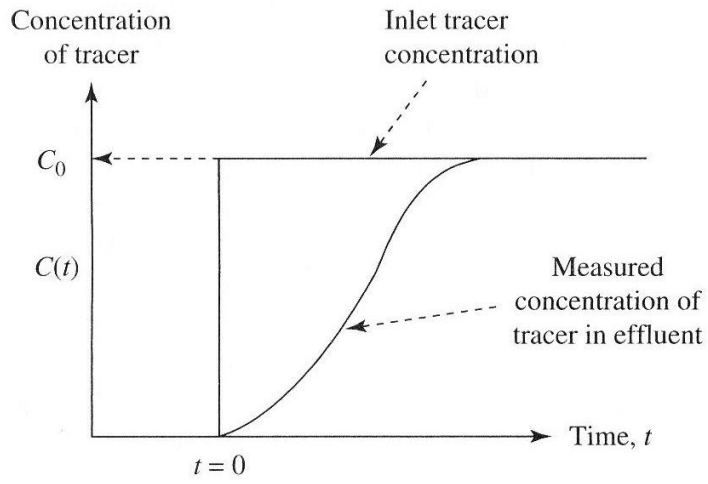

Figure 8. Cumulative exit-age distribution function, $F(t)$, resulting from a step input tracer test (Roberts, G. 2009)

The cumulative exit-age distribution function, $F(t)$, is defined as the fraction of fluid in the effluent stream that was in the vessel for a time less than t.

$$F(t) \equiv \left\{ \begin{array}{l} \text{fraction of fluid in the exit stream that was in the} \\ \text{vessel for a timer shorter than } t, \text{ i.e., between 0 and } t \end{array} \right\}$$

The cumulative exit-age distribution function can be obtained from the curve of tracer concentration versus time, as shown above. Suppose that the concentration of tracer in the feed to the vessel was changed from 0 to C_0 exactly at $t = 0$. If the concentration of tracer in the effluent stream is $C(t)$ at some time t, then the fraction of fluid that was in the vessel for a time less than t is $C(t)/C_0$. Therefore,

$$F(t) = \frac{C(t)}{C_0} \tag{54}$$

In equation 54, $C(t)$ is the concentration of tracer in the effluent stream after a sharp step change in the inlet tracer concentration from 0 to C_0 at $t = 0$.

3.2.3. Relationship between $F(t)$ and $E(t)$

From the definition of $E(t)$,

$$\int_0^t E(t)\mathrm{d}t = \left\{ \begin{array}{l} \text{fraction of fluid in the exit stream that} \\ \text{was in the vessel for a time less than } t \end{array} \right\}$$

However, the right-hand side of this equation is by definition $F(t)$. Therefore,

$$F(t) = \int_0^t E(t)\mathrm{d}t \tag{55}$$

Differentiating,

$$E(t) = \frac{\mathrm{d}F(t)}{\mathrm{d}t} \tag{56}$$

Equation 56 shows that $E(t)$ is the slope of the $F(t)$ curve at any point in time.

3.2.4. Moments of Residence Time Distributions

The n[th] moment of a function, $f(x)$, about the origin, is designated μ_n and is defined as

$$\mu_n = \int_0^\infty x^n f(x)\mathrm{d}x \tag{57}$$

The function $f(x)$, is a distribution function, just like $E(t)$.

3.2.4.1. The First Moment of $E(t)$ or the Average Residence Time

Consider the first moment of $E(t)$ about the origin,

$$\mu_1 = \int_0^\infty tE(t)\mathrm{d}t \tag{58}$$

And as previously described, $E(t)$ is just the fraction of fluid elements that stay in the reactor for a time between $t + \mathrm{d}t$. Integrating the above equation over the whole range of possible residence times gives the average time, $\overline{t}$, that an element of fluid spends in the reactor, so that

$$\overline{t} = \int_0^\infty tE(t)\mathrm{d}t = \mu_1 \tag{59}$$

As presented in section 3.1.1 for a PFR, assuming that the fluid enters and leaves the reactor only by convection, i.e., the reactor is a closed vessel, the following can be shown

$$\overline{t} = V/Q = \tau \tag{60}$$

Equation 60 is particularly useful in diagnosing the reactor's behavior and checking its operating conditions. In any reactor, the volumetric flow rate can be easily set or measured. This is not the case with the actual reactor volume or volume of reactor that is filled by fluid in which the reaction is taking place.

3.2.4.2. The Second Moment of $E(t)$ or Mixing

The second moment commonly used to compare RTDs is taken about the mean and is called the *variance*, or square of the standard deviation. It is defined as

$$\sigma^2 = \int_0^\infty (t-\overline{t})^2 E(t)\mathrm{d}t = \mu_2 - \tau^2 \tag{61}$$

The magnitude of this moment is an indication of the spread of the distribution or degree of mixing of fluid particles throughout the reactor. The greater the value of this moment is, the greater a distribution's spread will be.

3.2.4.3. The Third Moment of $E(t)$

The third moment is also taken about the mean and is related to the skewness.

The skewness is defined by

$$s^3 = \frac{1}{\sigma^{3/2}} \int_0^\infty (t-t_m)^3 E(t)\mathrm{d}t \tag{62}$$

The magnitude of this moment measures how extended a distribution is skewed in one direction or another in reference to the mean.

Rigorously, for complete description of a distribution, all moments must be determined. Practically, these three are usually sufficient for a reasonable characterization of an RTD.

3.2.5. Normalized RTD Function, $E(\Theta)$

Frequently, a normalized RTD is used instead of the function $E(t)$. If the parameter Θ is defined as

$$\Theta \equiv \frac{t}{\tau} \tag{63}$$

a dimensionless function $E(\Theta)$ can be defined as

$$E(\Theta) \equiv \tau E(t) \tag{64}$$

and plotted as a function of Θ. The quantity Θ represents the number of reactor volumes of fluid based on entrance conditions that have flowed through the reactor in time t.

The purpose of creating this normalized distribution function is that the flow performance inside reactors of different sizes can be compared directly.

4. Modeling Non-Ideal Reactors

Not all tank reactors are perfectly mixed nor do all tubular reactors exhibit plug-flow behavior. In these situations, some means must be used to allow for deviations from ideal behavior. When dealing with first order reactions, the RTD is sufficient to diagnose the reactor's performance, but in order to predict conversions and product distributions for such systems, a model of reactor flow pattern is necessary. In order to model these patterns, combinations and/or modifications of ideal reactors to represent real reactors are employed. The RTD is then used to evaluate the parameter(s) in the proposed model.

The overall goal is to use the following equation

$$\text{RTD data + Kinetics + Model = Prediction} \tag{65}$$

4.1. Dispersion Model

The dispersion model is used to describe non-ideal tubular reactors. This model assumes that there is an axial dispersion of the material, which is governed by an analogy to Fick's Law of Diffusion, superimposed on the flow as shown in figure 9. Therefore, in addition to transport by bulk flow, UA_FC (where the term U is the empty tube or superficial velocity and A_F is the reactor's cross-sectional area), every component in the mixture is transported through any cross section of the reactor at a rate equal to $\left[-DA_F\left(\mathrm{d}C/\mathrm{d}z\right)\right]$ resulting from molecular and convective diffusion, where D is referred as the dispersion coefficient in $m^2\,s^{-1}$. (Fogler, 2006). Convective

diffusion (i.e., dispersion) means either Aris-Taylor dispersion in laminar flow reactors or turbulent diffusion resulting from turbulent eddies. Radial concentration profiles for plug flow and a representative axial and radial profile for dispersive flow are shown in figure 9. Some molecules will diffuse ahead of molar average velocity while others will lag behind.

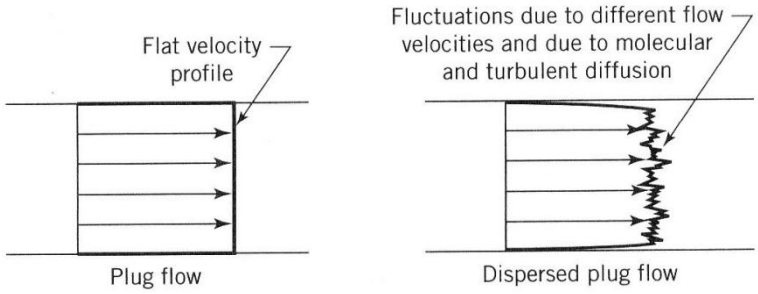

Figure 9. Representation of the dispersion model (Levenspiel, O. 1999)

4.1.1. Balance Equations

A mass balance is taken on a particular component of the mixture (say, species A) over a short length Δz of a tubular reactor of cross section A_F to arrive at

$$-\frac{1}{A_F}\frac{\mathrm{d}F_A}{\mathrm{d}z}+r_A=0 \tag{66}$$

Combining equation 66 and the appropriate equation for the molar flux F_A, an expression involving flow, reaction and dispersion can be written as

$$\frac{D}{U}\frac{\mathrm{d}^2C_A}{\mathrm{d}z^2}-\frac{\mathrm{d}C_A}{\mathrm{d}z}+\frac{r_A}{U}=0 \tag{67}$$

This equation is a second order ordinary differential equation. It is non-linear when r_A is other than zero or first order.

When the reaction rate r_A is first order, $r_A=-kC_{A,}$ then equation 68 is amenable to an analytical solution.

$$\frac{D}{U}\frac{\mathrm{d}^2C_A}{\mathrm{d}z^2}-\frac{\mathrm{d}C_A}{\mathrm{d}z}-\frac{kC_A}{U}=0 \tag{68}$$

However, by letting $\psi=C_A/C_{A0}$ and $\lambda=z/L$:

$$\frac{1}{Pe}\frac{\mathrm{d}^2\psi}{\mathrm{d}\lambda^2}-\frac{\mathrm{d}\psi}{\mathrm{d}\lambda}-Da.\psi=0 \tag{69}$$

The quantity Da in equation 69 is called the *Damkohler number* for convection in a first-order reaction and physically represents the ratio

$$Da = \frac{\text{Rate of consumption of A by reaction}}{\text{Rate of transport of A by convection}} = k\tau \tag{70}$$

The other dimensionless term is the *Peclet number*, Pe,

$$Pe = \frac{\text{Rate of transport by convection}}{\text{Rate of transport by diffusion or dispersion}} = \frac{UL}{D} \tag{71}$$

in which L is the characteristic length term.

4.1.2. Boundary Conditions

For a closed-closed vessel, we have plug flow (no dispersion) to the immediate left of the entrance line ($z = 0^-$) (closed) and to the immediate right of the exit $z = L = (z = L^+)$ (closed). However, between $z = 0^+$ and $z = L^-$, there are dispersion and reaction. The corresponding entrance boundary condition is (Fogler, 2006)

At $z = 0$: $\quad F_A(0^-) = F_A(0^+)$

Substituting for F_A yields

$$UA_cC_A(0^-) = -A_cDa\left(\frac{\partial C_A}{\partial z}\right)_{z=0^+} + UA_cC_A(0^+)$$

Solving for the entering concentration $C_A(0^-) = C_{A0}$,

$$C_{A0} = \frac{-Da}{U}\left(\frac{\partial C_A}{\partial z}\right)_{z=0^+} + C_A(0^+) \tag{72}$$

At the exit, the concentration is continuous and there is no gradient in tracer concentration.

$$\text{At } z = L: \quad \left.\begin{aligned} C_{A0}(L^-) &= C_A(L^+) \\ \frac{\partial C_A}{\partial z} &= 0 \end{aligned}\right\} \tag{73}$$

Now, solving the dispersion reaction balance (Eqn. 69) for a first order reaction and a closed-closed system, the boundary conditions in dimensionless form are

At $\lambda = 0$ then $1 = -\frac{1}{Pe}\frac{\mathrm{d}\psi}{\mathrm{d}\lambda}\Big|_{0^+} + \psi(0^+)$ (74)

At $\lambda = 1$ then $\frac{\mathrm{d}\psi}{\mathrm{d}\lambda} = 0$ (75)

At the end of the reactor, where $\lambda = 1$, the solution to equation 69 is (Levenspiel, 1999):

$$\psi_L = \frac{C_{AL}}{C_{A0}} = 1 - x_A = \frac{4q\exp(Pe/2)}{(1+q)^2\exp(qPe/2) - (1-q)^2\exp(-qPe/2)} \quad (76)$$

where

$$q = \sqrt{1 + 4Da/Pe} \quad (77)$$

Outside the limited case of a first order reaction, a numerical solution of the equation is required, and because this is a split-boundary- value problem, an iterative technique is required.

To evaluate the exit concentration or conversion given by equation 76, it is necessary to know both the Damkohler and Peclet numbers.

The Damkohler number and the dispersion coefficient can be determined using kinetic and RTD data through equation 70. Similarly, the Peclet number can be found experimentally by determining τ and σ^2 from the RTD data and then solving the following equation (Levenspiel, 1999):

$$\frac{\sigma^2}{\tau^2} = \frac{2}{Pe} - \frac{2}{Pe^2}\left[1 - \exp\left(-Pe\right)\right] \quad (78)$$

Some authors have questioned the accuracy of the method of moments approach represented by equation 78, concluding that it produces a biased estimate of mean residence time and dimensionless variance when compared, for example, to a nonlinear regression approach (Haas et al., 1997).

4.2. Tanks-in-Series Model

This model can be used in any case where the dispersion model has been applied. When deviation from plug-flow is small, both the dispersion model and the TIS model yield identical results.

The number of tanks in series can be determined by calculating the dimensionless variance σ_Θ^2 from a tracer experiment, and using the method of moments procedure

$$\sigma_{\Theta}^2 = \int_0^{\infty} \Theta^2 E(\Theta) \mathrm{d}\Theta - 1 \tag{79}$$

$$\sigma_{\Theta}^2 = \int_0^{\infty} \Theta^2 \frac{n(n\Theta)^{n-1}}{(n-1)!} e^{-n\Theta} \mathrm{d}\Theta - 1 = \frac{n^n}{(n-1)!} \int_0^{\infty} \Theta^{n+1} e^{-n\Theta} \mathrm{d}\Theta - 1 = \frac{n^n}{(n-1)!} \left[\frac{(n+1)!}{n^{n+2}} \right] - 1 = \frac{1}{n} \tag{80}$$

The number of tanks in series is

$$n = \frac{1}{\sigma_{\Theta}^2} = \frac{\tau^2}{\sigma^2} \tag{81}$$

This expression represents the number of tanks necessary to model the real reactor as n ideal tanks in series. If the number of reactors, n, turns out to be small, the reactor characteristics are those of one or two CSTR in series. On the other hand, when n turns out to be large, the reactor characteristics approach those of a PFR.

If the reaction is first order, equation 82 can be used to calculate the conversion,

$$x_A = 1 - \frac{1}{\left(1 + \frac{\tau k}{n}\right)^n} \tag{82}$$

It is acceptable (and usual) for the value of n calculated from equation 81 to be a noninteger in equation 82 to calculate the conversion.

III. Experimental Plan

The experimental plan followed herein consisted in:

- Using a continuous flow, bench-scale EC reactor with aluminum electrodes.
- Performing tracer tests using different reactor configurations and fluid velocities to obtain RTD data.
- Executing a series of electrocoagulation experiments using a synthetic oily wastewater in order to calculate the reaction order and kinetic constant for the oil and grease removal reaction.
- Performing reactor modeling using both the dispersion model and the TIS model.
- Conducting data analysis and interpretation of results.

IV. Laboratory Equipment and Experimental Set-Up

1. Electrocoagulation Reactor.

The reactor used in this research was purchased from Ecolotron Inc. of Seabrook, TX. Its design is property of Gavrel et al. under US Patent No.: 7087176 B2, registered on August 8th, 2006. It is described as "an apparatus for the high-pressure electrocoagulative treatment of aqueous and viscous fluids and sludge..." This unit includes a plate and frame design and can be tightly closed mechanically. Plates are individually separated by recessed, gasketed, non-electrical conductive spacer plates that completely enclose and isolate all fluids, electrical contacts and electrodes within the reactor structure. The reactor also exhibits an influent and effluent chamber at both ends to provide the means of fluid transfer between fluid conduits or tubing and the reactor chambers.

Metal plate and spacer dimensions are shown in figure 10.

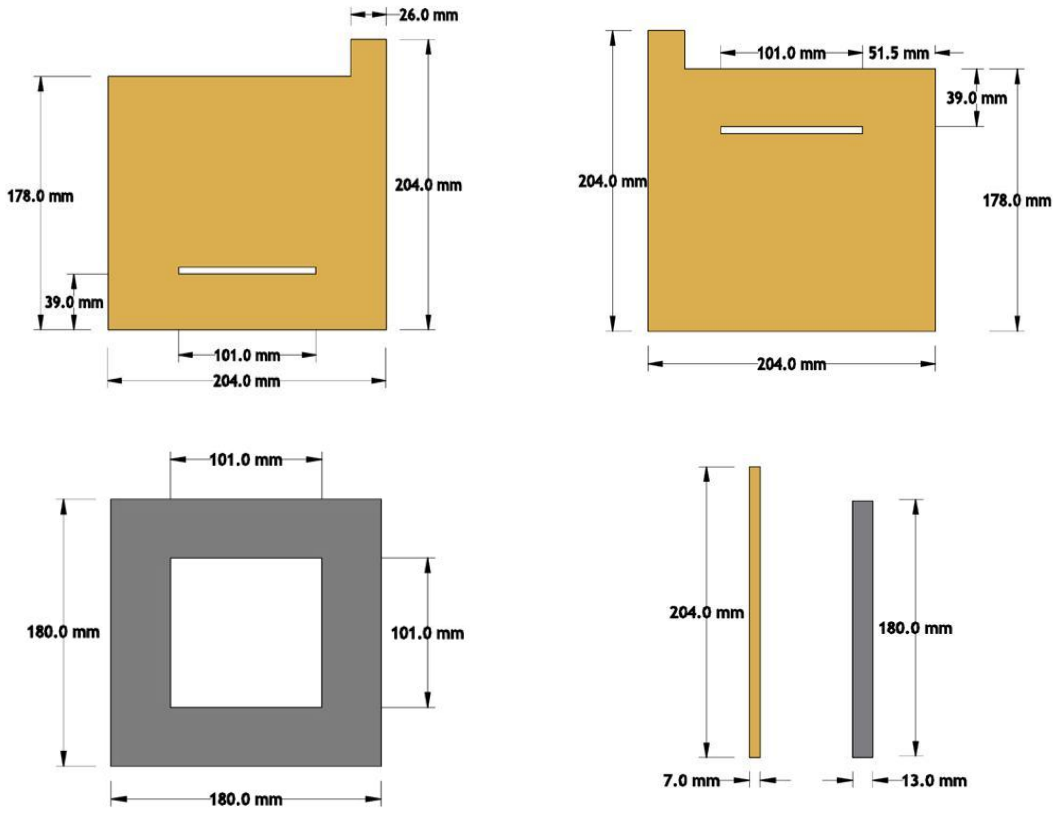

Figure 10. Plate and spacer dimensions (Andrade, M. 2009)

For the purposes of this research, an electrocoagulation cell or reactor cell is defined as the chamber formed between two metal plates and one spacer, as shown in figure 11.

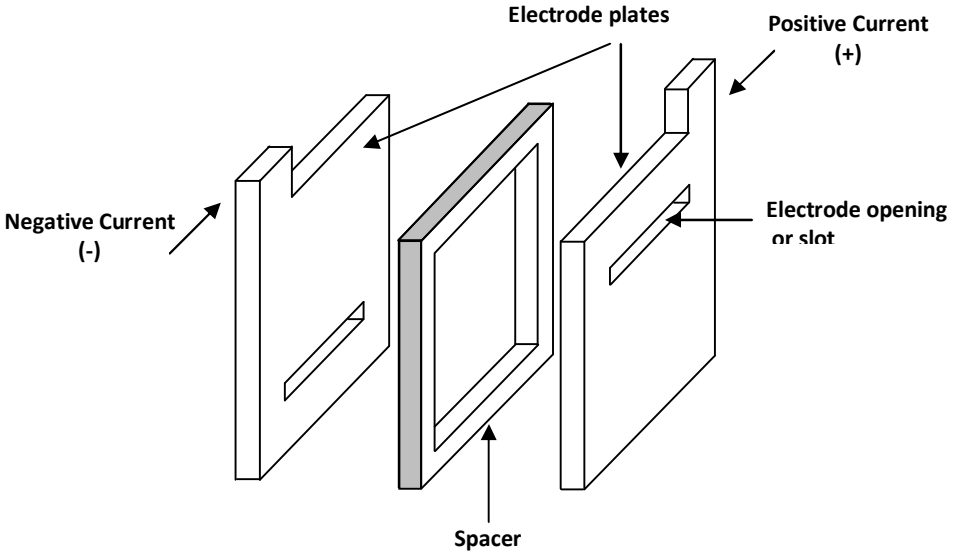

Figure 11. Electrocoagulation cell components (not to scale)

Inside each reactor cell, the fluid flows vertically either downward or upward and passes to the following cell through the electrode openings or slots. Therefore, the area perpendicular to the direction of flow, A_F, is considered to be equal to the area of this opening. Similarly, the active electrode area, A, or the area of electrode surface perpendicular to the direction of electrons flow and that is undergoing electrochemical reaction (metal dissolution), is given by the open section of the spacer.

This reactor design has the advantage of being versatile enough to allow for modifications of its original configuration. Thus, it is possible to vary the number of cells, electrode material and dimensions and even the positioning of the plates using the same frame. The supplier's reactor configuration calls for an 8-cell reactor with upward/downward flow, or the electrodes fixed so that their slots are in horizontal position. This has the purpose of promoting a turbulent flow along the reactor.

Figure 12 shows the effect of rotating the electrodes plates by 90 degrees. With the slots oriented vertically, the fluid follows a horizontal path toward either left or right.

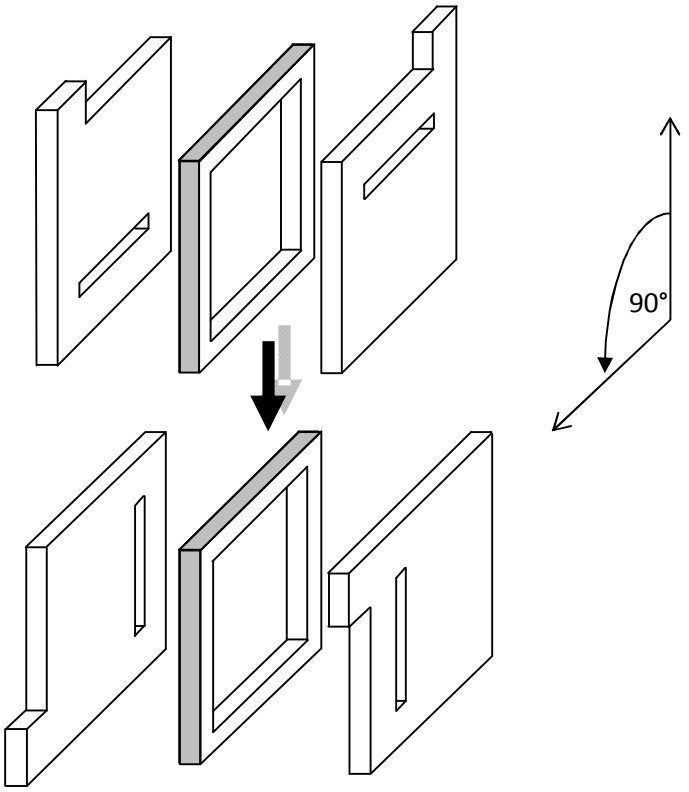

Figure 12. Rotation of electrode plates. The slots are re-oriented vertically, as a consequence the fluid follows a horizontal path.

As mentioned earlier, the reactor has influent and effluent chambers that allow the fluid to enter and exit the electrochemical cells from and toward the external conduits. This is true regardless the amount of cells or slots orientation. Therefore, in order to account for this additional, non-reactive volume, equation 83 is used

$$V_{CELL} = \frac{V_R}{2 + n_{CELL}} \tag{83}$$

where V_{CELL} is the individual cell volume, V_R the reactor volume calculated from the RTD data (see equation 85), and n_{CELL} is the number of cells corresponding to that V_R.

The reactor's characteristic length, L, is given by the following equation

$$L = \frac{V_R}{A_F} \tag{84}$$

2. Electrocoagulation Experiment

The experimental phase was executed using aluminum electrodes to which direct electric current was applied from a regulated power supply. The unit was operated as a monopolar reactor. A simplified diagram of the experimental set-up is shown in figure 13.

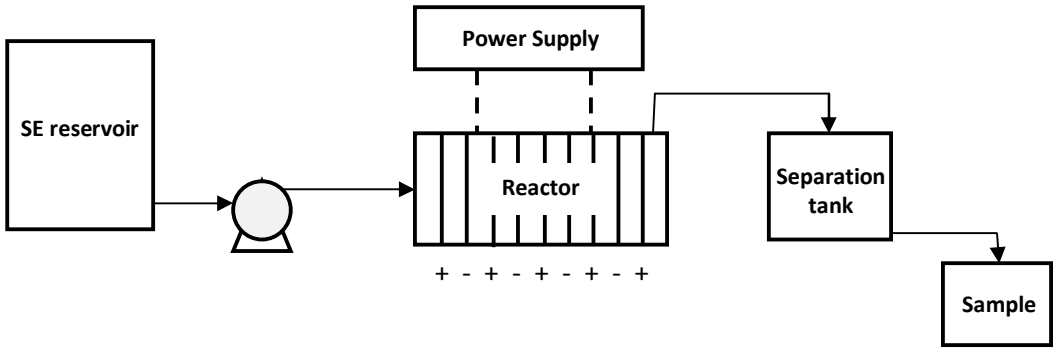

Figure 13. Bench-scale electrocoagulation experiment set-up.

The fluid to be treated was pumped from a 45-L plastic reservoir to the reactor with a peristaltic Masterflex® I/P® modular analog pump system (with benchtop controller) at fixed flow rates (0.5 L min^{-1} and 1.0 L min^{-1}). The reactor's effluent was collected in a 2-L clear plastic container where separation of electrocoagulated particles occurred by electrogenerated-hydrogen-gas flotation. The final sample was withdrawn from the bottom of this container into a 1-l glass beaker. All the fluid conduits were of 12.7-mm plastic tubing.

The fluid feed to the electrocoagulation reactor was prepared in the laboratory in order to simulate bilge water heavily contaminated with hydrocarbons. This synthetic emulsion (SE) consisted of 5000 mg L^{-1} of motor oil SAE-30, 2500 mg L^{-1} of diesel, 2500 mg L^{-1} of gasoline, 200 mg L^{-1} of sodium chloride and 2500 mg L^{-1} of Tween-40 as surfactant. The mixture was vigorously agitated for at least 12 hours at 800 rpm using an Arrow Engineering ® electric stirrer. The resulting emulsion had a conductivity of 960 µS cm^{-1} and a pH of 7.8.

Hydrocarbons concentration was determined through the hexane extractable gravimetric method (US EPA approved #10056, ASTM equivalent #5520B). Oil and grease and total petroleum hydrocarbons (TPH) include any material that may be recovered as a substance that is soluble in the n-hexane extractant. These include substances such as relatively non-volatile hydrocarbons, vegetable oils, animal fats, waxes, soaps, greases and related materials. When measuring oil and grease (HEM)

gravimetrically, the substances are extracted from the sample with n-hexane, then the n-hexane is evaporated. The residue left is weighed to determine the concentration of oil and grease materials in mg L^{-1}.

3. Tracer Experiment

Tracer tests were carried out using the same electrocoagulation reactor with aluminum electrodes, as described before. Note that in this case, no electric current was supplied to the electrodes.

The set-up for these experiments is illustrated in figure 14 and included two 45-L plastic tanks containing fluids of different conductivity, *A* and *B*. The peristaltic modular pump transferred the fluids at a constant flow rate from the reservoirs to the reactor through 12.7 mm plastic conduits. Proper tubing configuration allowed for switching between fluids and purging either of them from the system when required.

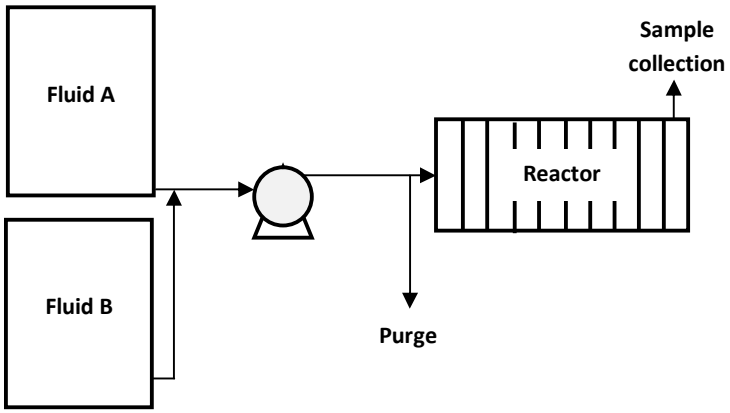

Figure 14. Bench-scale reactor tracer test set-up

The reactor effluent was collected in 30-mL vials and its conductivity measured with an Orion® benchtop multimeter. *Fluid A* consisted of a low conductivity solution, usually tap water (conductivity ≈ 400 µS cm^{-1}) while *fluid B* was a high conductivity brine (conductivity≈ 14000 µS cm^{-1}) prepared in the laboratory by adding sodium chloride to tap water until the desired conductivity was reached.

V. Experimental Procedures and Data Acquisition

1. Step-Input Tracer Tests

Working with a reactor at a bench scale imposes certain restrictions. Among them, the limited flow rate range due to reactor and tubing dimensions may be the most important one. It is virtually impossible to fully introduce a significant volume of tracer by an instantaneous pulse in the reactor's inlet. Consequently, performing an input step tracer experiment on such unit becomes challenging and the results are inaccurate. This was confirmed while running pulse step experiments for a previous research. Therefore, step input tracer tests were performed instead, using sodium chloride as a tracer and conductivity as the traced parameter.

To perform the step input tracer test in the laboratory, low conductivity water or *fluid A* was initially fed to the reactor at a constant flow rate until it was completely filled and steady state was achieved. Then, at a time designated as $t_0 = 0$, the influent to the reactor was rapidly switched to high conductivity water or *fluid B* and simultaneously, the first sample of the effluent stream taken. After this first sample, taken at t_0, the effluent stream was sampled every 5 seconds and its conductivity measured until the conductivities of the effluent and *fluid B* became equal.

The output data from this test was recorded as time vs. conductivity for a given reactor configuration, *fluids A* and *B* rate of flow and conductivity.

Step-input experiments were performed for different reactor configurations and flow rates. Tests were run with the electrode's openings oriented both horizontally and vertically and, in each case, with a flow rate through the reactor of 1.0 and 0.5 L min^{-1}.

The results of this first set of experiments with horizontal electrode's slots are presented graphically in figures 15 and 16. Figure 15 shows the tracer response for an 8-cell reactor with the slots in horizontal position and a flow rate of 0.5 L min^{-1} through it. Figure 16 shows the results for a similar experiment but with a flow rate of 1.0 l min^{-1} through the reactor. Detailed results are shown in the appendix, tables 4 and 5.

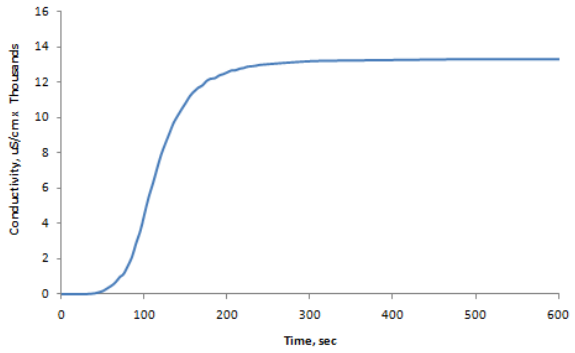

Figure 15. Tracer response curve for an 8-cell reactor with horizontal slots and Q=0.5 L min^{-1}

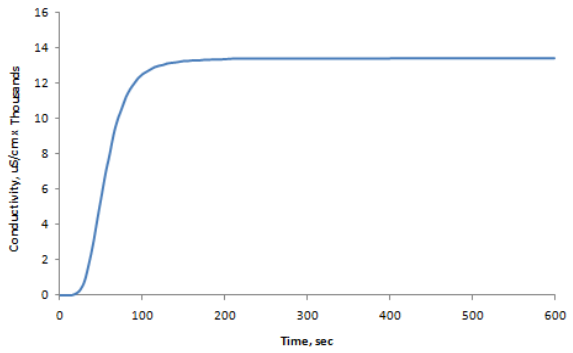

Figure 16. Tracer response curve for an 8-cell reactor with horizontal slots and Q=1.0 L min^{-1}

Similarly, another set of experiments was carried out using the same 8-cell configuration but rotating the electrodes by 90 degrees so that their slots were now oriented vertically. The tracer response was recorded for the 8-cell reactor with vertical slots and flow rate of 0.5 L min^{-1} and 1.0 L min^{-1} and plotted in figures 17 and 18, respectively. Results are summarized in the appendix, tables 6 and 7.

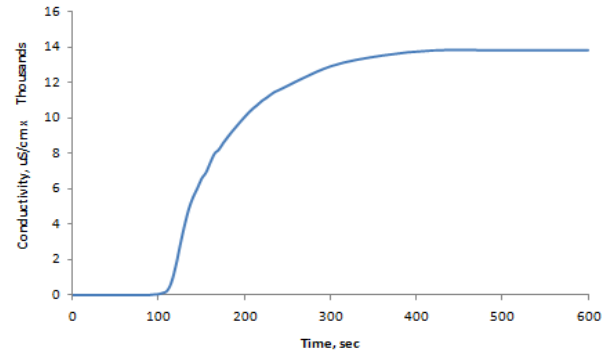

Figure 17. Tracer response curve for an 8-cell reactor with vertical slots and Q=0.5 L min^{-1}

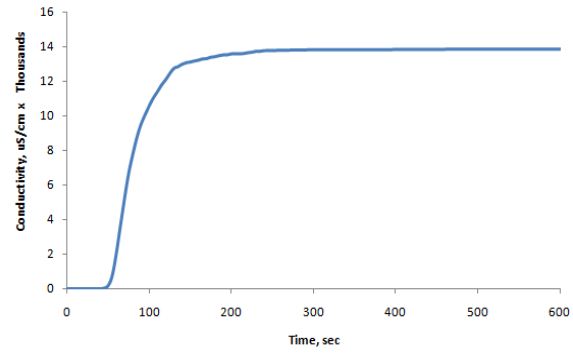

Figure 18. Tracer response curve for an 8-cell reactor with vertical slots and Q=1.0 L min^{-1}

The following group of experiments consisted in performing the same step input test but varying the number of cells from one to eight for a fixed flow rate. For these, the electrode's slots were kept vertically oriented. Figure 19 presents an example of the results obtained from the tracer tests corresponding to a 1-cell through a 4-cell reactor with a flow rate of 1 L min^{-1} through it. Note that the conductivity of *fluid A* and *B* was not the same for all the experiments in this series. Further data manipulation is necessary to be able to compare and analyze these results.

		1 cell	2 cell	3 cell	4 cell
Sample	Time, sec	C, uS/cm	C, uS/cm	C, uS/cm	C, uS/cm
1	0	392	394	411	443
2	5	428	394	411	443
3	10	1144	413	411	443
4	15	1846	618	430	446
5	20	5850	2710	744	451
6	25	9480	5910	1330	595
7	30	11390	8330	3640	1608
8	35	12880	10230	6620	4320
9	40	13550	11580	8910	6590
10	45	13890	12590	10940	8400
11	50	14230	13180	11980	10150
12	55	14380	13580	12830	11240
13	60	14570	13920	13500	12290
14	65	14690	14200	13950	12980
15	70	14730	14390	14190	13500
16	75	14790	14490	14510	13900
17	80	14820	14630	14740	14190
18	85	14870	14670	14860	14370
19	90	14910	14760	14930	14610
20	95	14910	14790	14990	14670
21	100	14960	14820	15080	14800
22	105	14960	14860	15140	14900
23	110	14960	14870	15140	14950
24	115	14960	14920	15170	15010
25	120	14980	14940	15200	15080
26	125	15000	14940	15210	15140
27	130	15020	14940	15220	15220
28	135	15040	14940	15250	15230
29	140		14970	15260	15310
30	145		14980	15280	15310
31	150		14990	15310	15310
32	155		15000	15320	15360
33	160		15020	15330	15360
34	165		15030	15340	15400
35	170		15030	15340	15400
36	175		15040	15350	15430
37	180			15380	15440
38	185			15380	15450
39	190			15380	15450
40	195			15390	15450
41	200			15390	15450
42	205			15390	15460
43	210			15390	15460
44	215			15390	15460
45	220			15390	15460
46	225			15390	15460
47	230			15390	15470
48	235			15390	15490
49	240			15400	15490
50	300			15420	15500
51	360				
52	420				
53	480				
54	540				
55	600				

Figure 19. Example of step input tracer test results for reactor with vertical slots and flow rate of 1.0 L min^{-1}

Complete results are presented in the appendix, tables 4 through 7, along with those obtained for a flow rate of 0.5 L min^{-1}.

2. Electrocoagulation Experiments

A series of electrocoagulation experiments were performed running a constant flow rate of 1 L min^{-1} of the synthetic emulsion described in the previous section through the reactor. Aluminum electrodes with their openings oriented vertically were used as both cathode and anode (the reasons for this configuration are detailed later). For each experiment, 8 L of SE were passes through the reactor, the effluent was collected after 5 min of operation in a clear 2-L capacity container and the final sample was drawn through a valve located at the bottom of the container after a 10-min separation time. Hexane extractable materials or HEM were measured in each sample using method 10056.

As with the step input tracer test, the reactor was fractioned in its individual electrochemical cells so that the effluent could be characterized at different lengths from the reactor's inlet point. Thus, electrocoagulation experiments were run in a 1-cell through an 8-cell reactor. The data obtained from these experiments was recorded as HEM in the effluent vs. number of cells for a given SE composition, flow rate current intensity and applied potential.

Table 1. Electrocoagulation experiments results

Flow rate, l/min	1.00			
Vol/run, l	8.00			
	No of Cells	Potential, volts	Current, amps	CHEM, mg/l
	0	0.0	0.0	583.5
	1	30.7	1.3	420
	2	32.8	2.6	345.6
	3	34.0	4.0	212
	4	33.7	5.4	108.1
	5	33.4	6.7	74.8
	6	33.4	8.0	64.8
	7	34.0	9.3	44.8
	8	34.0	10.8	23.4

Table 1 and figure 20 show the results obtained in electrocoagulation experiments running 1 L min^{-1} of a constant composition influent stream (SE), aluminum electrodes with vertical slots and average applied potential of 33 volts.

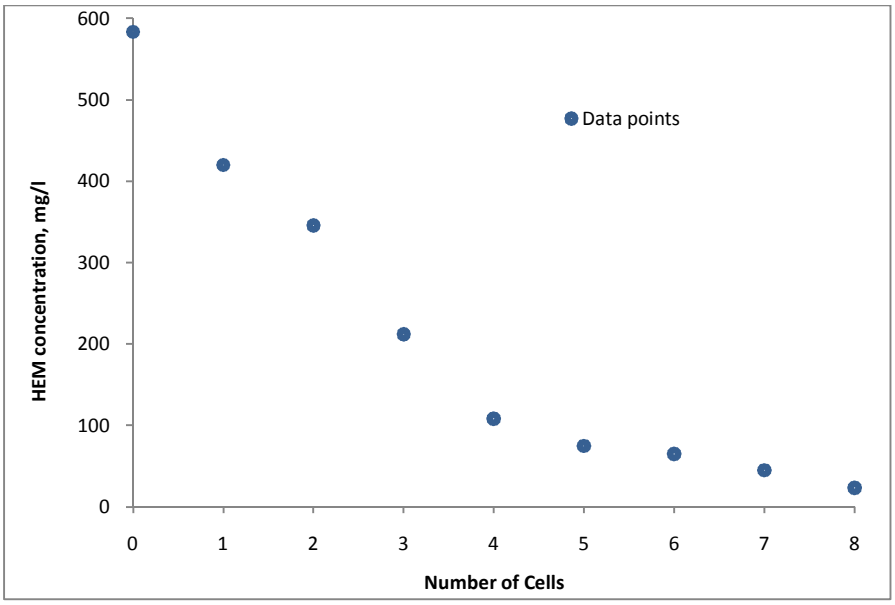

Figure 20. Electrocoagulation experiments shown as HEM vs. number of electrochemical cells.

Processing of this data is presented in the following section and will allow determining the kinetic constant k' for EC under similar operational conditions.

VI. Methodology for Data Processing

The procedure used for analyzing the experimental data followed the order stated in equation 65

$$\text{RTD data} + \text{Kinetics} + \text{Model} = \text{Prediction} \tag{65}$$

First, with the results obtained from the step input tracer test, RTD data was computed. Second, the results from the electrocoagulation experiments were used to confirm the assumed reaction order. Finally, the described non-ideal reactor models are applied to the data generated in the previous two steps. The resulting information is compared to that of ideal plug-flow behavior and will allow predicting the outcome of electrocoagulation treatment under different operational conditions and reactor configuration.

1. RTD Data Calculation

With the data collected from the step input tracer test, the cumulative exit-age distribution function, $F(t)$, is calculated using equation 54

$$F(t) = \frac{C(t)}{C_0} \tag{54}$$

with $C(t)$ being the conductivity of the sample from the reactor's effluent collected at time t and C_0 the conductivity of *fluid B.* $C(t)$ and C_0 have been corrected by subtracting the background conductivity or conductivity of *fluid A.*

Next, by equation 56, the exit-age distribution function, $E(t)$, is determined for each $F(t)$.

$$E(t) = \frac{\mathrm{d}F(t)}{\mathrm{d}t} \tag{56}$$

Once $E(t)$ has been obtained, the first moment of $E(t)$ or average residence time, τ can be calculated by graphical integration of equation 59.

$$\tau = \int_0^\infty tE(t)\mathrm{d}t \tag{59}$$

The upper limit of the integral in equation 59 is determined through equation 52. This is the time t in which the conductivity of the reactor's effluent equals that of *fluid B* and the tracer test ends.

$$\int_0^\infty E(t)\mathrm{d}t = 1 \tag{52}$$

Now, in a similar way, the second moment of $E(t)$ or variance can be found by integrating equation 61,

$$\sigma^2 = \int_0^\infty (t-\bar{t})^2 E(t)\mathrm{d}t \tag{61}$$

Also, and in order to be able to compare results from tracer tests corresponding to different reactor configurations, we can normalize the RTD data by means of equation 63 and 64 finding the dimensionless parameter Θ and dimensionless function $E(\Theta)$, respectively.

$$\Theta \equiv \frac{t}{\tau} \tag{63}$$

$$E(\Theta) \equiv \tau E(t) \tag{64}$$

A plot showing $E(\Theta)$ vs. Θ represents a useful tool for diagnosing reactor's performance and identifying deviations from ideal flow behavior.

Detailed results of RTD calculation for each of the reactor configurations examined is presented in Appendix A table A.1 through A.4.

Finally, the actual reactor volume is determined from the following equation

$$V_R = \tau Q \tag{85}$$

This volume is an important outcome from the tracer test because when compared to the maximum reactor volume, V_M, it shows the fraction of the reactor volume that is either empty or contains stagnant fluid (fluid not participating in the reaction). This is called the dead volume or V_D.

The average cell volume is then calculated by equation 83.

$$V_{CELL} = \frac{V_R}{2 + n_{CELL}} \tag{83}$$

Knowing the reactor volume, the reactor's characteristic length, L, is found with equation 84,

$$L = \frac{V_R}{A_F} \tag{84}$$

and the mean fluid velocity (in the direction of flow) in m s^{-1} using

$$v = \frac{L}{\tau} \tag{86}$$

Since the calculated characteristic length gives an indication of the effective distance traveled by any particle inside the reactor, it is feasible define the effective electrode area, A_E, as the electrode surface exposed to the fluid along the reactor. This area is of importance because it accounts for dead volume or empty space in the electrochemical PFR. Thus, assuming that the cell width, W, remains constant

$$A_E = \frac{LW}{2n_{CELL}} \tag{87}$$

A summary of these results is presented in Appendix A, table A.5 through A.8.

2. Reaction Rate Calculation

Using the data obtained from the electrocoagulation experiments, the integral method of analysis as described in section 2.2 is used herein for determining the reaction order and the kinetic constant k' for the reactor.

Assuming that the electrocoagulation of oil and grease is a first-order reaction process, and that the reactor behaves as an ideal PFR, according to equation 47, the points resulting from plotting the $\ln\left(C_{HEM,L}/C_{HEM,0}\right)$ vs. τ should fit a straight line which slope yields k'. The HEM concentration in the influent SE and the effluent samples have been measured as explained earlier and the average residence time, τ, have also been calculated from the RTD data.

$$\ln\left(\frac{C_{HEM,L}}{C_{HEM,0}}\right) = \ln\left(1 - x_{HEM}\right) = -k'\tau \tag{47}$$

A trendline through the data points was drawn using MS Excel. The values of slope, intercept with the ordinate and R^2 were found also with the same tool and are presented in the following section.

3. Reactor Modeling

In this section, both the data obtained from the step input tracer tests and the electrocoagulation experiments are correlated through non-ideal models in order to account for deviations from ideal flow and also be able to predict conversion under conditions distinct to the experimental ones. Results from applying the dispersion model and the tanks-in-series model are obtained and compared next.

For using the dispersion model, equation 76 has to be solved by non-linear regression to adjust the kinetic and RTD data.

$$\frac{C_{HEM,L}}{C_{HEM,0}} = \left(1 - x_{HEM}\right) = \frac{4q\exp(Pe/2)}{(1+q)^2\exp(qPe/2) - (1-q)^2\exp(-qPe/2)} \tag{76}$$

This was accomplished using the DataFit® software. Detailed results are presented in the appendix, table 12 and figure 30.

The Peclet number used in the dispersion model was calculated through equation 78 and corresponds to the for the 8-cell reactor. This approach is valid if similar hydraulic behavior of the fluid in each reactor cell is assumed.

$$\frac{\sigma^2}{\tau^2} = \frac{2}{Pe} - \frac{2}{Pe^2}\left[1 - \exp\left(-Pe\right)\right] \tag{78}$$

Finally, the RTD data is used to calculate the number of tanks in series according to equation 81

$$n = \frac{\tau^2}{\sigma^2} \tag{81}$$

and, as with the dispersion model, equation 82 is adjusted by non-linear regression to fit the experimental data and to determine the value of k' that satisfies the TIS model,

$$\frac{C_{HEM,L}}{C_{HEM,0}} = \left(1 - x_{HEM}\right) = 1 - \frac{1}{\left(1 + \frac{\tau k'}{n}\right)^n} \tag{82}$$

Detailed results are included in the appendix, table 13 and figure 31.

VII. Data Analysis and Results

1. RTD Data Analysis

The RTD data obtained from the step input tracer tests were used to identify the effect of electrode's slots orientation and volumetric flow rate on the reactor performance.

Plots of the dimensionless average residence time ($E(\Theta)$ vs. Θ) are useful for showing deviations from ideal plug-flow. In order to be able to sight such deviations, the generated RTD data is presented in the following set of figures as a tool for comparing how the slot orientation and volumetric flow rate influence the reactor's behavior. This side-by-side comparison indicates not only that our reactor does not behave as an ideal PFR but also that it is sensible to changes in its electrodes configuration and rate of flow.

Figure 21 and 22 show the $E(\Theta)$ vs. Θ curves obtained for different slot orientation at the same flow rate in an 8-cell reactor.

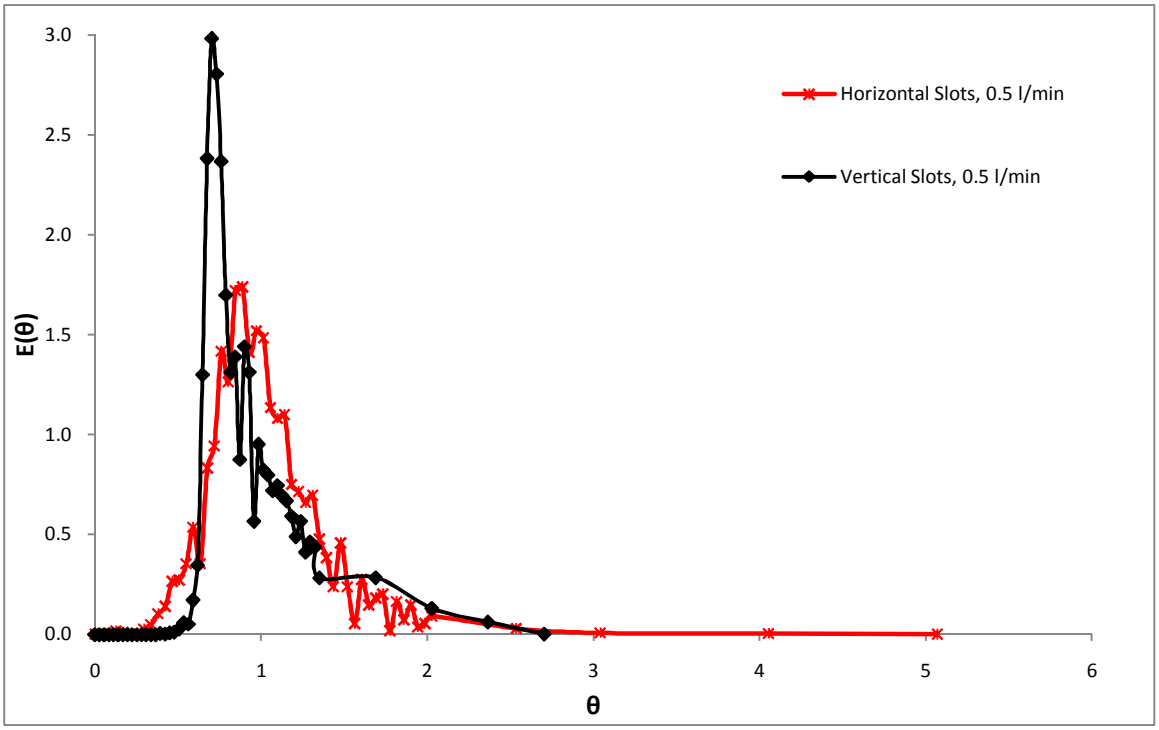

Figure 21. Comparison of the effect of slot orientation on RTD curves for an 8-cell reactor at Q= 0.5 L min^{-1}.

For both 0.5 L min^{-1} and 1.0 L min^{-1}, positioning the electrodes so that their openings were vertically oriented, produced a narrower peak. This is an indication of the fluid approximating plug-flow behavior under this plate arrangement. However, in the case of the lower flow rate and vertical slots, the sharpness of the peak and its earliness with respect to the mean residence time suggest some short-circuiting from inlet to outlet due to stagnant water. With horizontal slots the curve is more symmetrical but with several decaying peaks along the tail suggesting the occurrence of internal recirculation. At 1 L min $^{-1}$, having the slots oriented horizontally and forcing the fluid to follow a vertical upward-downward path makes the curve to spread out over the dimensionless time scale, which translates as slow internal circulation of the fluid.

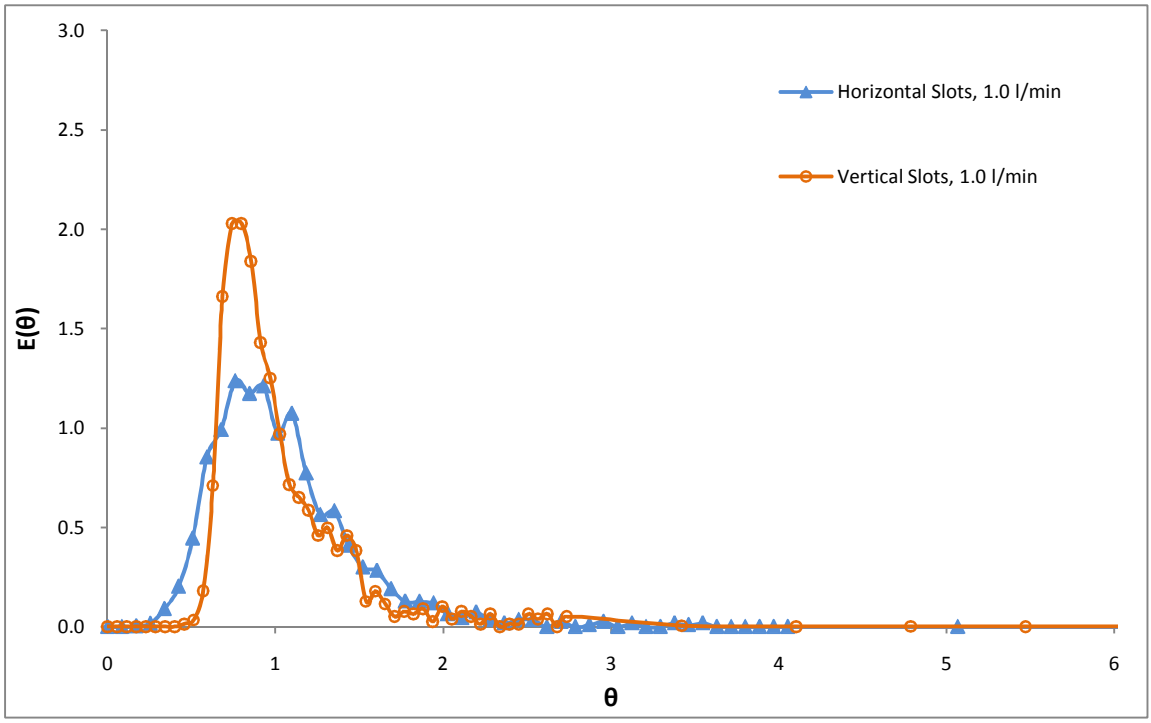

Figure 22. Comparison of the effect of slot orientation on RTD curves for an 8-cell reactor at Q= 1.0 L min^{-1}.

Figures 23 and 24 show a comparison of the $E(\Theta)$ vs. Θ curves for the same slot orientation and different rates of flow.

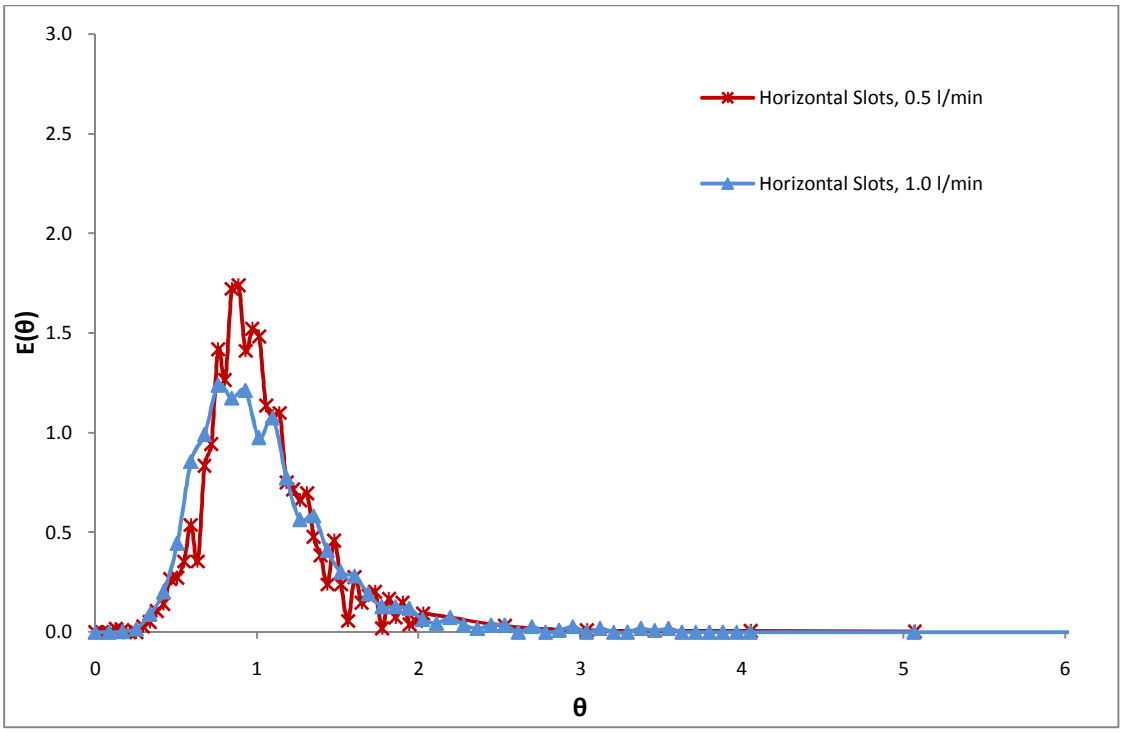

Figure 23. Comparison of the effect of volumetric flow rate on RTD curves for an 8-cell reactor with horizontal slots.

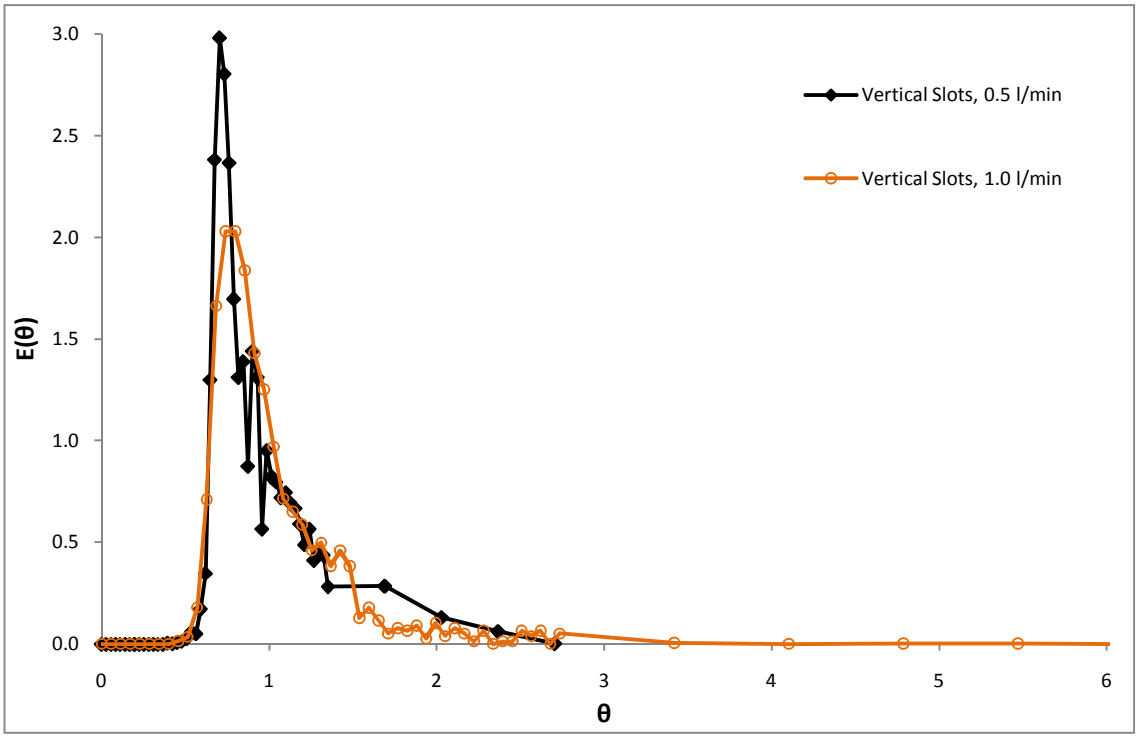

Figure 24. Comparison of the effect of volumetric flow rate on RTD curves for an 8-cell reactor with vertical slots.

These curves show the effect of flow rate variation on the reactors RTDs. For both slot orientations, having the fluid flowing at the lower velocity generates a narrower curve but also increases the amount and frequency of decaying peaks. Therefore, a flow rate of 0.5 L min^{-1} seems to generate problems of internal recirculation probably associated with the low speed of the fluid through the reactor. A wider curve symmetrical to the mean detention time is common for both fluid velocities when the slots are horizontal but even for the higher velocity, internal recirculation remains an issue.

If the reactor is operated with the slots in vertical position, the horizontal path of flow imposed to the fluid causes little fluid stagnation indicated by the early mean but it also minimizes internal recirculation and improves the overall flow behavior, especially at higher velocities. This is observed in the curve for vertical slots and 1.0 L min^{-1} in figure 24, which is nicely shaped and exhibits few signs of plug flow misbehavior.

Table 2 summarizes the calculated RTD parameters, which are presented in detail in the appendix, tables 8 through 11. These results clearly indicate that the plate's slot orientation has a significant effect on the overall performance of this reactor. In general, by orienting the electrodes' openings vertically, the reactor's average residence time increases by 50% as compared to having the slots oriented horizontally. This effect will be exacerbated by the accumulation of electro-generated gas at the top of the cells when the slots are horizontal. Similar behavior was observed for both fluid velocities.

Table 2. Summary of RTD results for the 8-cell reactor operated under different configurations and volumetric flow rates.

Flow rate, l/min	0.5		1.0	
Slot orientation	Horizontal	Vertical	Horizontal	Vertical
Avg. res. time, s	90.9	140.3	46.4	69.9
Actual volume, ml	946.8	1449.8	967.4	1433.2
Avg. Cell Vol, ml	94.7	146.1	96.7	145.6
Cell avg. det. time, s	11.4	17.5	5.8	8.7
Reactor L, m	1.50	2.38	1.53	2.22
Mean Fluid Velocity, m/s	0.016	0.017	0.032	0.032
Effective Electrode Area, m^2	0.0095	0.0150	0.0097	0.0140
Peclet number	21.6	15.7	15.3	15.1

A larger τ translates into a larger effective volume, characteristic reactor's length and ultimately a bigger effective electrode area, which means higher treatment efficiency. This is equivalent to add additional cells to the same reactor with horizontal slots.

In this bench-scale reactor, the upward-downward path of flow resulting from plate's slots horizontally oriented causes a significant loss of reactive volume. This lost or dead volume may be occupied by stagnant fluid or gas and remains as empty pockets along the reactor and throughout the entire operation.

The Peclet number, which gives an indication of the amount of dispersion, does not vary importantly among the explored configurations, but the lowest value resulted when operating the reactor with vertical slots and 1.0 L min^{-1}. Electrocoagulation experiments and subsequent results were obtained for this configuration.

2. Electrocoagulation Kinetics

The results from the electrocoagulation experiments presented previously along with the average residence times calculated from the tracer tests for 1-cell through 8-cell reactors with plate's openings oriented vertically are shown in table 3.

Table 3. Electrocoagulation experiments and RTD results as used for verification of reaction order

No of Cells	CHEM, mg/l	τ, sec	Δτ, sec	τcorr., sec	CHEM/CHEM,0	ln(CHEM/CHEM,0)	xHEM
0	583.5	0.0	0.0	0.0	1.00	0.00	0.00
1	420	28.0	28.0	9.3	0.72	-0.33	0.28
2	345.6	35.5	7.5	16.8	0.59	-0.52	0.41
3	212	44.9	9.4	26.2	0.36	-1.01	0.64
4	108.1	52.4	7.5	33.7	0.19	-1.69	0.81
5	74.8	60.1	7.7	41.4	0.13	-2.05	0.87
6	64.8	70.4	10.3	51.7	0.11	-2.20	0.89
7	44.8	79.1	8.7	60.4	0.08	-2.57	0.92
8	23.4	87.8	8.7	69.1	0.04	-3.22	0.96

The data points and the trendline through them were drawn on a $\ln\left(C_{HEM,L}/C_{HEM,0}\right)$ vs. τ plot and are presented in figure 25.

This result confirms that the electrocoagulation of the HEM in the synthetic emulsion follows first-order reaction kinetics and, under the present operational conditions, assuming ideal plug-flow reactor behavior, the kinetic constant, k', is $0.0447\ s^{-1}$. R^2 for the linear regression is 0.979.

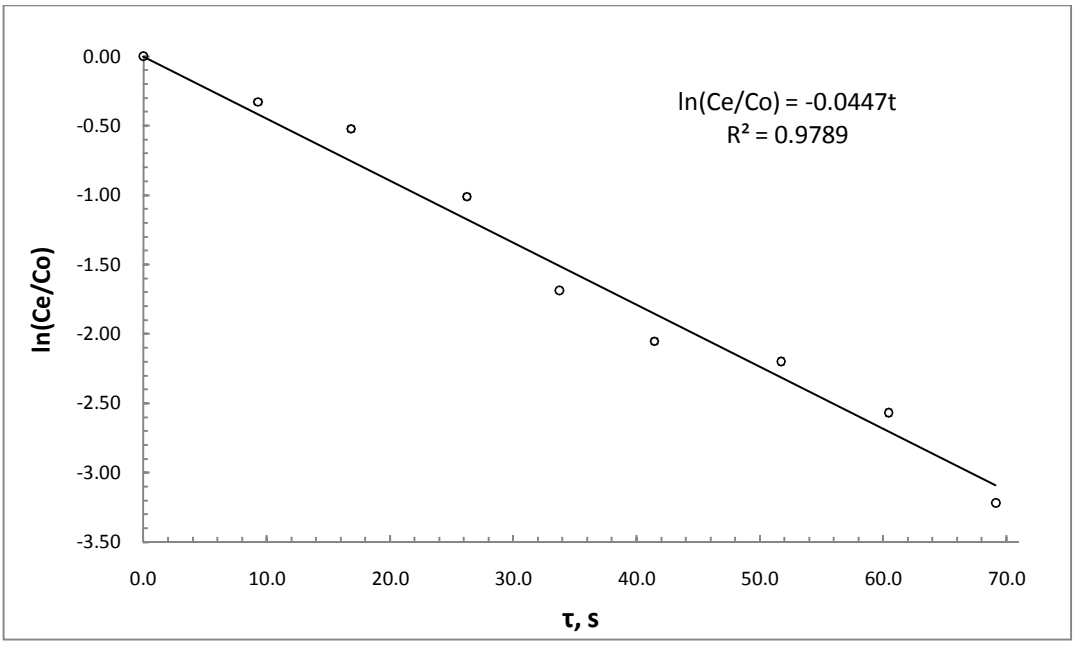

Figure 25. Data points fitting by linear regression using ideal PFR first-order kinetics

3. Reactor Modeling

From the previous result, the design equation for the EC reactor assuming ideal plug-flow behavior is

$$\frac{C_{HEM,L}}{C_{HEM,0}} = \exp\left(-0.0447\tau\right) \tag{88}$$

Figure 26 shows the $C_{HEM,L}/C_{HEM,0}$ vs. $k'\tau$ plot for equation 88.

Non-linear regression of the expression for the dispersion model for a first-order reaction in a closed vessel as presented in equation 76 yields a kinetic constant $k' = 0.0441\ \text{s}^{-1}$ with a R^2 of 0.974.

Calculation of the number of complete mixed reactor in series, n, according to equation 81, resulted in $n = 8.1$. Applying the TIS model equation to the experimental data and using this value of n resulted in a kinetic constant $k' = 0.0443\ \text{s}^{-1}$ with a R^2 of 0.97.

The design equation based on the dispersion model is

$$\frac{C_{HEM,L}}{C_{HEM,0}} = \frac{30.2\sqrt{1+0.012\tau}}{\left(1+\sqrt{1+0.012\tau}\right)^2 \exp\left(7.55\sqrt{1+0.012\tau}\right) - \left(1-\sqrt{1+0.012\tau}\right)^2 \exp\left(-7.55\sqrt{1+0.012\tau}\right)} \tag{89}$$

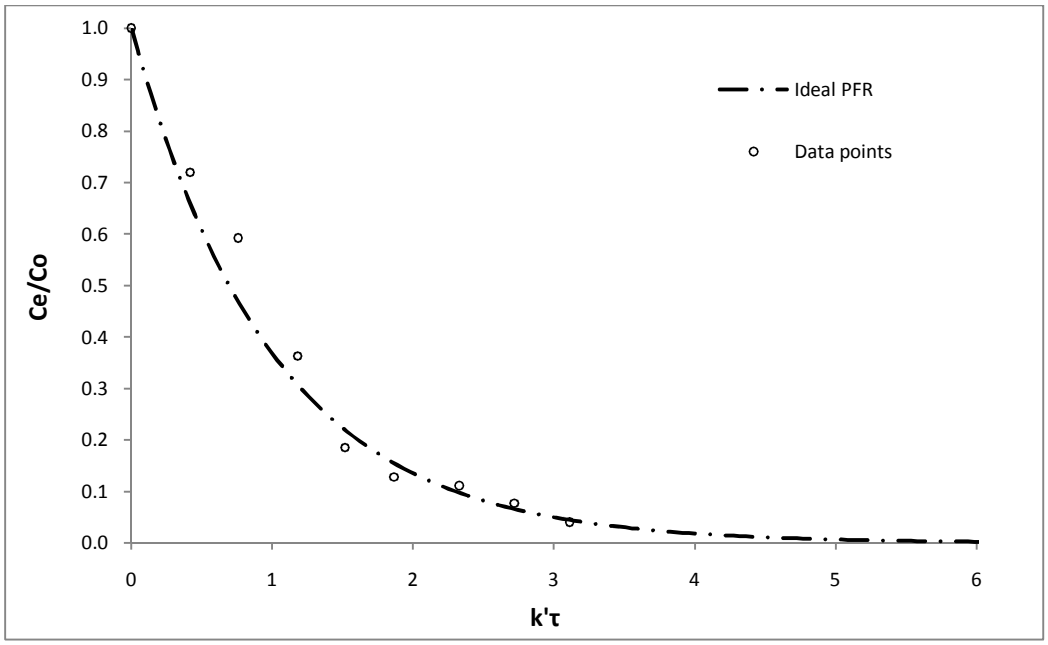

Figure 26. $C_{HEM,L}/C_{HEM,0}$ vs. $k'\tau$ curve for ideal PFR

and figure 27 presents the corresponding $C_{HEM,L}/C_{HEM,0}$ vs. $k'\tau$ plot.

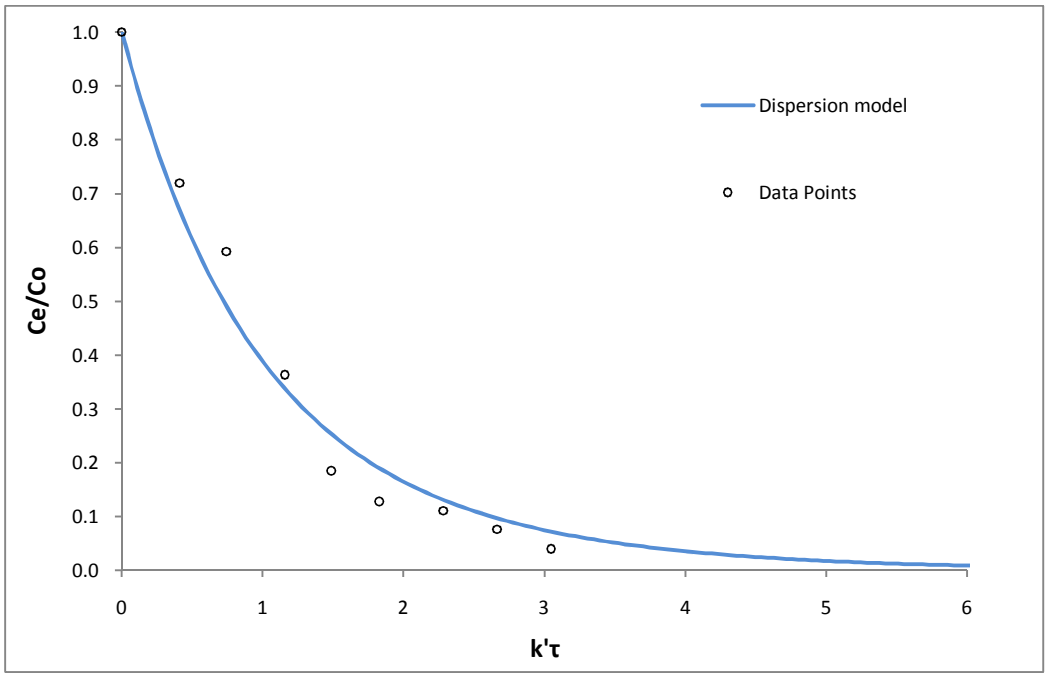

Figure 27. $C_{HEM,L}/C_{HEM,0}$ vs. $k'\tau$ curve for dispersion model

The TIS model, given for this reactor by design equation 90, is presented graphically in figure 28.

$$\frac{C_{HEM,L}}{C_{HEM,0}} = \frac{1}{(1+0.0055\tau)^8} \tag{90}$$

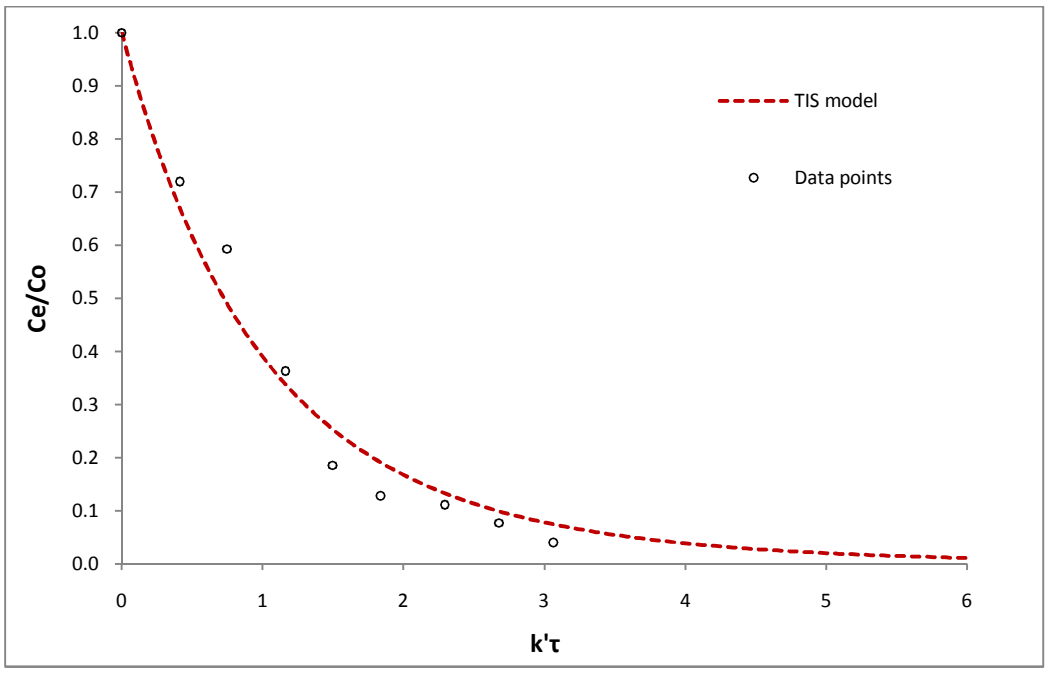

Figure 28. $C_{HEM,L}/C_{HEM,0}$ vs. $k'\tau$ curve for TIS model

Figure 29 shows the $C_{HEM,L}/C_{HEM,0}$ vs. τ curves for the ideal PFR and the two non-ideal plug-flow models studied. The dispersion and TIS models show very good agreement and both curves practically overlap each other. This is a reasonable result since the number of tanks in series obtained for the latter coincided with the number of cells in the 8-cell reactor, which confirms that assuming TIS behavior is valid whenever the dispersion model applies and for reactors with small deviations from plug flow, as is the case of the reactor being tested. This means that each individual cell of the 8-cell reactor behaves as an independent CSTR, and, consequently, both models can be used interchangeably since they yield similar conversion efficiency.

Another indication of the quasi-ideal flow pattern in the experimental EC reactor with vertical slots is the proximity of both non-ideal models' curves to the ideal PFR curve. As expected though, assuming ideal behavior yields higher conversion rate for the same reactor volume, as can be derived from figure 29. Such "more-optimistic" performance described by the ideal PFR equation does not take

into consideration the anomalies that occur in a real reactor operation, therefore, other than for comparison purposes, it has no validity in reactor modeling.

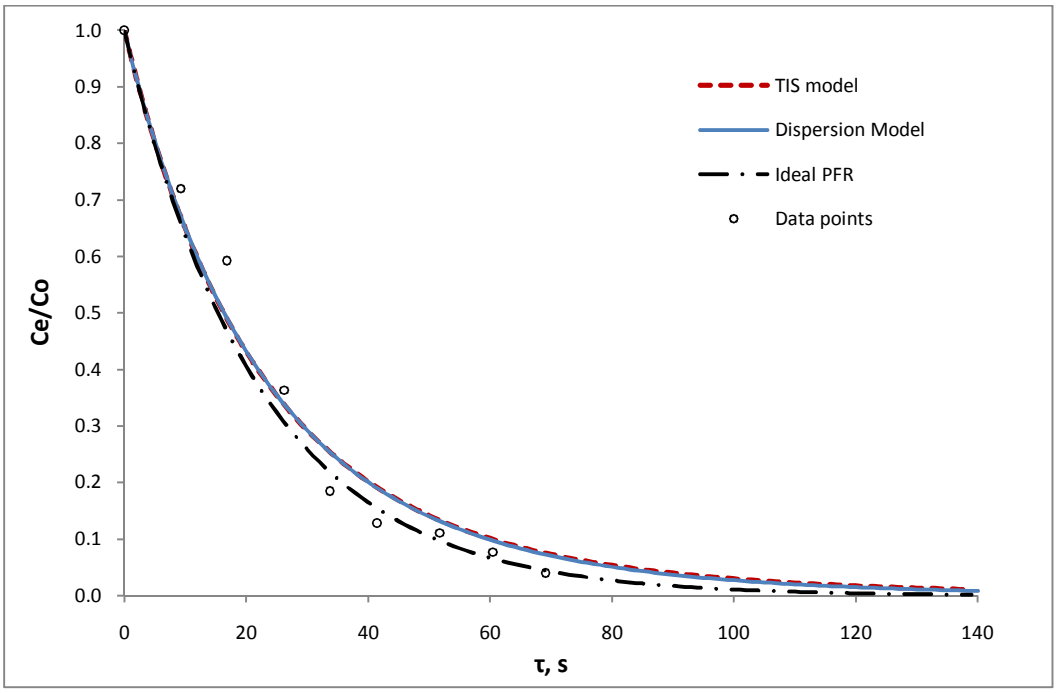

Figure 29. Comparison of $C_{HEM,L}/C_{HEM,0}$ vs τ curves for different kinetic models applied to the experimental data

Regarding the effect of electrode's slot orientation on conversion efficiency, rotating the electrodes may increase the average retention time from 46 s for horizontally oriented slots to 70 s for vertically oriented electrodes in an 8-cell reactor, as shown in table 2, and according to figure 29 this would represent a change of the $C_{HEM,L}/C_{HEM,0}$ fraction from 0.16 to 0.07, i.e., a boost in the conversion efficiency of 14%.

These estimations are based on the RTD data obtained from the step input tracer tests performed using a high conductivity brine. The increased density of the tracer fluid (from 997 kg m^{-3} for tap water at 20 °C to approximately 1004 Kg m^{-3} for brine with conductivity of 14000 µS cm^{-1}) could promote the formation of density currents inside the reactor, favoring the horizontal path of flow over the vertical one. However, considering the small cell volume and the high operating pressure of the reactor, these density effects may be overcome by turbulence and mixing, as suggested by the TIS model, which indicates that the EC reactor behaves as 8 individual CSTRs.

VIII. Conclusions and Recommendations

1. Conclusions

- Tracer tests performed on the electrocoagulation reactor indicated the possibility of abnormal internal flow patterns of fluids throughout the reactor. These anomalies were manifested in the form of internal recirculation and pockets of stagnant fluid or gas that originate dead volume and shortcircuiting.
- Rotation of the electrode plates by 90 degrees so that the electrode's opening change orientation from horizontal to vertical and the fluid through the reactor follows a vertical path instead of horizontal, could have a quantifiable effect on the reactor's performance.
- Stagnant water is the main problem observed in the operation with horizontally oriented slots. It was shortcircuiting in the case of slots oriented vertically. In each case, these problems were increased when the fluid velocity through the reactor was decreased under 0.032 m s^{-1}.
- Having the electrode's slot oriented vertically instead of horizontally may increase the reactor average detention time up to 50% and the HEM removal efficiency up to 14%.
- Though flow pattern in the reactor is not ideal, the magnitude of longitudinal dispersion is low.
- Electrocoagulation with aluminum electrodes is effective for HEM removal from stable emulsions and follows first-order reaction kinetics.
- Both the dispersion model and the tanks-in-series model correlate the experimental data very well, yielding a R^2 of approximately 0.97. The calculated kinetic constant based on the dispersion model was $k' = 0.0441\ s^{-1}$ and according to the TIS mode, it was $k' = 0.0443\ s^{-1}$. However, the TIS model is preferred over the dispersion model for it offers a simpler approach to modeling this type of reactors.

2. Recommendations

- Based on the results of this research, it is recommended to perform a more extensive study on the kinetics of the electrocoagulation of HEM under different operational conditions. Electrocoagulation experiments similar to the ones carried out for this research should be done over a wider range of flow rates and HEM concentrations. EC efficiency under different current intensities and electrode materials is also an aspect of this process requiring further investigation.

- For better performance and HEM removal efficiency, this reactor should be operated with the fluid flowing at a velocity higher than 0.032 m s^{-1} and following a horizontal path (slots oriented vertically).
- If the reactor is to be operated under any configuration different to the ones examined in this research, a tracer test must be performed in order to identify potential anomalies in flow pattern behavior.

IX. References

Andrade, M. “Heavy metal removal from bilge water by electrocoagulation treatment, A thesis”. University of New Orleans, December, 2009.

Bensadok, K., S. Benammar, F. Lapicque, and G. Nezzal. "Electrocoagulation of cutting oil emulsions using aluminium plate electrodes." *Journal of Hazardous Materials* 152, no. 1 (2008): 423-430.

Canizares, P., Jimenez, C., Martinez, F., Rodrigo, M., and Saez, C. “The pH as a key parameter in the choice between coagulation and electrocoagulation for the treatment of wastewaters.” *Journal of Hazardous Materials* 163 (2009): 158-164.

Canizares, P., Jimenez, C., Martinez, F., Saez, C., and Rodrigo, M. “Study of the electrocoagulation process using aluminum and iron electrodes.” *Industrial and Engineering Chemistry Research* 46 (2007): 6189-6195.

Canizares, P., Martinez, F., Lobato, J., and Rodrigo M. “Break-up of oil-in-water emulsions by electrochemical techniques.” *Journal of Hazardous Materials* 145 (2007): 233-240.

Chen, G., and Hung, Y. Electrochemical Wastewater Treatment Processes. From *Handbook of Environmental Engineering, Volume 5: Advaqnced Physicochemical Treatment Technologies*, Chapter 2. Wang, L., Hung, Y., and Shammas, N. (eds.), Humana Press, 2007.

Chen, Guohua. "Electrochemical technologies in wastewater treatment." *Separation and Purification Techonology* (Elsevier B.V.) 38, no. 1 (2004): 11-41.

Chen, X. M., G. Chen, and P.L. Yue. "Separation of pollutants from restaurant wastewater by electrocoagulation." *Separation and Purification Technology* (Elsevier Science) 19, no. 1-2 (2000): 65-76.

Chen, Xueming, Guohua Chen, and Po Lock Yue. "Electrocoagulation and electroflotation of restaurant wastewater." *Journal of Environmental Engineering* (ASCE) 126, no. 9 (September 2000): 858-863.

Chen, Xueming, Guohua Chen, and Po Lock Yue. "Investigation on the electrolysis voltage of electrocoagulation." *Chemical Engineering Sciences* (Elsevier) 57, no. 13 (July 2002): 2449-2455.

Donini, J., Kan, J., Szynkarczuk, J., Hassan, T., and Kar, K. “The operating cost of electrocoagulation.” *The Canadian Journal of Chemical Engineering* 72 (1994): 1007-1012.

Fogler, H. Scott. *Elements of Chemical Reaction Engineering*. Fourth Edition. Prentice Hall, 2006.

Gavrel et al. “High pressure process and apparatus for the electrocoagulative treatment of aqueous and viscous fluids”. *United States Patent No.: 7,087,176 B2,* August 8, 2006.

Haas, C., Joffe, J., Heath, M., and Jacangelo, J. “Continuous flow residence time distribution function characterization”. *Journal of Environmental Engineering* 123, no. 2 (1997): 107-114.

Holt, P., Barton, G., and Mitchell, C. “The future for electrocoagulation as a localized water treatment technology.” *Chemosphere* 59 (2005): 355-367.

Holt, P., Barton, G., Wark, M., and Mitchell, C., “A quantitative comparison between chemical dosing and electrocoagulation.” *Colloids and Surfaces A: Physicochemical and Engineering Aspects*211 (2002): 233-248.

Jia qian, J. “An anodic passivation of electrocoagulator in the process of water treatment.” *Water Treatment* 3 (1988): 344-352.

Jiang, J., Graham, N., Andre, C., Kelsall, G., and Brandon, N. “Laboratory study of electrocoagulation-flotation for water treatment.” *Water Research* 36 (2002): 4064-4078.

Kobya, Mehmet, Orhan Taner Can, and Mahmut Bayramoglu. "Treatment of textile wastewaters by electrocoagulation using iron and aluminum electrodes." *Journal of Hazardous Materials* (Elsevier Science B.V.) 100, no. 1-3 (June 2003): 163-178.

Kura, B., La Motta, E., Tittlebaum, M., and Alawady, M., “Macroscopic BOD kinetic model for microbial rock plant filter design.” Advances in Environmental Research 1 (1997): 36-43.

Levenspiel, Octave. *Chemical Reaction Engineering*, Third Edition. John Wiley & Sons, 1999.

Liu, H., Zhao, X., and Qu, J. “Electrocoagulation in Water Treatment.” From: *Electrochemistry for the Environment*, Chapter 10. Comninellis, C and Chen, G. (eds.), Springer, 2010.

MARPOL. "International convention for the prevention of the pollution from the ships." International Maritime Organization, London, 1973.

Matteson, M., Dobson, R., Glenn, R., Kukunoor, N., Waits, W., and Clayfield, E. “Electrocoagulation and separation of aqueous suspensions of ultrafine particles”. *Colloids and Surfaces A: Physicochemical and Engineering Aspects* 104 (1995):101-109.

Mollah, Mohammad Y.A., Paul Morkovsky, Jewel A.G. Gomes, Mehmet Kesmez, José Parga, and David L. Cocke. "Fundamentals, present and future perspectives of electrocoagulation." *Journal of Hazardous Materials* (Elesevier Scientific Pub. Co.) 114, no. 1-3 (2004): 199-210.

Moreno, Hector A., et al. "Electrochemical Reactions for Electrocoagulation Using Iron Electrodes." *Industrial & Engineering Chemistry Research* 48, no. 4 (2009): 2275-2282.

Nahui, F.N.B., et al. ' Electroflotation of Emulsified Oil in Industrial Wasted Evaluated with a Full Factorial Design". *Brazilian Journal of Chemical Engineering* 25, no. 03 (2008)

Ogutveren, Ulker Bakir, and Savas Koparal. "Electrocoagulation for oil-water emulsion treatment." *Journal of Environmental Science and Health* 32, no. 9 & 10 (1997): 2507-2520.

Oldham, Heith B., and Jan C. Myland. *Fundamentals of Electrochemical Science.* Peterborough, Ontario: Academic Press, Inc, 1994.

Picard, T., Cathalifaud-Feuillade, G., Mazet, M., and Vandensteendam, C. “Cathodic dissolution in the electrocoagulation process using aluminum electrodes.” *Journal of Environmental Monitoring* 2 (2000): 77-80.

Rajeshwar, K., and Ibanez, J. *Environmental Electrochemistry, Fundamentals and Applications in Pollution Abatement*, Academic Press, 1997.

Roberts, George. *Chemical Reactions and Chemical Reactors*. John Wiley & Sons, 2009.

Trinidad, P., and Walsh, F. “Conversion expressions for electrochemical reactors which operate under mass transport controlled reaction conditions, part I: batch reactor, PFR and CSTR.” *International Journal of Engineering Education* 14, no. 6 (1998): 431-441.

U.S. Environmental Protection Agency. "Cruise ship discharge assessment report." Oceans and Coastal Protection Division. Office of Wetlands, Oceans, and Watersheds, U.S. Environmental Protection Agency (EPA), USA, 2008.

Vik, E., Carlson, D., Eikun, A., and Gjessing, E. “Electrocoagulation of potable water.” *Water Research* 18 (1984):1355-1360.

Walsh, F. “ Electrochemical technology for environmental treatment and clean energy conversion.” *Pure and Applied Chemistry* 73, no. 12 (2001): 1819-1837.

Wehner, J., and Wilhelm, R. “Boundary conditions of flow reactor.” *Chemical Engineering Science* 6 (1956): 89-93.

Wong, H., Shang, C., Cheung, Y., and Chen, G. “Chloride assisted electrochemical disinfection.” *Proceedings of the Eighth Mainland-Taiwan Environmental Protection Conference*, 2002.

Yang, Chen-Lu. "Electrochemical coagulation for oily water demulsification." *Separation and Purification Technology* 54 (2007): 388-395.

Yousuf, M., Schennach, R., Parga, J., and Cocke, D. “Electrocoagulation (EC)-science and applications.” *Journal of Hazardous Materials* B84 (2001): 29-41.

X. Appendix

Table 4. Step input tracer test results for an 8-cell reactor with horizontal slots and Q=1 l min^{-1}

	8 cells (Horizontal slots)													
Flow rate, L/min	0.98													
C back, uS/cm	397													
Co, uS/cm	13413													
Mean det. time, sec	59.23													
Actual volume, ml	967.40													
Sample	Time, sec	C, uS/cm	C corr, uS/cm	F(t)	E(t)	Partial E(t)	Cum. E(t)	tE(t)	Partial tE(t)	Cum. tE(t)	θ	E(θ)	(t−τ)*E(t)	Partial (t−τ)*E(t)	Cum. (t−τ)*E(t)=σ²
1	0	397	0	0.00000	0.00000	0.00000	0.00000	0.00000	0.00000	0.00000	0.00000	0.00000	0.00000	0.00000	0.00000
2	5	397	0	0.00000	0.00000	0.00000	0.00000	0.00000	0.00000	0.00000	0.08442	0.00000	0.00000	0.00000	0.00000
3	10	402	5	0.00038	0.00008	0.00019	0.00019	0.00077	0.00192	0.00192	0.16884	0.00455	0.18619	0.46548	0.46548
4	15	420	23	0.00177	0.00028	0.00088	0.00108	0.00415	0.01229	0.01421	0.25326	0.01638	0.54104	1.81809	2.28356
5	20	520	123	0.00945	0.00154	0.00453	0.00561	0.03073	0.08720	0.10141	0.33767	0.09101	2.36461	7.26413	9.54769
6	25	742	345	0.02651	0.00341	0.01237	0.01798	0.08528	0.29003	0.39144	0.42209	0.20204	3.99655	15.90288	25.45057
7	30	1232	835	0.06415	0.00753	0.02735	0.04533	0.22588	0.77789	1.16933	0.50651	0.44594	6.43229	26.07210	51.52267
8	35	2171	1774	0.13629	0.01443	0.05489	0.10022	0.50499	1.82717	2.99650	0.59093	0.85457	8.46986	37.25538	88.77805
9	40	3260	2863	0.21996	0.01673	0.07790	0.17813	0.66933	2.93581	5.93231	0.67535	0.99109	6.18696	36.64206	125.42010
10	45	4620	4223	0.32445	0.02090	0.09408	0.27220	0.94038	4.02428	9.95659	0.75977	1.23772	4.23076	26.04431	151.46441
11	50	5910	5513	0.42356	0.01982	0.10180	0.37400	0.99109	4.82867	14.78526	0.84419	1.17402	1.68818	14.79734	166.26174
12	55	7240	6843	0.52574	0.02044	0.10065	0.47465	1.12400	5.28772	20.07299	0.92860	1.21042	0.36543	5.13402	171.39576
13	60	8310	7913	0.60794	0.01644	0.09219	0.56684	0.98648	5.27620	25.34919	1.01302	0.97380	0.00978	0.93803	172.33380
14	65	9490	9093	0.69860	0.01813	0.08643	0.65327	1.17855	5.41257	30.76175	1.09744	1.07391	0.60394	1.53429	173.86809
15	70	10340	9943	0.76391	0.01306	0.07798	0.73125	0.91426	5.23202	35.99378	1.18186	0.77358	1.51535	5.29821	179.16630
16	75	10960	10563	0.81154	0.00953	0.05647	0.78772	0.71451	4.07191	40.06569	1.26628	0.56426	2.36964	9.71247	188.87877
17	80	11600	11203	0.86071	0.00983	0.04840	0.83612	0.78672	3.75307	43.81876	1.35070	0.58246	4.24289	16.53134	205.41010
18	85	12050	11653	0.89528	0.00691	0.04187	0.87800	0.58774	3.43616	47.25492	1.43512	0.40954	4.59240	22.08823	227.49834
19	90	12380	11983	0.92064	0.00507	0.02996	0.90796	0.45636	2.61025	49.86517	1.51954	0.30033	4.80131	23.48427	250.98261
20	95	12690	12293	0.94445	0.00476	0.02459	0.93254	0.45252	2.27220	52.13737	1.60395	0.28213	6.09516	27.24117	278.22378
21	100	12900	12503	0.96059	0.00323	0.01998	0.95252	0.32268	1.93800	54.07537	1.68837	0.19112	5.36392	28.64769	306.87147
22	105	13040	12643	0.97134	0.00215	0.01344	0.96596	0.22588	1.37139	55.44676	1.77279	0.12741	4.50680	24.67679	331.54826
23	110	13180	12783	0.98210	0.00215	0.01076	0.97672	0.23663	1.15627	56.60303	1.85721	0.12741	5.54521	25.13002	356.67828
24	115	13310	12913	0.99209	0.00200	0.01037	0.98709	0.22972	1.16587	57.76890	1.94163	0.11831	6.21324	29.39613	386.07441
25	120	13380	12983	0.99746	0.00108	0.00768	0.99478	0.12907	0.89697	58.66587	2.02605	0.06371	3.97236	25.46400	411.53841
26	125	13430	13033	1.00131	0.00077	0.00461	0.99939	0.09604	0.56277	59.22864	2.11047	0.04550	3.32350	18.23965	429.77807
27	130	13510	13113	1.00745	0.00123	0.00499	1.00438	0.15980	0.63960	59.86824	2.19488	0.07281	6.15683	23.70084	453.47891
28	135	13550	13153	1.01053	0.00061	0.00461	1.00899	0.08297	0.60695	60.47518	2.27930	0.03640	3.52876	24.21400	477.69291
29	140	13570	13173	1.01206	0.00031	0.00230	1.01129	0.04302	0.31500	60.79018	2.36372	0.01820	2.00492	13.83421	491.52712
30	145	13610	13213	1.01514	0.00061	0.00230	1.01360	0.08912	0.33036	61.12054	2.44814	0.03640	4.52165	16.31643	507.84355
31	150	13650	13253	1.01821	0.00061	0.00307	1.01667	0.09219	0.45329	61.57383	2.53256	0.03640	5.06419	23.96461	531.80815
32	155	13650	13253	1.01821	0.00000	0.00154	1.01821	0.00000	0.23049	61.80432	2.61698	0.00000	0.00000	12.66048	544.46863
33	160	13680	13283	1.02051	0.00046	0.00115	1.01936	0.07376	0.18439	61.98871	2.70140	0.02730	4.68110	11.70275	556.17138
34	165	13680	13283	1.02051	0.00000	0.00115	1.02051	0.00000	0.18439	62.17309	2.78581	0.00000	0.00000	11.70275	567.87413
35	170	13690	13293	1.02128	0.00015	0.00038	1.02090	0.02612	0.06530	62.23840	2.87023	0.00910	1.88542	4.71354	572.58768
36	175	13720	13323	1.02359	0.00046	0.00154	1.02243	0.08067	0.26698	62.50538	2.95465	0.02730	6.17840	20.15954	592.74722
37	180	13720	13323	1.02359	0.00000	0.00115	1.02359	0.00000	0.20167	62.70705	3.03907	0.00000	0.00000	15.44600	608.19321
38	185	13740	13343	1.02512	0.00031	0.00077	1.02435	0.05685	0.14213	62.84919	3.12349	0.01820	4.86123	12.15307	620.34628
39	190	13740	13343	1.02512	0.00000	0.00077	1.02512	0.00000	0.14213	62.99132	3.20791	0.00000	0.00000	12.15307	632.49935
40	195	13740	13343	1.02512	0.00000	0.00000	1.02512	0.00000	0.00000	62.99132	3.29233	0.00000	0.00000	0.00000	632.49935
41	200	13760	13363	1.02666	0.00031	0.00077	1.02589	0.06146	0.15366	63.14498	3.37674	0.01820	6.08991	15.22478	647.72413
42	205	13770	13373	1.02743	0.00015	0.00115	1.02704	0.03150	0.23241	63.37738	3.46116	0.00910	3.26510	23.38754	671.11167
43	210	13790	13393	1.02896	0.00031	0.00115	1.02820	0.06454	0.24009	63.61747	3.54558	0.01820	6.98586	25.62742	696.73909
44	215	13790	13393	1.02896	0.00000	0.00077	1.02896	0.00000	0.16134	63.77881	3.63000	0.00000	0.00000	17.46466	714.20375
45	220	13790	13393	1.02896	0.00000	0.00000	1.02896	0.00000	0.00000	63.77881	3.71442	0.00000	0.00000	0.00000	714.20375
46	225	13790	13393	1.02896	0.00000	0.00000	1.02896	0.00000	0.00000	63.77881	3.79884	0.00000	0.00000	0.00000	714.20375
47	230	13790	13393	1.02896	0.00000	0.00000	1.02896	0.00000	0.00000	63.77881	3.88326	0.00000	0.00000	0.00000	714.20375
48	235	13790	13393	1.02896	0.00000	0.00000	1.02896	0.00000	0.00000	63.77881	3.96767	0.00000	0.00000	0.00000	714.20375
49	240	13790	13393	1.02896	0.00000	0.00000	1.02896	0.00000	0.00000	63.77881	4.05209	0.00000	0.00000	0.00000	714.20375
50	300	13790	13393	1.02896	0.00000	0.00000	1.02896	0.00000	0.00000	63.77881	5.06512	0.00000	0.00000	0.00000	714.20375
51	360	13790	13393	1.02896	0.00000	0.00000	1.02896	0.00000	0.00000	63.77881	6.07814	0.00000	0.00000	0.00000	714.20375
52	480	13810	13413	1.03050	0.00001	0.00077	1.02973	0.00615	0.36878	64.14759	8.10419	0.00076	2.26706	136.02377	850.22752
53	600	13810	13413	1.03050	0.00000	0.00077	1.03050	0.00000	0.36878	64.51636	10.13023	0.00000	0.00000	136.02377	986.25129
54															
55															

Table 5. Step input tracer test results for an 8-cell reactor with horizontal slots and Q=0.5 l min^{-1}

	8 cells (Horizontal slots)														
Flow rate, L/min	0.48														
C back, uS/cm	413														
Co, uS/cm	13337														
Mean det. time, sec	118.34														
Actual volume, ml	946.76														
Sample	Time, sec	C, uS/cm	C corr, uS/cm	F(t)	E(t)	Partial E(t)	Cum. E(t)	tE(t)	Partial tE(t)	Cum. tE(t)	θ	E(θ)	(t−τ)²E(t)	Partial (t−τ)²E(t)	Cum. (t−τ)²E(t)=σ²
1	0	413	0	0.00000	0.00000	0.00000	0.00000	0.00000	0.00000	0.00000	0.00000	0.00000	0.00000	0.00000	0.00000
2	5	413	0	0.00000	0.00000	0.00000	0.00000	0.00000	0.00000	0.00000	0.04225	0.00000	0.00000	0.00000	0.00000
3	10	413	0	0.00000	0.00000	0.00000	0.00000	0.00000	0.00000	0.00000	0.08450	0.00000	0.00000	0.00000	0.00000
4	15	422	9	0.00070	0.00014	0.00035	0.00035	0.00209	0.00522	0.00522	0.12675	0.01648	1.48748	3.71870	3.71870
5	20	427	14	0.00108	0.00008	0.00054	0.00089	0.00155	0.00909	0.01431	0.16900	0.00916	0.74835	5.58957	9.30826
6	25	427	14	0.00108	0.00000	0.00019	0.00108	0.00000	0.00387	0.01818	0.21125	0.00000	0.00000	1.87087	11.17913
7	30	427	14	0.00108	0.00000	0.00000	0.00108	0.00000	0.00000	0.01818	0.25350	0.00000	0.00000	0.00000	11.17913
8	35	442	29	0.00224	0.00023	0.00058	0.00166	0.00812	0.02031	0.03849	0.29575	0.02747	1.61242	4.03106	15.21019
9	40	469	56	0.00433	0.00042	0.00162	0.00329	0.01671	0.06209	0.10059	0.33800	0.04945	2.56457	10.44248	25.65267
10	45	526	113	0.00874	0.00088	0.00325	0.00654	0.03969	0.14102	0.24160	0.38025	0.10439	4.74508	18.27413	43.92679
11	50	603	190	0.01470	0.00119	0.00518	0.01172	0.05958	0.24818	0.48979	0.42250	0.14102	5.56585	25.77733	69.70412
12	55	748	335	0.02592	0.00224	0.00859	0.02031	0.12341	0.45748	0.94727	0.46474	0.26555	9.00367	36.42380	106.12793
13	60	897	484	0.03745	0.00231	0.01137	0.03169	0.13835	0.65440	1.60167	0.50699	0.27288	7.84910	42.13193	148.25986
14	65	1090	677	0.05238	0.00299	0.01323	0.04492	0.19413	0.83121	2.43288	0.54924	0.35346	8.49905	40.87039	189.13024
15	70	1383	970	0.07505	0.00453	0.01880	0.06372	0.31739	1.27882	3.71170	0.59149	0.53660	10.59731	47.74091	236.87116
16	75	1576	1163	0.08999	0.00299	0.01880	0.08252	0.22400	1.35349	5.06519	0.63374	0.35346	5.61125	40.52140	277.39256
17	80	2031	1618	0.12519	0.00704	0.02507	0.10759	0.56329	1.96824	7.03343	0.67599	0.83328	10.35266	39.90976	317.30232
18	85	2546	2133	0.16504	0.00797	0.03753	0.14512	0.67742	3.10179	10.13521	0.71824	0.94317	8.86115	48.03451	365.33683
19	90	3320	2907	0.22493	0.01198	0.04987	0.19499	1.07799	4.38854	14.52375	0.76049	1.41750	9.62306	46.21053	411.54736
20	95	4010	3597	0.27832	0.01068	0.05664	0.25162	1.01439	5.23097	19.75472	0.80274	1.26366	5.81907	38.60532	450.15267
21	100	4950	4537	0.35105	0.01455	0.06306	0.31469	1.45466	6.17262	25.92734	0.84499	1.72151	4.89525	26.78580	476.93847
22	105	5900	5487	0.42456	0.01470	0.07312	0.38781	1.54364	7.49574	33.42309	0.88724	1.73982	2.61797	18.78306	495.72153
23	110	6670	6257	0.48414	0.01192	0.06654	0.45435	1.31074	7.13595	40.55904	0.92949	1.41017	0.82972	8.61922	504.34075
24	115	7500	7087	0.54836	0.01284	0.06190	0.51625	1.47710	6.96959	47.52863	0.97174	1.52006	0.14368	2.43348	506.77423
25	120	8310	7897	0.61103	0.01253	0.06345	0.57970	1.50418	7.45319	54.98182	1.01399	1.48343	0.03435	0.44507	507.21930
26	125	8930	8517	0.65901	0.00959	0.05532	0.63502	1.19932	6.75874	61.74056	1.05624	1.13546	0.42499	1.14836	508.36766
27	130	9520	9107	0.70466	0.00913	0.04681	0.68183	1.18694	5.96565	67.70621	1.09849	1.08052	1.24035	4.16334	512.53100
28	135	10120	9707	0.75108	0.00929	0.04604	0.72787	1.25348	6.10105	73.80726	1.14074	1.09884	2.57571	9.54014	522.07114
29	140	10530	10117	0.78281	0.00634	0.03907	0.76695	0.88827	5.35438	79.16164	1.18299	0.75087	2.97544	13.87787	535.94901
30	145	10920	10507	0.81298	0.00604	0.03095	0.79790	0.87512	4.40846	83.57010	1.22524	0.71424	4.28815	18.15897	554.10798
31	150	11280	10867	0.84084	0.00557	0.02902	0.82691	0.83565	4.27693	87.84703	1.26749	0.65930	5.58255	24.67674	578.78471
32	155	11660	11247	0.87024	0.00588	0.02863	0.85554	0.91148	4.36784	92.21487	1.30973	0.69593	7.90121	33.70940	612.49411
33	160	11920	11507	0.89036	0.00402	0.02476	0.88030	0.64376	3.88812	96.10299	1.35198	0.47616	6.98152	37.20683	649.70094
34	165	12130	11717	0.90661	0.00325	0.01818	0.89848	0.53621	2.94994	99.05292	1.39423	0.38459	7.07387	35.13847	684.83942
35	170	12260	11847	0.91667	0.00201	0.01315	0.91164	0.34200	2.19553	101.24845	1.43648	0.23808	5.36795	31.10456	715.94397
36	175	12510	12097	0.93601	0.00387	0.01470	0.92634	0.67703	2.54759	103.79604	1.47873	0.45785	12.41814	44.46522	760.40919
37	180	12640	12227	0.94607	0.00201	0.01470	0.94104	0.36212	2.59788	106.39392	1.52098	0.23808	7.64750	50.16408	810.57327
38	185	12670	12257	0.94839	0.00046	0.00619	0.94723	0.08589	1.12001	107.51393	1.56323	0.05494	2.06265	24.27537	834.84864
39	190	12820	12407	0.96000	0.00232	0.00696	0.95419	0.44104	1.31732	108.83124	1.60548	0.27471	11.91853	34.95295	869.80159
40	195	12900	12487	0.96619	0.00124	0.00890	0.96309	0.24141	1.70613	110.53737	1.64773	0.14651	7.27460	47.98283	917.78442
41	200	13000	12587	0.97392	0.00155	0.00696	0.97006	0.30950	1.37728	111.91465	1.68998	0.18314	10.31819	43.98196	961.76638
42	205	13110	12697	0.98244	0.00170	0.00812	0.97818	0.34896	1.64616	113.56082	1.73223	0.20145	12.78255	57.75184	1019.51822
43	210	13120	12707	0.98321	0.00015	0.00464	0.98282	0.03250	0.95365	114.51447	1.77448	0.01831	1.30002	35.20642	1054.72464
44	215	13210	12797	0.99017	0.00139	0.00387	0.98669	0.29944	0.82985	115.34432	1.81673	0.16483	13.01153	35.77886	1090.50350
45	220	13250	12837	0.99327	0.00062	0.00503	0.99172	0.13618	1.08906	116.43338	1.85898	0.07326	6.39668	48.52050	1139.02401
46	225	13330	12917	0.99946	0.00124	0.00464	0.99636	0.27855	1.03683	117.47021	1.90123	0.14651	14.08280	51.19870	1190.22271
47	230	13350	12937	1.00101	0.00031	0.00387	1.00023	0.07119	0.87434	118.34455	1.94348	0.03663	3.85854	44.85336	1235.07606
48	235	13380	12967	1.00333	0.00046	0.00193	1.00217	0.10910	0.45071	118.79526	1.98573	0.05494	6.31778	25.44079	1260.51685
49	240	13430	13017	1.00720	0.00077	0.00310	1.00526	0.18570	0.73700	119.53227	2.02798	0.09157	11.45160	44.42344	1304.94030
50	300	13630	13217	1.02267	0.00026	0.03095	1.03621	0.07738	7.89229	127.42456	2.53497	0.03052	8.51096	598.87686	1903.81715
51	360	13680	13267	1.02654	0.00006	0.00967	1.04588	0.02321	3.01764	130.44220	3.04197	0.00763	3.76543	368.29186	2272.10902
52	480	13740	13327	1.03118	0.00004	0.00619	1.05207	0.01857	2.50696	132.94916	4.05595	0.00458	5.06015	529.53479	2801.64381
53	600	13750	13337	1.03196	0.00001	0.00271	1.05478	0.00387	1.34633	134.29550	5.06994	0.00076	1.49587	393.36117	3195.00497

Table 6. Step input tracer test results for 1-cell through 8-cell reactor with vertical slots and Q=1 l min^{-1}

		1 cell													
Flow rate, L/min		0.98													
C back, uS/cm		392													
Co, uS/cm		14960													
Mean det. time, seg		27.96													
Actual volume, ml		456.60													
Sample	Time, sec	C, uS/cm	C corr, uS/cm	F(t)	E(t)	Partial E(t)	Cum. E(t)	tE(t)	Partial tE(t)	Cum. tE(t)	θ	E(θ)	(t−τ)²E(t)	Partial (t−τ)²E(t)	Cum. (t−τ)²E(t)=σ²
1	0	392	0	0.00000	0.00000	0.00000	0.00000	0.00000	0.00000	0.00000	0.00000	0.00000	0.00000	0.00000	0.00000
2	5	428	36	0.00247	0.00049	0.00124	0.00124	0.00247	0.00618	0.00618	0.17886	0.01382	0.26043	0.65108	0.65108
3	10	1144	752	0.05162	0.00983	0.02581	0.02705	0.09830	0.25192	0.25810	0.35772	0.27479	3.16898	8.57352	9.22459
4	15	1846	1454	0.09981	0.00964	0.04867	0.07571	0.14456	0.60715	0.86525	0.53657	0.26942	1.61752	11.96624	21.19083
5	20	5850	5458	0.37466	0.05497	0.16152	0.23723	1.09940	3.10990	3.97515	0.71543	1.53669	3.47869	12.74053	33.93136
6	25	9480	9088	0.62383	0.04984	0.26201	0.49924	1.24588	5.86319	9.83834	0.89429	1.39315	0.43519	9.78472	43.71608
7	30	11390	10998	0.75494	0.02622	0.19014	0.68939	0.78666	5.08134	14.91969	1.07315	0.73303	0.10965	1.36211	45.07819
8	35	12880	12488	0.85722	0.02046	0.11669	0.80608	0.71595	3.75652	18.67621	1.25201	0.57184	1.01523	2.81220	47.89039
9	40	13550	13158	0.90321	0.00920	0.07414	0.88022	0.36793	2.70971	21.38591	1.43087	0.25714	1.33448	5.87427	53.76466
10	45	13890	13498	0.92655	0.00467	0.03467	0.91488	0.21005	1.44495	22.83086	1.60972	0.13049	1.35612	6.72649	60.49114
11	50	14230	13838	0.94989	0.00467	0.02334	0.93822	0.23339	1.10859	23.93946	1.78858	0.13049	2.26843	9.06136	69.55251
12	55	14380	13988	0.96019	0.00206	0.01682	0.95504	0.11326	0.86663	24.80608	1.96744	0.05757	1.50623	9.43665	78.98916
13	60	14570	14178	0.97323	0.00261	0.01167	0.96671	0.15651	0.67442	25.48051	2.14630	0.07292	2.67856	10.46198	89.45114
14	65	14690	14298	0.98147	0.00165	0.01064	0.97735	0.10708	0.65898	26.13948	2.32516	0.04605	2.26083	12.34848	101.79961
15	70	14730	14338	0.98421	0.00055	0.00549	0.98284	0.03844	0.36381	26.50329	2.50401	0.01535	0.97077	8.07900	109.87862
16	75	14790	14398	0.98833	0.00082	0.00343	0.98627	0.06178	0.25055	26.75384	2.68287	0.02303	1.82308	6.98463	116.86325
17	80	14820	14428	0.99039	0.00041	0.00309	0.98936	0.03295	0.23682	26.99066	2.86173	0.01151	1.11560	7.34670	124.20995
18	85	14870	14478	0.99382	0.00069	0.00275	0.99211	0.05835	0.22824	27.21890	3.04059	0.01919	2.23375	8.37336	132.58330
19	90	14910	14518	0.99657	0.00055	0.00309	0.99519	0.04942	0.26943	27.48833	3.21945	0.01535	2.11399	10.86933	143.45263
20	95	14910	14518	0.99657	0.00000	0.00137	0.99657	0.00000	0.12356	27.61189	3.39831	0.00000	0.00000	5.28497	148.73760
21	100	14960	14568	1.00000	0.00069	0.00172	0.99828	0.06864	0.17161	27.78350	3.57716	0.01919	3.56292	8.90731	157.64490
22	105	14960	14568	1.00000	0.00000	0.00172	1.00000	0.00000	0.17161	**27.95511**	3.75602	0.00000	0.00000	8.90731	166.55221
23	110	14960	14568	1.00000	0.00000	0.00000	1.00000	0.00000	0.00000	27.95511	3.93488	0.00000	0.00000	0.00000	166.55221
24	115	14960	14568	1.00000	0.00000	0.00000	1.00000	0.00000	0.00000	27.95511	4.11374	0.00000	0.00000	0.00000	166.55221
25	120	14980	14588	1.00137	0.00027	0.00069	1.00069	0.03295	0.08237	28.03748	4.29260	0.00768	2.32627	5.81567	172.36788
26	125	15000	14608	1.00275	0.00027	0.00137	1.00206	0.03432	0.16818	28.20566	4.47145	0.00768	2.58586	12.28032	184.64820
27	130	15020	14628	1.00412	0.00027	0.00137	1.00343	0.03569	0.17504	28.38070	4.65031	0.00768	2.85919	13.61262	198.26083
28	135	15040	14648	1.00549	0.00027	0.00000	1.00343	0.03707	0.18191	28.56260	4.82917	0.00768	3.14624	15.01357	213.27440
29	140														
30	145														
31	150														
32	155														
33	160														
34	165														
35	170														
36	175														
37	180														
38	185														
39	190														
40	195														
41	200														
42	205														
43	210														
44	215														
45	220														
46	225														
47	230														
48	235														
49	240														
50	300														
51	360														
52	420														
53	480														
54	540														
55	600														

									2 cells							
Flow rate, L/min									1.01							
C back, uS/cm									394							
Co, uS/cm									14940							
Mean det. time, sec									35.51							
Actual volume, ml									597.78							
Sample	Time, sec	C, uS/cm	C corr., uS/cm	F(t)	E(t)	Partial E(t)	Cum. E(t)	tE(t)	Partial tE(t)	Cum. tE(t)	θ	E(θ)	(t−τ)*E(t)	Partial (t−τ)*E(t)	Cum. (t−τ)*E(t)=σ²
1	0	394	0	0.00000	0.00000	0.00000	0.00000	0.00000	0.00000	0.00000	0.00000	0.00000	0.00000	0.00000	0.00000
2	5	394	0	0.00000	0.00000	0.00000	0.00000	0.00000	0.00000	0.00000	0.14080	0.00000	0.00000	0.00000	0.00000
3	10	413	19	0.00131	0.00026	0.00065	0.00065	0.00261	0.00653	0.00653	0.28160	0.00928	0.17003	0.42507	0.42507
4	15	618	224	0.01540	0.00282	0.00770	0.00835	0.04228	0.11223	0.11876	0.42239	0.10010	1.18590	3.38983	3.81490
5	20	2710	2316	0.15922	0.02876	0.07896	0.08731	0.57528	1.54390	1.66266	0.56319	1.02146	6.92108	20.26746	24.08236
6	25	5910	5516	0.37921	0.04400	0.18191	0.26921	1.09996	4.18809	5.85075	0.70399	1.56246	4.86175	29.45707	53.53943
7	30	8330	7936	0.54558	0.03327	0.19318	0.46240	0.99821	5.24543	11.09618	0.84479	1.18161	1.01086	14.68153	68.22096
8	35	10230	9836	0.67620	0.02612	0.14849	0.61089	0.91434	4.78138	15.87756	0.98559	0.92771	0.00684	2.54427	70.76523
9	40	11580	11186	0.76901	0.01856	0.11171	0.72260	0.74247	4.14203	20.01959	1.12639	0.65916	0.37390	0.95187	71.71710
10	45	12590	12196	0.83844	0.01389	0.08112	0.80373	0.62491	3.41847	23.43806	1.26718	0.49315	1.25018	4.06021	75.77731
11	50	13180	12786	0.87900	0.00811	0.05500	0.85872	0.40561	2.57631	26.01437	1.40798	0.28808	1.70281	7.38248	83.15979
12	55	13580	13186	0.90650	0.00550	0.03403	0.89275	0.30249	1.77025	27.78461	1.54878	0.19531	2.08876	9.47892	92.63871
13	60	13920	13526	0.92988	0.00467	0.02544	0.91819	0.28049	1.45745	29.24206	1.68958	0.16601	2.80336	12.23029	104.86900
14	65	14200	13806	0.94913	0.00385	0.02131	0.93950	0.25024	1.32683	30.56888	1.83038	0.13672	3.34765	15.37752	120.24652
15	70	14390	13996	0.96219	0.00261	0.01616	0.95566	0.18287	1.08277	31.65166	1.97117	0.09277	3.10728	16.13733	136.38385
16	75	14490	14096	0.96906	0.00137	0.00997	0.96563	0.10312	0.71497	32.36663	2.11197	0.04883	2.14398	13.12815	149.51200
17	80	14630	14236	0.97869	0.00192	0.00825	0.97388	0.15399	0.64279	33.00942	2.25277	0.06836	3.80981	14.88448	164.39648
18	85	14670	14276	0.98144	0.00055	0.00619	0.98006	0.04675	0.50186	33.51127	2.39357	0.01953	1.34694	12.89189	177.28837
19	90	14760	14366	0.98763	0.00124	0.00447	0.98453	0.11137	0.39530	33.90657	2.53437	0.04394	3.67395	12.55224	189.84061
20	95	14790	14396	0.98969	0.00041	0.00412	0.98866	0.03919	0.37639	34.28296	2.67517	0.01465	1.45972	12.83417	202.67478
21	100	14820	14426	0.99175	0.00041	0.00206	0.99072	0.04125	0.20109	34.48405	2.81596	0.01465	1.71541	7.93782	210.61260
22	105	14860	14466	0.99450	0.00055	0.00241	0.99313	0.05775	0.24749	34.73154	2.95676	0.01953	2.65563	10.92761	221.54021
23	110	14870	14476	0.99519	0.00014	0.00172	0.99484	0.01512	0.18218	34.91372	3.09756	0.00488	0.76289	8.54631	230.08652
24	115	14920	14526	0.99863	0.00069	0.00206	0.99691	0.07906	0.23546	35.14918	3.23836	0.02441	4.34372	12.76651	242.85303
25	120	14940	14546	1.00000	0.00027	0.00241	0.99931	0.03300	0.28015	35.42933	3.37916	0.00977	1.96295	15.76666	258.61969
26	125	14940	14546	1.00000	0.00000	0.00069	1.00000	0.00000	0.08250	35.51182	3.51995	0.00000	0.00000	4.90736	263.52705
27	130	14940	14546	1.00000	0.00000	0.00000	1.00000	0.00000	0.00000	35.51182	3.66075	0.00000	0.00000	0.00000	263.52705
28	135	14940	14546	1.00000	0.00000	0.00000	1.00000	0.00000	0.00000	35.51182	3.80155	0.00000	0.00000	0.00000	263.52705
29	140	14970	14576	1.00206	0.00041	0.00103	1.00103	0.05775	0.14437	35.65619	3.94235	0.01465	4.50341	11.25854	274.78559
30	145	14980	14586	1.00275	0.00014	0.00137	1.00241	0.01994	0.19421	35.85041	4.08315	0.00488	1.64824	15.37914	290.16473
31	150	14990	14596	1.00344	0.00014	0.00069	1.00309	0.02062	0.10140	35.95181	4.22395	0.00488	1.80222	8.62615	298.79088
32	155	15000	14606	1.00412	0.00014	0.00069	1.00378	0.02131	0.10484	36.05665	4.36474	0.00488	1.96307	9.41323	308.20411
33	160	15020	14626	1.00550	0.00027	0.00103	1.00481	0.04400	0.16328	36.21992	4.50554	0.00977	4.26160	15.56168	323.76579
34	165	15030	14636	1.00619	0.00014	0.00103	1.00584	0.02269	0.16671	36.38664	4.64634	0.00488	2.30540	16.41750	340.18329
35	170	15030	14636	1.00619	0.00000	0.00034	1.00619	0.00000	0.05672	36.44335	4.78714	0.00000	0.00000	5.76350	345.94680
36	175	15040	14646	1.00687	0.00014	0.00034	1.00653	0.02406	0.06015	36.50351	4.92794	0.00488	2.67523	6.68808	352.63487
37	180														
38	185														
39	190														
40	195														
41	200														
42	205														
43	210														
44	215														
45	220														
46	225														
47	230														
48	235														
49	240														
50	300														
51	360														
52	420														
53	480														
54	540														
55	600														

		3 cells													
Flow rate, L/min		0.99													
C back, uS/cm		411													
Co, uS/cm		15340													
Mean det. time, sec		44.87													
Actual volume, ml		740.41													
Sample	Time, sec	C, uS/cm	C corr., uS/cm	F(t)	E(t)	Partial E(t)	Cum. E(t)	tE(t)	Partial tE(t)	Cum. tE(t)	θ	E(θ)	(t−τ)²E(t)	Partial (t−τ)²E(t)	Cum. (t−τ)²E(t)=σ²
1	0	411	0	0.00000	0.00000	0.00000	0.00000	0.00000	0.00000	0.00000	0.00000	0.00000	0.00000	0.00000	0.00000
2	5	411	0	0.00000	0.00000	0.00000	0.00000	0.00000	0.00000	0.00000	0.11142	0.00000	0.00000	0.00000	0.00000
3	10	411	0	0.00000	0.00000	0.00000	0.00000	0.00000	0.00000	0.00000	0.22285	0.00000	0.00000	0.00000	0.00000
4	15	430	19	0.00127	0.00025	0.00064	0.00064	0.00382	0.00955	0.00955	0.33427	0.01142	0.22715	0.56789	0.56789
5	20	744	333	0.02231	0.00421	0.01115	0.01179	0.08413	0.21987	0.22942	0.44570	0.18876	2.60255	7.07427	7.64215
6	25	1330	919	0.06156	0.00785	0.03014	0.04193	0.19626	0.70098	0.93040	0.55712	0.35228	3.10057	14.25780	21.89995
7	30	3640	3229	0.21629	0.03095	0.09699	0.13892	0.92839	2.81164	3.74205	0.66855	1.38867	6.84592	24.86622	46.76617
8	35	6620	6209	0.41590	0.03992	0.17717	0.31610	1.39728	5.81419	9.55623	0.77937	1.79145	3.89179	26.84427	73.61044
9	40	8910	8499	0.56929	0.03068	0.17650	0.49260	1.22714	6.56106	16.11729	0.89140	1.37665	0.72862	11.55101	85.16145
10	45	10940	10529	0.70527	0.02720	0.14468	0.63728	1.22379	6.12734	22.24462	1.00282	1.22035	0.00044	1.82263	86.98408
11	50	11980	11569	0.77493	0.01393	0.10282	0.74010	0.69663	4.80106	27.04568	1.11425	0.62520	0.36618	0.91653	87.90061
12	55	12830	12419	0.83187	0.01139	0.06330	0.80340	0.62630	3.30732	30.35300	1.22567	0.51098	1.16774	3.83479	91.73540
13	60	13500	13089	0.87675	0.00898	0.05091	0.85431	0.53855	2.91212	33.26512	1.33710	0.40278	2.05379	8.05383	99.78923
14	65	13950	13539	0.90689	0.00603	0.03751	0.89182	0.39185	2.32601	35.59113	1.44852	0.27052	2.44204	11.23958	111.02881
15	70	14190	13779	0.92297	0.00322	0.02311	0.91493	0.22507	1.54230	37.13343	1.55994	0.14428	2.02992	11.17989	122.20869
16	75	14510	14099	0.94440	0.00429	0.01876	0.93369	0.32152	1.36647	38.49990	1.67137	0.19237	3.89089	14.80203	137.01072
17	80	14740	14329	0.95981	0.00308	0.01842	0.95211	0.24650	1.42005	39.91995	1.78279	0.13827	3.80189	19.23196	156.24268
18	85	14860	14449	0.96785	0.00161	0.01172	0.96383	0.13665	0.95787	40.87782	1.89422	0.07214	2.58848	15.97593	172.21860
19	90	14930	14519	0.97254	0.00094	0.00636	0.97019	0.08440	0.55262	41.43044	2.00564	0.04208	1.90969	11.24543	183.46403
20	95	14990	14579	0.97656	0.00080	0.00435	0.97455	0.07636	0.40190	41.83234	2.11707	0.03607	2.01970	9.82347	193.28750
21	100	15080	14669	0.98258	0.00121	0.00502	0.97957	0.12057	0.49233	42.32467	2.22849	0.05410	3.66407	14.20944	207.49694
22	105	15140	14729	0.98660	0.00080	0.00502	0.98459	0.08440	0.51243	42.83710	2.33992	0.03607	2.90592	16.42499	223.92192
23	110	15140	14729	0.98660	0.00000	0.00201	0.98660	0.00000	0.21100	43.04809	2.45134	0.00000	0.00000	7.26480	231.18673
24	115	15170	14759	0.98861	0.00040	0.00100	0.98761	0.04622	0.11555	43.16364	2.56277	0.01803	1.97645	4.94113	236.12786
25	120	15200	14789	0.99062	0.00040	0.00201	0.98962	0.04823	0.23612	43.39976	2.67419	0.01803	2.26834	10.61198	246.73983
26	125	15210	14799	0.99129	0.00013	0.00134	0.99096	0.01675	0.16244	43.56219	2.78561	0.00601	0.86011	7.82112	254.56095
27	130	15220	14809	0.99196	0.00013	0.00067	0.99163	0.01742	0.08540	43.64760	2.89704	0.00601	0.97080	4.57727	259.13822
28	135	15250	14839	0.99397	0.00040	0.00134	0.99297	0.05426	0.17918	43.82678	3.00846	0.01803	3.26457	10.58844	269.72665
29	140	15260	14849	0.99464	0.00013	0.00134	0.99431	0.01876	0.18253	44.00931	3.11989	0.00601	1.21228	11.19214	280.91879
30	145	15280	14869	0.99598	0.00027	0.00100	0.99531	0.03885	0.14402	44.15333	3.23131	0.01202	2.68614	9.74605	290.66483
31	150	15310	14899	0.99799	0.00040	0.00167	0.99699	0.06029	0.24784	44.40117	3.34274	0.01803	4.44166	17.81950	308.48434
32	155	15320	14909	0.99866	0.00013	0.00134	0.99833	0.02076	0.20263	44.60379	3.45416	0.00601	1.62474	15.16601	323.65035
33	160	15330	14919	0.99933	0.00013	0.00067	0.99900	0.02143	0.10550	44.70929	3.56559	0.00601	1.77562	8.50090	332.15125
34	165	15340	14929	1.00000	0.00013	0.00067	0.99967	0.02210	0.10885	44.81814	3.67701	0.00601	1.93320	9.27207	341.42332
35	170	15340	14929	1.00000	0.00000	0.00033	1.00000	0.00000	0.05526	44.87340	3.78844	0.00000	0.00000	4.83301	346.25633
36	175	15350	14939	1.00067	0.00013	0.00033	1.00033	0.02344	0.05861	44.93201	3.89986	0.00601	2.26846	5.67115	351.92748
37	180	15380	14969	1.00268	0.00040	0.00134	1.00167	0.07234	0.23947	45.17148	4.01129	0.01803	7.33841	24.01719	375.94467
38	185	15380	14969	1.00268	0.00000	0.00100	1.00268	0.00000	0.18086	45.35233	4.12271	0.00000	0.00000	18.34604	394.29071
39	190	15380	14969	1.00268	0.00000	0.00000	1.00268	0.00000	0.00000	45.35233	4.23413	0.00000	0.00000	0.00000	394.29071
40	195	15390	14979	1.00335	0.00013	0.00033	1.00301	0.02612	0.06531	45.41764	4.34556	0.00601	3.01936	7.54839	401.83910
41	200	15390	14979	1.00335	0.00000	0.00033	1.00335	0.00000	0.06531	45.48295	4.45698	0.00000	0.00000	7.54839	409.38750
42	205	15390	14979	1.00335	0.00000	0.00000	1.00335	0.00000	0.00000	45.48295	4.56841	0.00000	0.00000	0.00000	409.38750
43	210	15390	14979	1.00335	0.00000	0.00000	1.00335	0.00000	0.00000	45.48295	4.67983	0.00000	0.00000	0.00000	409.38750
44	215	15390	14979	1.00335	0.00000	0.00000	1.00335	0.00000	0.00000	45.48295	4.79126	0.00000	0.00000	0.00000	409.38750
45	220	15390	14979	1.00335	0.00000	0.00000	1.00335	0.00000	0.00000	45.48295	4.90268	0.00000	0.00000	0.00000	409.38750
46	225	15390	14979	1.00335	0.00000	0.00000	1.00335	0.00000	0.00000	45.48295	5.01411	0.00000	0.00000	0.00000	409.38750
47	230	15390	14979	1.00335	0.00000	0.00000	1.00335	0.00000	0.00000	45.48295	5.12553	0.00000	0.00000	0.00000	409.38750
48	235	15390	14979	1.00335	0.00000	0.00000	1.00335	0.00000	0.00000	45.48295	5.23696	0.00000	0.00000	0.00000	409.38750
49	240	15400	14989	1.00402	0.00013	0.00033	1.00368	0.03215	0.08038	45.56333	5.34838	0.00601	5.10073	12.75182	422.13932
50	300	15420	15009	1.00536	0.00002	0.00469	1.00837	0.00670	1.16552	46.72885	6.68548	0.00100	1.45331	196.62129	618.76061
51	360														
52	420														
53	480														
54	540														
55	600														

							4 cells								
Flow rate, L/min							0.99								
C back, uS/cm							443								
Co, uS/cm							15450								
Mean det. time, sec							52.43								
Actual volume, ml							865.08								
Sample	Time, sec	C, uS/cm	C corr., uS/cm	F(t)	E(t)	Partial E(t)	Cum. E(t)	tE(t)	Partial tE(t)	Cum. tE(t)	θ	E(θ)	(t−τ)²E(t)	Partial (t−τ)²E(t)	Cum. (t−τ)²E(t)=σ²
1	0	443	0	0.00000	0.00000	0.00000	0.00000	0.00000	0.00000	0.00000	0.00000	0.00000	0.00000	0.00000	0.00000
2	5	443	0	0.00000	0.00000	0.00000	0.00000	0.00000	0.00000	0.00000	0.09537	0.00000	0.00000	0.00000	0.00000
3	10	443	0	0.00000	0.00000	0.00000	0.00000	0.00000	0.00000	0.00000	0.19073	0.00000	0.00000	0.00000	0.00000
4	15	446	3	0.00020	0.00004	0.00010	0.00010	0.00060	0.00150	0.00150	0.28610	0.00210	0.05601	0.14003	0.14003
5	20	451	8	0.00053	0.00007	0.00027	0.00037	0.00133	0.00483	0.00633	0.38147	0.00349	0.07008	0.31522	0.45525
6	25	595	152	0.01013	0.00192	0.00496	0.00533	0.04798	0.12328	0.12961	0.47683	0.10062	1.44386	3.78484	4.24009
7	30	1608	1165	0.07763	0.01350	0.03855	0.04388	0.40501	1.13247	1.26208	0.57220	0.70781	6.79162	20.58869	24.82878
8	35	4320	3877	0.25835	0.03614	0.12411	0.16799	1.26501	4.17505	5.43713	0.66757	1.89496	10.97945	44.42767	69.25645
9	40	6590	6147	0.40961	0.03025	0.16599	0.33398	1.21010	6.18778	11.62491	0.76293	1.58612	4.67357	39.13254	108.38900
10	45	8400	7957	0.53022	0.02412	0.13594	0.46991	1.08549	5.73899	17.36390	0.85830	1.26470	1.33137	15.01234	123.40134
11	50	10150	9707	0.64683	0.02332	0.11861	0.58853	1.16612	5.62904	22.99294	0.95367	1.22278	0.13763	3.67249	127.07383
12	55	11240	10797	0.71946	0.01453	0.09462	0.68315	0.79896	4.91271	27.90564	1.04903	0.76162	0.09601	0.58408	127.65791
13	60	12290	11847	0.78943	0.01399	0.07130	0.75445	0.83961	4.09642	32.00207	1.14440	0.73367	0.80206	2.24518	129.90308
14	65	12980	12537	0.83541	0.00920	0.05797	0.81242	0.59772	3.59332	35.59539	1.23977	0.48212	1.45315	5.63804	135.54112
15	70	13500	13057	0.87006	0.00693	0.04031	0.85274	0.48511	2.70707	38.30246	1.33513	0.36334	2.13955	8.98176	144.52288
16	75	13900	13457	0.89671	0.00533	0.03065	0.88339	0.39981	2.21230	40.51476	1.43050	0.27949	2.71575	12.13825	156.66113
17	80	14190	13747	0.91604	0.00386	0.02299	0.90638	0.30919	1.77251	42.28727	1.52587	0.20263	2.93787	14.13406	170.79519
18	85	14370	13927	0.92803	0.00240	0.01566	0.92204	0.20390	1.28273	43.57000	1.62123	0.12577	2.54487	13.70685	184.50204
19	90	14610	14167	0.94403	0.00320	0.01399	0.93603	0.28787	1.22943	44.79943	1.71660	0.16770	4.51490	17.64943	202.15147
20	95	14670	14227	0.94802	0.00080	0.01000	0.94603	0.07596	0.90958	45.70900	1.81197	0.04192	1.44914	14.91011	217.06158
21	100	14800	14357	0.95669	0.00173	0.00633	0.95236	0.17325	0.62304	46.33205	1.90733	0.09083	3.92067	13.42453	230.48611
22	105	14900	14457	0.96335	0.00133	0.00766	0.96002	0.13993	0.78297	47.11501	2.00270	0.06987	3.68320	19.00968	249.49579
23	110	14950	14507	0.96668	0.00067	0.00500	0.96502	0.07330	0.53308	47.64810	2.09807	0.03494	2.20857	14.72942	264.22521
24	115	15010	14567	0.97068	0.00080	0.00366	0.96868	0.09196	0.41314	48.06124	2.19343	0.04192	3.13062	13.34798	277.57318
25	120	15080	14637	0.97534	0.00093	0.00433	0.97301	0.11195	0.50976	48.57100	2.28880	0.04891	4.25944	18.47515	296.04833
26	125	15140	14697	0.97934	0.00080	0.00433	0.97734	0.09995	0.52975	49.10075	2.38417	0.04192	4.21125	21.17672	317.22506
27	130	15220	14777	0.98467	0.00107	0.00466	0.98201	0.13860	0.59639	49.69714	2.47953	0.05590	6.41538	26.56659	343.79165
28	135	15230	14787	0.98534	0.00013	0.00300	0.98501	0.01799	0.39148	50.08863	2.57490	0.00699	0.90863	18.31005	362.10169
29	140	15310	14867	0.99067	0.00107	0.00300	0.98801	0.14926	0.41814	50.50676	2.67027	0.05590	8.17607	22.71177	384.81346
30	145	15310	14867	0.99067	0.00000	0.00267	0.99067	0.00000	0.37316	50.87992	2.76563	0.00000	0.00000	20.44018	405.25364
31	150	15310	14867	0.99067	0.00000	0.00000	0.99067	0.00000	0.00000	50.87992	2.86100	0.00000	0.00000	0.00000	405.25364
32	155	15360	14917	0.99400	0.00067	0.00167	0.99234	0.10329	0.25821	51.13814	2.95637	0.03494	7.01057	17.52644	422.78008
33	160	15360	14917	0.99400	0.00000	0.00167	0.99400	0.00000	0.25821	51.39635	3.05173	0.00000	0.00000	17.52644	440.30651
34	165	15400	14957	0.99667	0.00053	0.00133	0.99534	0.08796	0.21990	51.61625	3.14710	0.02795	6.75535	16.88837	457.19488
35	170	15400	14957	0.99667	0.00000	0.00133	0.99667	0.00000	0.21990	51.83614	3.24247	0.00000	0.00000	16.88837	474.08324
36	175	15430	14987	0.99867	0.00040	0.00100	0.99767	0.06997	0.17492	52.01106	3.33783	0.02096	6.00664	15.01659	489.09984
37	180	15440	14997	0.99933	0.00013	0.00133	0.99900	0.02399	0.23489	52.24595	3.43320	0.00699	2.16890	20.43883	509.53867
38	185	15450	15007	1.00000	0.00013	0.00067	0.99967	0.02466	0.12161	52.36756	3.52857	0.00699	2.34224	11.27785	520.81651
39	190	15450	15007	1.00000	0.00000	0.00033	1.00000	0.00000	0.06164	52.42920	3.62393	0.00000	0.00000	5.85561	526.67212
40	195	15450	15007	1.00000	0.00000	0.00000	1.00000	0.00000	0.00000	52.42920	3.71930	0.00000	0.00000	0.00000	526.67212
41	200	15450	15007	1.00000	0.00000	0.00000	1.00000	0.00000	0.00000	52.42920	3.81467	0.00000	0.00000	0.00000	526.67212
42	205	15460	15017	1.00067	0.00013	0.00033	1.00033	0.02732	0.06830	52.49750	3.91003	0.00699	3.10227	7.75566	534.42779
43	210	15460	15017	1.00067	0.00000	0.00033	1.00067	0.00000	0.06830	52.56580	4.00540	0.00000	0.00000	7.75566	542.18345
44	215	15460	15017	1.00067	0.00000	0.00000	1.00067	0.00000	0.00000	52.56580	4.10077	0.00000	0.00000	0.00000	542.18345
45	220	15460	15017	1.00067	0.00000	0.00000	1.00067	0.00000	0.00000	52.56580	4.19614	0.00000	0.00000	0.00000	542.18345
46	225	15460	15017	1.00067	0.00000	0.00000	1.00067	0.00000	0.00000	52.56580	4.29150	0.00000	0.00000	0.00000	542.18345
47	230	15470	15027	1.00133	0.00013	0.00033	1.00100	0.03065	0.07663	52.64243	4.38687	0.00699	4.20222	10.50556	552.68901
48	235	15490	15047	1.00267	0.00027	0.00100	1.00200	0.06264	0.23322	52.87566	4.48224	0.01397	8.88441	32.71659	585.40560
49	240	15490	15047	1.00267	0.00000	0.00067	1.00267	0.00000	0.15659	53.03225	4.57760	0.00000	0.00000	22.21103	607.61664
50	300	15500	15057	1.00333	0.00001	0.00033	1.00300	0.00333	0.09995	53.13220	5.72200	0.00058	0.68070	20.42090	628.03754
51	360														
52	420														
53	480														
54	540														
55	600														

				5 cells												
Flow rate, L/min				1.01												
C back, uS/cm				447												
Co, uS/cm				15440												
Mean det. time, sec				60.12												
Actual volume, ml				1011.98												
Sample	Time, sec	C, uS/cm	C corr., uS/cm	F(t)	E(t)	Partial E(t)	Cum. E(t)	tE(t)	Partial tE(t)	Cum. tE(t)	θ	E(θ)	(t−τ)*E(t)	Partial (t−τ)*E(t)	Cum. (t−τ)*E(t)=σ²
1	0	447	0	0.00000	0.00000	0.00000	0.00000	0.00000	0.00000	0.00000	0.17886	0.00000	0.00000	0.00000	0.00000
2	5	447	0	0.00000	0.00000	0.00000	0.00000	0.00000	0.00000	0.00000	0.16634	0.00000	0.00000	0.00000	0.00000
3	10	447	0	0.00000	0.00000	0.00000	0.00000	0.00000	0.00000	0.00000	0.24951	0.00000	0.00000	0.00000	0.00000
4	15	447	0	0.00000	0.00000	0.00000	0.00000	0.00000	0.00000	0.00000	0.33268	0.00000	0.00000	0.00000	0.00000
5	20	450	3	0.00020	0.00004	0.00010	0.00010	0.00080	0.00200	0.00200	0.41585	0.00241	0.06441	0.16102	0.16102
6	25	500	53	0.00353	0.00067	0.00177	0.00187	0.01667	0.04369	0.04569	0.49902	0.04010	0.82255	2.21740	2.37842
7	30	740	293	0.01954	0.00320	0.00967	0.01154	0.09604	0.28180	0.32749	0.58219	0.19247	2.90400	9.31639	11.69481
8	35	1350	903	0.06023	0.00814	0.02835	0.03989	0.28480	0.95211	1.27960	0.66536	0.48919	5.13372	20.09429	31.78910
9	40	2663	2216	0.14780	0.01751	0.06413	0.10402	0.70059	2.46348	3.74308	0.74853	1.05295	7.08865	30.55592	62.34503
10	45	5560	5113	0.34103	0.03864	0.14040	0.24441	1.73901	6.09301	9.84209	0.83170	2.32323	8.83207	39.80182	102.14684
11	50	7570	7123	0.47509	0.02681	0.16364	0.40806	1.34063	7.69909	17.54119	0.91487	1.61191	2.74475	28.94206	131.08890
12	55	9220	8773	0.58514	0.02201	0.12206	0.53011	1.21056	6.37798	23.91916	0.99804	1.32321	0.57647	8.30306	139.39196
13	60	10540	10093	0.67318	0.01761	0.09305	0.62316	1.05649	5.66764	29.58681	1.08121	1.05857	0.00024	1.44179	140.83375
14	65	11820	11373	0.75855	0.01707	0.08671	0.71587	1.10985	5.41586	35.00267	1.16438	1.02649	0.40700	1.01811	141.85187
15	70	12450	12003	0.80057	0.00840	0.06370	0.77956	0.58827	4.24531	39.24798	1.24755	0.50522	0.82072	3.06931	144.92118
16	75	13060	12613	0.84126	0.00814	0.04135	0.82092	0.61028	2.99640	42.24438	1.33072	0.48919	1.80223	6.55738	151.47856
17	80	13560	13113	0.87461	0.00667	0.03702	0.85793	0.53358	2.85967	45.10405	1.41389	0.40097	2.63660	11.09707	162.57562
18	85	13970	13523	0.90195	0.00547	0.03035	0.88828	0.46488	2.49616	47.60021	1.49706	0.32880	3.38615	15.05686	177.63248
19	90	14250	13803	0.92063	0.00374	0.02301	0.91129	0.33616	2.00260	49.60281	1.58023	0.22454	3.33524	16.80346	194.43594
20	95	14460	14013	0.93464	0.00280	0.01634	0.92763	0.26612	1.50570	51.10852	1.66340	0.16841	3.40856	16.85949	211.29543
21	100	14580	14133	0.94264	0.00160	0.01101	0.93864	0.16007	1.06550	52.17401	1.74657	0.09623	2.54614	14.88675	226.18217
22	105	14700	14253	0.95064	0.00160	0.00800	0.94664	0.16808	0.82038	52.99440	1.82974	0.09623	3.22458	14.42679	240.60896
23	110	14850	14403	0.96065	0.00200	0.00900	0.95565	0.22010	0.97045	53.96485	1.91291	0.12029	4.97881	20.50845	261.11742
24	115	14920	14473	0.96532	0.00093	0.00734	0.96298	0.10738	0.81872	54.78357	1.99608	0.05614	2.81257	19.47845	280.59587
25	120	14970	14523	0.96865	0.00067	0.00400	0.96698	0.08004	0.46855	55.25212	2.07925	0.04010	2.39171	13.01070	293.60657
26	125	15040	14593	0.97332	0.00093	0.00400	0.97099	0.11672	0.49190	55.74401	2.16242	0.05614	3.93090	15.80651	309.41308
27	130	15090	14643	0.97666	0.00067	0.00400	0.97499	0.08671	0.50857	56.25258	2.24559	0.04010	3.25721	17.97026	327.38334
28	135	15160	14713	0.98132	0.00093	0.00400	0.97899	0.12606	0.53191	56.78450	2.32876	0.05614	5.23598	21.23296	348.61630
29	140	15160	14713	0.98132	0.00000	0.00233	0.98132	0.00000	0.31515	57.09965	2.41193	0.00000	0.00000	13.08994	361.70624
30	145	15240	14793	0.98666	0.00107	0.00267	0.98399	0.15474	0.38685	57.48649	2.49510	0.06416	7.68892	19.22231	380.92855
31	150	15260	14813	0.98799	0.00027	0.00333	0.98733	0.04002	0.48689	57.97339	2.57827	0.01604	2.15536	24.61070	405.53925
32	155	15290	14843	0.99000	0.00040	0.00167	0.98899	0.06203	0.25512	58.22851	2.66144	0.02406	3.60274	14.39525	419.93450
33	160	15330	14883	0.99266	0.00053	0.00233	0.99133	0.08537	0.36851	58.59701	2.74461	0.03208	5.32327	22.31502	442.24952
34	165	15350	14903	0.99400	0.00027	0.00200	0.99333	0.04402	0.32348	58.92050	2.82779	0.01604	2.93478	20.64512	462.89464
35	170	15370	14923	0.99533	0.00027	0.00133	0.99466	0.04535	0.22344	59.14393	2.91096	0.01604	3.22127	15.39012	478.28476
36	175	15380	14933	0.99600	0.00013	0.00100	0.99566	0.02334	0.17175	59.31568	2.99413	0.00802	1.76055	12.45453	490.73930
37	180	15390	14943	0.99667	0.00013	0.00067	0.99633	0.02401	0.11839	59.43407	3.07730	0.00802	1.91713	9.19419	499.93349
38	185	15430	14983	0.99933	0.00053	0.00167	0.99800	0.09871	0.30681	59.74088	3.16047	0.03208	8.32153	25.59664	525.53013
39	190	15430	14983	0.99933	0.00000	0.00133	0.99933	0.00000	0.24678	59.98766	3.24364	0.00000	0.00000	20.80382	546.33395
40	195	15440	14993	1.00000	0.00013	0.00033	0.99967	0.02601	0.06503	60.05269	3.32681	0.00802	2.42690	6.06724	552.40119
41	200	15440	14993	1.00000	0.00000	0.00033	1.00000	0.00000	0.06503	60.11772	3.40998	0.00000	0.00000	6.06724	558.46843
42	205	15440	14993	1.00000	0.00000	0.00000	1.00000	0.00000	0.00000	60.11772	3.49315	0.00000	0.00000	0.00000	558.46843
43	210	15460	15013	1.00133	0.00027	0.00067	1.00067	0.05603	0.14007	60.25779	3.57632	0.01604	5.99338	14.98346	573.45189
44	215	15490	15043	1.00333	0.00040	0.00167	1.00233	0.08604	0.35517	60.61295	3.65949	0.02406	9.59989	38.98318	612.43507
45	220	15490	15043	1.00333	0.00000	0.00100	1.00333	0.00000	0.21510	60.82805	3.74266	0.00000	0.00000	23.99372	636.43479
46	225	15500	15053	1.00400	0.00013	0.00033	1.00367	0.03001	0.07504	60.90309	3.82583	0.00802	3.62651	9.06629	645.50107
47	230	15500	15053	1.00400	0.00000	0.00033	1.00400	0.00000	0.07504	60.97812	3.90900	0.00000	0.00000	9.06629	654.56736
48	235	15500	15053	1.00400	0.00000	0.00000	1.00400	0.00000	0.00000	60.97812	3.99217	0.00000	0.00000	0.00000	654.56736
49	240	15500	15053	1.00400	0.00000	0.00000	1.00400	0.00000	0.00000	60.97812	4.99021	0.00000	0.00000	0.00000	654.56736
50	300	15550	15103	1.00734	0.00006	0.00167	1.00567	0.01667	0.50023	61.47836	5.98825	0.00334	3.19835	95.95062	750.51798
51	360														
52	420														
53	480														
54	540														
55	600														

								6 cells								
Flow rate, L/min								0.98								
C back, uS/cm								479								
Co, uS/cm								14350								
Mean det. time, sec								70.14								
Actual volume, ml								1145.63								
Sample	Time, sec	C, uS/cm	C corr., uS/cm	F(t)	E(t)	Partial E(t)	Cum. E(t)	tE(t)	Partial tE(t)	Cum. tE(t)	θ	E(θ)	$(t-\tau)^2E(t)$	Partial $(t-\tau)^2E(t)$	Cum. $(t-\tau)^2E(t)=\sigma^2$	
1	0	479	0	0.00000	0.00000	0.00000	0.00000	0.00000	0.00000	0.00000	0.00000	0.00000	0.00000	0.00000	0.00000	
2	5	479	0	0.00000	0.00000	0.00000	0.00000	0.00000	0.00000	0.00000	0.07129	0.00000	0.00000	0.00000	0.00000	
3	10	479	0	0.00000	0.00000	0.00000	0.00000	0.00000	0.00000	0.00000	0.14257	0.00000	0.00000	0.00000	0.00000	
4	15	479	0	0.00000	0.00000	0.00000	0.00000	0.00000	0.00000	0.00000	0.21386	0.00000	0.00000	0.00000	0.00000	
5	20	479	0	0.00000	0.00000	0.00000	0.00000	0.00000	0.00000	0.00000	0.28514	0.00000	0.00000	0.00000	0.00000	
6	25	483	4	0.00029	0.00006	0.00014	0.00014	0.00144	0.00360	0.00360	0.35643	0.00405	0.11752	0.29380	0.29380	
7	30	484	5	0.00036	0.00001	0.00018	0.00032	0.00043	0.00469	0.00829	0.42771	0.00101	0.02323	0.35188	0.64569	
8	35	536	57	0.00411	0.00075	0.00191	0.00223	0.02624	0.06669	0.07498	0.49900	0.05259	0.92586	2.37272	3.01841	
9	40	923	444	0.03201	0.00558	0.01582	0.01806	0.22320	0.62360	0.69858	0.57028	0.39138	5.06917	14.98755	18.00596	
10	45	2465	1986	0.14318	0.02223	0.06953	0.08759	1.00050	3.05926	3.75784	0.64157	1.55947	14.05262	47.80446	65.81042	
11	50	4240	3761	0.27114	0.02559	0.11957	0.20716	1.27965	5.70038	9.45822	0.71285	1.79511	10.38161	61.08556	126.89598	
12	55	6130	5651	0.40740	0.02725	0.13211	0.33927	1.49881	6.94615	16.40437	0.78414	1.91141	6.24697	41.57143	168.46741	
13	60	7530	7051	0.50833	0.02019	0.11859	0.45786	1.21116	6.77493	23.17929	0.85542	1.41586	2.07575	20.80680	189.27421	
14	65	8770	8291	0.59772	0.01788	0.09516	0.55302	1.16214	5.93324	29.11254	0.92671	1.25405	0.47246	6.37054	195.64475	
15	70	9640	9161	0.66044	0.01254	0.07606	0.62908	0.87809	5.10057	34.21311	0.99800	0.87985	0.00025	1.18178	196.82653	
16	75	10580	10101	0.72821	0.01355	0.06524	0.69433	1.01651	4.73650	38.94961	1.06928	0.95065	0.32005	0.80075	197.62728	
17	80	11190	10711	0.77219	0.00880	0.05587	0.75020	0.70363	4.30034	43.24995	1.14057	0.61691	0.85498	2.93757	200.56485	
18	85	11820	11341	0.81761	0.00908	0.04470	0.79490	0.77211	3.68935	46.93930	1.21185	0.63714	2.00570	7.15170	207.71655	
19	90	12200	11721	0.84500	0.00548	0.03641	0.83130	0.49312	3.16307	50.10237	1.28314	0.38430	2.16092	10.41656	218.13310	
20	95	12630	12151	0.87600	0.00620	0.02920	0.86050	0.58900	2.70528	52.80766	1.35442	0.43487	3.83153	14.98114	233.11424	
21	100	12900	12421	0.89547	0.00389	0.02523	0.88573	0.38930	2.44575	55.25341	1.42571	0.27306	3.47095	18.25622	251.37046	
22	105	13180	12701	0.91565	0.00404	0.01983	0.90556	0.42391	2.03302	57.28642	1.49699	0.28317	4.90592	20.94218	272.31264	
23	110	13390	12911	0.93079	0.00303	0.01766	0.92322	0.33307	1.89244	59.17886	1.56828	0.21238	4.81065	24.29142	296.60406	
24	115	13560	13081	0.94305	0.00245	0.01370	0.93692	0.28188	1.53738	60.71624	1.63956	0.17193	4.93263	24.35819	320.96225	
25	120	13610	13131	0.94665	0.00072	0.00793	0.94485	0.08651	0.92099	61.63723	1.71085	0.05057	1.79220	16.81207	337.77432	
26	125	13710	13231	0.95386	0.00144	0.00541	0.95026	0.18023	0.66686	62.30409	1.78214	0.10113	4.33935	15.32888	353.10320	
27	130	13800	13321	0.96035	0.00130	0.00685	0.95710	0.16870	0.87232	63.17641	1.85342	0.09102	4.64975	22.47275	375.57595	
28	135	13870	13391	0.96540	0.00101	0.00577	0.96287	0.13626	0.76238	63.93879	1.92471	0.07079	4.24587	22.23905	397.81499	
29	140	13890	13411	0.96684	0.00029	0.00324	0.96612	0.04037	0.44157	64.38036	1.99599	0.02023	1.40735	14.13304	411.94804	
30	145	13950	13471	0.97116	0.00087	0.00288	0.96900	0.12544	0.41453	64.79490	2.06728	0.06068	4.84804	15.63848	427.58652	
31	150	14020	13541	0.97621	0.00101	0.00469	0.97369	0.15139	0.69209	65.48699	2.13856	0.07079	6.43684	28.21220	455.79872	
32	155	14060	13581	0.97909	0.00058	0.00397	0.97765	0.08940	0.60198	66.08896	2.20985	0.04045	4.15320	26.47508	482.27380	
33	160	14090	13611	0.98126	0.00043	0.00252	0.98017	0.06921	0.39651	66.48547	2.28113	0.03034	3.49278	19.11493	501.38872	
34	165	14120	13641	0.98342	0.00043	0.00216	0.98234	0.07137	0.35145	66.83693	2.35242	0.03034	3.89228	18.46265	519.85137	
35	170	14130	13651	0.98414	0.00014	0.00144	0.98378	0.02451	0.23971	67.07663	2.42370	0.01011	1.43781	13.32522	533.17659	
36	175	14180	13701	0.98774	0.00072	0.00216	0.98594	0.12616	0.37669	67.45332	2.49499	0.05057	7.92697	23.41194	556.58853	
37	180	14220	13741	0.99063	0.00058	0.00324	0.98919	0.10381	0.57494	68.02826	2.56627	0.04045	6.96076	37.21933	593.80785	
38	185	14240	13761	0.99207	0.00029	0.00216	0.99135	0.05335	0.39291	68.42117	2.63756	0.02023	3.80439	26.91289	620.72074	
39	190	14270	13791	0.99423	0.00043	0.00180	0.99315	0.08219	0.33884	68.76000	2.70885	0.03034	6.21424	25.04658	645.76732	
40	195	14280	13801	0.99495	0.00014	0.00144	0.99459	0.02812	0.27576	69.03576	2.78013	0.01011	2.24784	21.15519	666.92251	
41	200	14280	13801	0.99495	0.00000	0.00036	0.99495	0.00000	0.07029	69.10605	2.85142	0.00000	0.00000	5.61959	672.54210	
42	205	14350	13871	1.00000	0.00101	0.00252	0.99748	0.20691	0.51727	69.62331	2.92270	0.07079	18.35620	45.89051	718.43261	
43	210	14350	13871	1.00000	0.00000	0.00252	1.00000	0.00000	0.51727	70.14058	2.99399	0.00000	0.00000	45.89051	764.32311	
44	215	14350	13871	1.00000	0.00000	0.00000	1.00000	0.00000	0.00000	70.14058	3.06527	0.00000	0.00000	0.00000	764.32311	
45	220	14360	13881	1.00072	0.00014	0.00036	1.00036	0.03172	0.07930	70.21988	3.13656	0.01011	3.23810	8.09525	772.41836	
46	225	14370	13891	1.00144	0.00014	0.00072	1.00108	0.03244	0.16041	70.38029	3.20784	0.01011	3.45778	16.73970	789.15806	
47	230	14390	13911	1.00288	0.00029	0.00108	1.00216	0.06633	0.24692	70.62721	3.27913	0.02023	7.36934	27.06781	816.22587	
48	235	14390	13911	1.00288	0.00000	0.00072	1.00288	0.00000	0.16581	70.79302	3.35041	0.00000	0.00000	18.42335	834.64922	
49	240	14400	13921	1.00360	0.00014	0.00036	1.00324	0.03460	0.08651	70.87953	3.42170	0.01011	4.16008	10.40020	845.04942	
50	300	14400	13921	1.00360	0.00000	0.00433	1.00757	0.00000	1.03814	71.91767	4.27712	0.00000	0.00000	124.80235	969.85177	
51	360	14440	13961	1.00649	0.00005	0.00144	1.00901	0.01730	0.51907	72.43674	5.13255	0.00337	4.03809	121.14265	1090.99441	
52	420	14450	13971	1.00721	0.00001	0.00180	1.01081	0.00505	0.67046	73.10720	5.98797	0.00084	1.47071	165.26406	1256.25847	
53	480	14460	13981	1.00793	0.00001	0.00072	1.01153	0.00577	0.32442	73.43162	6.84340	0.00084	2.01842	104.67391	1360.93238	
54	540															
55	600															

		7 cells													
Flow rate, L/min				1											
C back, uS/cm				467											
Co, uS/cm				11610											
Mean det. time, sec				79.12											
Actual volume, ml				1318.73											
Sample	Time, sec	C, uS/cm	C corr., uS/cm	F(t)	E(t)	Partial E(t)	Cum. E(t)	tE(t)	Partial tE(t)	Cum. tE(t)	θ	E(θ)	(t−τ)²E(t)	Partial (t−τ)²E(t)	Cum. (t−τ)²E(t)=σ²
1	0	467	0	0.00000	0.00000	0.00000	0.00000	0.00000	0.00000	0.00000	0.00000	0.00000	0.00000	0.00000	0.00000
2	5	467	0	0.00000	0.00000	0.00000	0.00000	0.00000	0.00000	0.00000	0.06319	0.00000	0.00000	0.00000	0.00000
3	10	467	0	0.00000	0.00000	0.00000	0.00000	0.00000	0.00000	0.00000	0.12638	0.00000	0.00000	0.00000	0.00000
4	15	467	0	0.00000	0.00000	0.00000	0.00000	0.00000	0.00000	0.00000	0.18958	0.00000	0.00000	0.00000	0.00000
5	20	467	0	0.00000	0.00000	0.00000	0.00000	0.00000	0.00000	0.00000	0.25277	0.00000	0.00000	0.00000	0.00000
6	25	467	0	0.00000	0.00000	0.00000	0.00000	0.00000	0.00000	0.00000	0.31596	0.00000	0.00000	0.00000	0.00000
7	30	467	0	0.00000	0.00000	0.00000	0.00000	0.00000	0.00000	0.00000	0.37915	0.00000	0.00000	0.00000	0.00000
8	35	480	13	0.00117	0.00023	0.00058	0.00058	0.00817	0.02042	0.02042	0.44235	0.01846	0.45427	1.13568	1.13568
9	40	549	82	0.00736	0.00124	0.00368	0.00426	0.04954	0.14426	0.16468	0.50554	0.09799	1.89564	5.87478	7.01045
10	45	785	318	0.02854	0.00424	0.01369	0.01795	0.19061	0.60038	0.76505	0.56873	0.33516	4.93232	17.06390	24.08035
11	50	1156	689	0.06183	0.00666	0.02724	0.04519	0.33294	1.30889	2.07395	0.63192	0.52688	5.64799	26.45077	50.53113
12	55	1986	1519	0.13632	0.01490	0.05389	0.09908	0.81935	2.88073	4.95468	0.69511	1.17872	8.66947	35.79365	86.32477
13	60	3570	3103	0.27847	0.02843	0.10832	0.20739	1.70582	6.31293	11.26761	0.75831	2.24952	10.39741	47.66721	133.99198
14	65	5110	4643	0.41667	0.02764	0.14018	0.34757	1.79664	8.75617	20.02378	0.82150	2.18703	5.51370	39.77779	173.76977
15	70	6420	5953	0.53424	0.02351	0.12788	0.47546	1.64588	8.60630	28.63008	0.88469	1.86040	1.95721	18.67729	192.44706
16	75	7380	6913	0.62039	0.01723	0.10186	0.57731	1.29229	7.34542	35.97550	0.94788	1.36334	0.29300	5.62553	198.07259
17	80	8110	7643	0.68590	0.01310	0.07583	0.65315	1.04819	5.85121	41.82671	1.01108	1.03671	0.01006	0.75765	198.83024
18	85	8940	8473	0.76039	0.01490	0.07000	0.72314	1.26627	5.78614	47.61285	1.07427	1.17872	0.51442	1.31121	200.14145
19	90	9310	8843	0.79359	0.00664	0.05385	0.77699	0.59768	4.65988	52.27273	1.13746	0.52546	0.78559	3.25002	203.39147
20	95	9730	9263	0.83128	0.00754	0.03545	0.81244	0.71614	3.28457	55.55730	1.20065	0.59646	1.90011	6.71423	210.10570
21	100	10090	9623	0.86359	0.00646	0.03500	0.84744	0.64615	3.40573	58.96303	1.26384	0.51125	2.81604	11.79036	221.89607
22	105	10290	9823	0.88154	0.00359	0.02513	0.87257	0.37692	2.55766	61.52069	1.32704	0.28403	2.40361	13.04912	234.94518
23	110	10470	10003	0.89769	0.00323	0.01705	0.88962	0.35538	1.83075	63.35143	1.39023	0.25563	3.08001	13.70904	248.65422
24	115	10620	10153	0.91115	0.00269	0.01481	0.90442	0.30961	1.66248	65.01391	1.45342	0.21302	3.46526	16.36316	265.01738
25	120	10810	10343	0.92821	0.00341	0.01526	0.91968	0.40923	1.79709	66.81100	1.51661	0.26983	5.69804	22.90823	287.92561
26	125	10920	10453	0.93808	0.00197	0.01346	0.93314	0.24679	1.64004	68.45105	1.57981	0.15622	4.15526	24.63324	312.55885
27	130	10970	10503	0.94256	0.00090	0.00718	0.94032	0.11667	0.90864	69.35969	1.64300	0.07101	2.32289	16.19538	328.75424
28	135	11050	10583	0.94974	0.00144	0.00583	0.94615	0.19384	0.77627	70.13596	1.70619	0.11361	4.48305	17.01486	345.76910
29	140	11090	10623	0.95333	0.00072	0.00538	0.95154	0.10051	0.73589	70.87185	1.76938	0.05681	2.66063	17.85921	363.62831
30	145	11160	10693	0.95962	0.00126	0.00494	0.95647	0.18218	0.70672	71.57857	1.83257	0.09941	5.45236	20.28249	383.91080
31	150	11180	10713	0.96141	0.00036	0.00404	0.96051	0.05385	0.59006	72.16863	1.89577	0.02840	1.80327	18.13908	402.04987
32	155	11240	10773	0.96680	0.00108	0.00359	0.96410	0.16692	0.55192	72.72054	1.95896	0.08521	6.20000	20.00818	422.05805
33	160	11270	10803	0.96949	0.00054	0.00404	0.96814	0.08615	0.63268	73.35323	2.02215	0.04260	3.52202	24.30506	446.36311
34	165	11380	10913	0.97936	0.00197	0.00628	0.97442	0.32577	1.02979	74.38302	2.08534	0.15622	14.56021	45.20557	491.56868
35	170	11390	10923	0.98026	0.00018	0.00538	0.97981	0.03051	0.89069	75.27371	2.14854	0.01420	1.48228	40.10621	531.67489
36	175	11450	10983	0.98564	0.00108	0.00314	0.98295	0.18846	0.54743	75.82114	2.21173	0.08521	9.89324	28.45380	560.12869
37	180	11480	11013	0.98833	0.00054	0.00404	0.98699	0.09692	0.71345	76.53460	2.27492	0.04260	5.47933	38.44644	598.57513
38	185	11480	11013	0.98833	0.00000	0.00135	0.98833	0.00000	0.24230	76.77690	2.33811	0.00000	0.00000	13.69833	612.27346
39	190	11530	11063	0.99282	0.00090	0.00224	0.99058	0.17051	0.42628	77.20318	2.40130	0.07101	11.03254	27.58136	639.85482
40	195	11530	11063	0.99282	0.00000	0.00224	0.99282	0.00000	0.42628	77.62945	2.46450	0.00000	0.00000	27.58136	667.43617
41	200	11550	11083	0.99462	0.00036	0.00090	0.99372	0.07179	0.17948	77.80894	2.52769	0.02840	5.24494	13.11235	680.54852
42	205	11560	11093	0.99551	0.00018	0.00135	0.99506	0.03679	0.27147	78.08041	2.59088	0.01420	2.84391	20.22213	700.77065
43	210	11590	11123	0.99821	0.00054	0.00179	0.99686	0.11308	0.37467	78.45508	2.65407	0.04260	9.22298	30.16723	730.93788
44	215	11610	11143	1.00000	0.00036	0.00224	0.99910	0.07718	0.47563	78.93072	2.71727	0.02840	6.62744	39.62604	770.56392
45	220	11610	11143	1.00000	0.00000	0.00090	1.00000	0.00000	0.19295	79.12367	2.78046	0.00000	0.00000	16.56859	787.13251
46	225	11610	11143	1.00000	0.00000	0.00000	1.00000	0.00000	0.00000	79.12367	2.84365	0.00000	0.00000	0.00000	787.13251
47	230	11610	11143	1.00000	0.00000	0.00000	1.00000	0.00000	0.00000	79.12367	2.90684	0.00000	0.00000	0.00000	787.13251
48	235	11620	11153	1.00090	0.00018	0.00045	1.00045	0.04218	0.10545	79.22911	2.97003	0.01420	4.36102	10.90255	798.03507
49	240	11620	11153	1.00090	0.00000	0.00045	1.00090	0.00000	0.10545	79.33456	3.03323	0.00000	0.00000	10.90255	808.93762
50	300	11640	11173	1.00269	0.00003	0.00090	1.00179	0.00897	0.26923	79.60379	3.79153	0.00237	1.45940	43.78207	852.71969
51	360	11670	11203	1.00538	0.00004	0.00224	1.00404	0.01615	0.75384	80.35762	4.54984	0.00355	3.53996	149.98082	1002.70051
52	420	11670	11203	1.00538	0.00000	0.00135	1.00538	0.00000	0.48461	80.84223	5.30815	0.00000	0.00000	106.19876	1108.89926
53	480	11680	11213	1.00628	0.00001	0.00045	1.00583	0.00718	0.21538	81.05761	6.06645	0.00118	2.40363	72.10887	1181.00814
54	540	11680	11213	1.00628	0.00000	0.00045	1.00628	0.00000	0.21538	81.27300	6.82476	0.00000	0.00000	72.10887	1253.11701
55	600														

		8 cells														
Flow rate, L/min		0.98														
C back, uS/cm		393														
Co, uS/cm		14140														
Mean det. time, sec		87.75														
Actual volume, ml		1433.20														
Sample	Time, sec	C, uS/cm	C corr., uS/cm	F(t)	E(t)	Partial E(t)	Cum. E(t)	tE(t)	Partial tE(t)	Cum. tE(t)	θ	E(θ)	(t−τ)²E(t)	Partial (t−τ)²E(t)	Cum. (t−τ)²E(t)=σ²	
1	0	393	0	0.00000	0.00000	0.00000	0.00000	0.00000	0.00000	0.00000	0.00000	0.00000	0.00000	0.00000		
2	5	393	0	0.00000	0.00000	0.00000	0.00000	0.00000	0.00000	0.00000	0.05698	0.00000	0.00000	0.00000	0.00000	
3	10	393	0	0.00000	0.00000	0.00000	0.00000	0.00000	0.00000	0.00000	0.11396	0.00000	0.00000	0.00000	0.00000	
4	15	393	0	0.00000	0.00000	0.00000	0.00000	0.00000	0.00000	0.00000	0.17095	0.00000	0.00000	0.00000	0.00000	
5	20	393	0	0.00000	0.00000	0.00000	0.00000	0.00000	0.00000	0.00000	0.22793	0.00000	0.00000	0.00000	0.00000	
6	25	393	0	0.00000	0.00000	0.00000	0.00000	0.00000	0.00000	0.00000	0.28491	0.00000	0.00000	0.00000	0.00000	
7	30	393	0	0.00000	0.00000	0.00000	0.00000	0.00000	0.00000	0.00000	0.34189	0.00000	0.00000	0.00000	0.00000	
8	35	393	0	0.00000	0.00000	0.00000	0.00000	0.00000	0.00000	0.00000	0.39888	0.00000	0.00000	0.00000	0.00000	
9	40	404	11	0.00080	0.00016	0.00040	0.00040	0.00640	0.01600	0.01600	0.45586	0.01404	0.36484	0.91210	0.91210	
10	45	431	38	0.00276	0.00039	0.00138	0.00178	0.01768	0.06019	0.07620	0.51284	0.03447	0.71778	2.70656	3.61866	
11	50	572	179	0.01302	0.00205	0.00611	0.00789	0.10257	0.30061	0.37681	0.56982	0.18000	2.92281	9.10149	12.72015	
12	55	1128	735	0.05347	0.00809	0.02535	0.03324	0.44490	1.36866	1.74547	0.62680	0.70979	8.67429	28.99276	41.71291	
13	60	2430	2037	0.14818	0.01894	0.06758	0.10082	1.13654	3.95359	5.69906	0.68379	1.66213	14.58338	58.14419	99.85710	
14	65	4020	3627	0.26384	0.02313	0.10519	0.20601	1.50360	6.60035	12.29941	0.74077	2.02979	11.96903	66.38104	166.23814	
15	70	5610	5217	0.37950	0.02313	0.11566	0.32167	1.61926	7.80716	20.10657	0.79775	2.02979	7.28548	48.13629	214.37443	
16	75	7050	6657	0.48425	0.02095	0.11021	0.43188	1.57125	7.97629	28.08285	0.85473	1.83830	3.40397	26.72363	241.09806	
17	80	8170	7777	0.56572	0.01629	0.09311	0.52499	1.30356	7.18702	35.26988	0.91171	1.42979	0.97787	10.95461	252.05267	
18	85	9150	8757	0.63701	0.01426	0.07638	0.60137	1.21190	6.28864	41.55852	0.96870	1.25106	0.10757	2.71361	254.76628	
19	90	9910	9517	0.69230	0.01106	0.06329	0.66465	0.99513	5.51757	47.07609	1.02568	0.97021	0.05614	0.40927	255.17555	
20	95	10470	10077	0.73303	0.00815	0.04801	0.71266	0.77399	4.42278	51.49887	1.08266	0.71489	0.42862	1.21189	256.38744	
21	100	10980	10587	0.77013	0.00742	0.03892	0.75158	0.74198	3.78992	55.28879	1.13964	0.65106	1.11402	3.85660	260.24403	
22	105	11440	11047	0.80359	0.00669	0.03528	0.78686	0.70270	3.61170	58.90049	1.19663	0.58723	1.99214	7.76540	268.00943	
23	110	11800	11407	0.82978	0.00524	0.02982	0.81669	0.57613	3.19706	62.09755	1.25361	0.45957	2.59364	11.46446	279.47390	
24	115	12190	11797	0.85815	0.00567	0.02728	0.84397	0.65251	3.07158	65.16913	1.31059	0.49787	4.21427	17.01978	296.49368	
25	120	12490	12097	0.87997	0.00436	0.02510	0.86906	0.52375	2.94064	68.10977	1.36757	0.38298	4.54035	21.88655	318.38023	
26	125	12850	12457	0.90616	0.00524	0.02401	0.89307	0.65469	2.94610	71.05587	1.42455	0.45957	7.26862	29.52244	347.90266	
27	130	13150	12757	0.92798	0.00436	0.02401	0.91707	0.56740	3.05521	74.11108	1.48154	0.38298	7.79225	37.65219	385.55485	
28	135	13250	12857	0.93526	0.00145	0.01455	0.93162	0.19641	1.90951	76.02059	1.53852	0.12766	3.24851	27.60191	413.15676	
29	140	13390	12997	0.94544	0.00204	0.00873	0.94035	0.28515	1.20390	77.22449	1.59550	0.17872	5.56130	22.02453	435.18130	
30	145	13480	13087	0.95199	0.00131	0.00837	0.94872	0.18986	1.18753	78.41202	1.65248	0.11489	4.29205	24.63336	459.81466	
31	150	13520	13127	0.95490	0.00058	0.00473	0.95344	0.08729	0.69288	79.10490	1.70946	0.05106	2.25531	16.36838	476.18304	
32	155	13580	13187	0.95926	0.00087	0.00364	0.95708	0.13530	0.55649	79.66138	1.76645	0.07660	3.94820	15.50877	491.69182	
33	160	13630	13237	0.96290	0.00073	0.00400	0.96108	0.11639	0.62923	80.29061	1.82343	0.06383	3.79758	19.36445	511.05626	
34	165	13700	13307	0.96799	0.00102	0.00436	0.96545	0.16804	0.71106	81.00167	1.88041	0.08936	6.07790	24.68868	535.74494	
35	170	13720	13327	0.96945	0.00029	0.00327	0.96872	0.04947	0.54376	81.54543	1.93739	0.02553	1.96860	20.11624	555.86119	
36	175	13800	13407	0.97527	0.00116	0.00364	0.97236	0.20368	0.63287	82.17829	1.99438	0.10213	8.86084	27.07361	582.93480	
37	180	13830	13437	0.97745	0.00044	0.00400	0.97636	0.07856	0.70561	82.88390	2.05136	0.03830	3.71455	31.43848	614.37328	
38	185	13890	13497	0.98181	0.00087	0.00327	0.97963	0.16149	0.60013	83.48403	2.10834	0.07660	8.25622	29.92693	644.30021	
39	190	13930	13537	0.98472	0.00058	0.00364	0.98327	0.11057	0.68015	84.16418	2.16532	0.05106	6.08466	35.85219	680.15240	
40	195	13940	13547	0.98545	0.00015	0.00182	0.98509	0.02837	0.34735	84.51153	2.22230	0.01277	1.67357	19.39555	699.54795	
41	200	13990	13597	0.98909	0.00073	0.00218	0.98727	0.14549	0.43464	84.94617	2.27929	0.06383	9.16621	27.09943	726.64739	
42	205	13990	13597	0.98909	0.00000	0.00182	0.98909	0.00000	0.36372	85.30989	2.33627	0.00000	0.00000	22.91552	749.56290	
43	210	14000	13607	0.98982	0.00015	0.00036	0.98945	0.03055	0.07638	85.38627	2.39325	0.01277	2.17442	5.43604	754.99894	
44	215	14010	13617	0.99054	0.00015	0.00073	0.99018	0.03128	0.15458	85.54085	2.45023	0.01277	2.35591	11.32583	766.32477	
45	220	14060	13667	0.99418	0.00073	0.00218	0.99236	0.16003	0.47829	86.01913	2.50721	0.06383	12.72344	37.69839	804.02316	
46	225	14090	13697	0.99636	0.00044	0.00291	0.99527	0.09820	0.64560	86.66473	2.56420	0.03830	8.22221	52.36412	856.38728	
47	230	14140	13747	1.00000	0.00073	0.00291	0.99818	0.16731	0.66378	87.32851	2.62118	0.06383	14.72029	57.35623	913.74351	
48	235	14140	13747	1.00000	0.00000	0.00182	1.00000	0.00000	0.41827	87.74678	2.67816	0.00000	0.00000	36.80072	950.54423	
49	240	14180	13787	1.00291	0.00058	0.00145	1.00145	0.13967	0.34917	88.09595	2.73514	0.05106	13.49010	33.72524	984.26947	
50	300	14230	13837	1.00655	0.00006	0.01928	1.02073	0.01819	4.73558	92.83153	3.41893	0.00532	2.73099	486.63243	1470.90190	
51	360	14230	13837	1.00655	0.00000	0.00182	1.02255	0.00000	0.54557	93.37710	4.10271	0.00000	0.00000	81.92956	1552.83146	
52	420	14250	13857	1.00800	0.00002	0.00073	1.02328	0.01018	0.30552	93.68262	4.78650	0.00213	2.67676	80.30276	1633.13422	
53	480	14260	13867	1.00873	0.00001	0.00109	1.02437	0.00582	0.48010	94.16273	5.47029	0.00106	1.86541	136.26500	1769.39922	
54	540	14260	13867	1.00873	0.00000	0.00036	1.02473	0.00000	0.17458	94.33731	6.15407	0.00000	0.00000	55.96224	1825.36146	
55	600	14260	13867	1.00873	0.00000	0.00000	1.02473	0.00000	0.00000	94.33731	6.83786	0.00000	0.00000	0.00000	1825.36146	

Table 7. Step input tracer test results for 1-cell through 8-cell reactor with vertical slots and Q=0.5 l min^{-1}

	1 cell													
Flow rate, L/min	0.53													
C back, uS/cm	396													
Co, uS/cm	14980													
Mean det. time, sec	49.01													
Actual volume, ml	432.89													
Sample	**Time, sec**	**C, uS/cm**	**C corr, uS/cm**	**F(t)**	**E(t)**	**Partial E(t)**	**Cum. E(t)**	**tE(t)**	**Partial tE(t)**	**Cum. tE(t)**	**θ**	**E(θ)**	**(t−τ)²E(t)**	**Partial (t−τ)²E(t)**	**Cum. (t−τ)²E(t)=σ²**
1	0	396	0	0.00000	0.00000	0.00000	0.00000	0.00000	0.00000	0.00000	0.00000	0.00000	0.00000	0.00000	0.00000
2	5	396	0	0.00000	0.00000	0.00000	0.00000	0.00000	0.00000	0.00000	0.10203	0.00000	0.00000	0.00000	0.00000
3	10	407	11	0.00075	0.00015	0.00038	0.00038	0.00151	0.00377	0.00377	0.20405	0.00739	0.22952	0.57380	0.57380
4	15	484	88	0.00603	0.00106	0.00302	0.00339	0.01584	0.04337	0.04714	0.30608	0.05175	1.22114	3.62666	4.20045
5	20	503	107	0.00734	0.00026	0.00329	0.00669	0.00521	0.05263	0.09977	0.40811	0.01277	0.21923	3.60093	7.80138
6	25	1322	926	0.06349	0.01123	0.02873	0.03542	0.28079	0.71500	0.81476	0.51014	0.55042	6.47281	16.73010	24.53148
7	30	2950	2554	0.17512	0.02233	0.08389	0.11931	0.66978	2.37641	3.19117	0.61216	1.09411	8.06510	36.34477	60.87625
8	35	5080	4684	0.32117	0.02921	0.12884	0.24815	1.02235	4.23032	7.42149	0.71419	1.43148	5.73045	34.48887	95.36512
9	40	8340	7944	0.54471	0.04471	0.18479	0.43294	1.78826	7.02654	14.44803	0.81622	2.19091	3.62642	23.39217	118.75729
10	45	9610	9214	0.63179	0.01742	0.15531	0.58825	0.78374	6.42939	20.87802	0.91825	0.85351	0.27956	9.76494	128.52223
11	50	10570	10174	0.69761	0.01317	0.07645	0.66470	0.65826	3.60498	24.48300	1.02027	0.64518	0.01300	0.73139	129.25362
12	55	11350	10954	0.75110	0.01070	0.05965	0.72436	0.58832	3.11643	27.59942	1.12230	0.52420	0.38425	0.99312	130.24674
13	60	12070	11674	0.80047	0.00987	0.05143	0.77578	0.59243	2.95187	30.55129	1.22433	0.48388	1.19333	3.94397	134.19071
14	65	12640	12244	0.83955	0.00782	0.04423	0.82001	0.50809	2.75130	33.30259	1.32636	0.38307	1.99949	7.98205	142.17276
15	70	13060	12664	0.86835	0.00576	0.03394	0.85395	0.40318	2.27818	35.58077	1.42838	0.28226	2.53848	11.34493	153.51768
16	75	13500	13104	0.89852	0.00603	0.02948	0.88343	0.45255	2.13933	37.72010	1.53041	0.29571	4.07697	16.53863	170.05632
17	80	13820	13424	0.92046	0.00439	0.02606	0.90949	0.35107	2.00905	39.72916	1.63244	0.21506	4.21547	20.73110	190.78742
18	85	14050	13654	0.93623	0.00315	0.01886	0.92835	0.26810	1.54793	41.27708	1.73447	0.15457	4.08630	20.75444	211.54185
19	90	14270	13874	0.95132	0.00302	0.01543	0.94377	0.27153	1.34908	42.62617	1.83649	0.14785	5.06999	22.89074	234.43259
20	95	14330	13934	0.95543	0.00082	0.00960	0.95337	0.07817	0.87425	43.50041	1.93852	0.04032	1.74060	17.02647	251.45906
21	100	14490	14094	0.96640	0.00219	0.00754	0.96092	0.21942	0.74397	44.24438	2.04055	0.10753	5.70563	18.61558	270.07464
22	105	14620	14224	0.97532	0.00178	0.00994	0.97086	0.18719	1.01652	45.26090	2.14258	0.08737	5.58950	28.23783	298.31247
23	110	14660	14264	0.97806	0.00055	0.00583	0.97669	0.06034	0.61883	45.87973	2.24460	0.02688	2.04071	19.07552	317.38799
24	115	14700	14304	0.98080	0.00055	0.00274	0.97943	0.06308	0.30856	46.18829	2.34663	0.02688	2.38900	11.07428	328.46227
25	120	14760	14364	0.98491	0.00082	0.00343	0.98286	0.09874	0.40455	46.59284	2.44866	0.04032	4.14708	16.34020	344.80247
26	125	14770	14374	0.98560	0.00014	0.00240	0.98526	0.01714	0.28970	46.88254	2.55068	0.00672	0.79197	12.34762	357.15009
27	130	14820	14424	0.98903	0.00069	0.00206	0.98731	0.08914	0.26570	47.14824	2.65271	0.03360	4.49805	13.22504	370.37513
28	135	14850	14454	0.99109	0.00041	0.00274	0.99006	0.05554	0.36170	47.50994	2.75474	0.02016	3.04233	18.85095	389.22608
29	140	14890	14494	0.99383	0.00055	0.00240	0.99246	0.07680	0.33084	47.84078	2.85677	0.02688	4.54187	18.96050	408.18658
30	145	14900	14504	0.99451	0.00014	0.00171	0.99417	0.01988	0.24170	48.08249	2.95879	0.00672	1.26368	14.51387	422.70045
31	150	14940	14544	0.99726	0.00055	0.00171	0.99589	0.08228	0.25542	48.33790	3.06082	0.02688	5.59501	17.14672	439.84717
32	155	14940	14544	0.99726	0.00000	0.00137	0.99726	0.00000	0.20570	48.54361	3.16285	0.00000	0.00000	13.98752	453.83469
33	160	14950	14554	0.99794	0.00014	0.00034	0.99760	0.02194	0.05485	48.59846	3.26488	0.00672	1.68946	4.22366	458.05835
34	165	14970	14574	0.99931	0.00027	0.00103	0.99863	0.04526	0.16799	48.76646	3.36690	0.01344	3.69021	13.44918	471.50753
35	170	14970	14574	0.99931	0.00000	0.00069	0.99931	0.00000	0.11314	48.87959	3.46893	0.00000	0.00000	9.22552	480.73306
36	175	14970	14574	0.99931	0.00000	0.00000	0.99931	0.00000	0.00000	48.87959	3.57096	0.00000	0.00000	0.00000	480.73306
37	180	14970	14574	0.99931	0.00000	0.00000	0.99931	0.00000	0.00000	48.87959	3.67299	0.00000	0.00000	0.00000	480.73306
38	185	14980	14584	1.00000	0.00014	0.00034	0.99966	0.02537	0.06343	48.94302	3.77501	0.00672	2.53624	6.34059	487.07365
39	190	14980	14584	1.00000	0.00000	0.00034	1.00000	0.00000	0.06343	49.00645	3.87704	0.00000	0.00000	6.34059	493.41425
40	195	14980	14584	1.00000	0.00000	0.00000	1.00000	0.00000	0.00000	49.00645	3.97907	0.00000	0.00000	0.00000	493.41425
41	200	15000	14604	1.00137	0.00027	0.00069	1.00069	0.05485	0.13714	49.14358	4.08110	0.01344	6.25317	15.63292	509.04717
42	205	15010	14614	1.00206	0.00014	0.00103	1.00171	0.02811	0.20742	49.35100	4.18312	0.00672	3.33708	23.97562	533.02279
43	210	15020	14624	1.00274	0.00014	0.00069	1.00240	0.02880	0.14228	49.49328	4.28515	0.00672	3.55443	17.22878	550.25158
44	215	15020	14624	1.00274	0.00000	0.00034	1.00274	0.00000	0.07200	49.56528	4.38718	0.00000	0.00000	8.88608	559.13766
45	220	15040	14644	1.00411	0.00027	0.00069	1.00343	0.06034	0.15085	49.71613	4.48921	0.01344	8.01942	20.04854	579.18620
46	225	15040	14644	1.00411	0.00000	0.00069	1.00411	0.00000	0.15085	49.86698	4.59123	0.00000	0.00000	20.04854	599.23474
47	230														
48	235														
49	240														
50	300														
51	360														
52	420														
53	480														
54	540														
55	600														

	2 cells														
Flow rate, L/min	0.52														
C back, uS/cm	408														
Co, uS/cm	14940														
Mean det. time, sec	65.60														
Actual volume, ml	568.55														
Sample	Time, sec	C, uS/cm	C corr., uS/cm	F(t)	E(t)	Partial E(t)	Cum. E(t)	tE(t)	Partial tE(t)	Cum. tE(t)	θ	E(θ)	(t−τ)*E(t)	Partial (t−τ)*E(t)	Cum. (t−τ)*E(t)=σ²
1	0	408	0	0.00000	0.00000	0.00000	0.00000	0.00000	0.00000	0.00000	0.00000	0.00000	0.00000	0.00000	0.00000
2	5	408	0	0.00000	0.00000	0.00000	0.00000	0.00000	0.00000	0.00000	0.07622	0.00000	0.00000	0.00000	0.00000
3	10	408	0	0.00000	0.00000	0.00000	0.00000	0.00000	0.00000	0.00000	0.15243	0.00000	0.00000	0.00000	0.00000
4	15	408	0	0.00000	0.00000	0.00000	0.00000	0.00000	0.00000	0.00000	0.22865	0.00000	0.00000	0.00000	0.00000
5	20	411	3	0.00021	0.00004	0.00010	0.00010	0.00083	0.00206	0.00206	0.30487	0.00271	0.08586	0.21466	0.21466
6	25	446	38	0.00261	0.00048	0.00131	0.00141	0.01204	0.03217	0.03423	0.38108	0.03160	0.79410	2.19992	2.41457
7	30	673	265	0.01824	0.00312	0.00901	0.01043	0.09372	0.26442	0.29865	0.45730	0.20495	3.95996	11.88515	14.29973
8	35	984	576	0.03964	0.00428	0.01851	0.02894	0.14981	0.60883	0.90748	0.53352	0.28079	4.00846	19.92105	34.22078
9	40	2677	2269	0.15614	0.02330	0.06895	0.09789	0.93201	2.70455	3.61203	0.60973	1.52856	15.27303	48.20372	82.42449
10	45	5080	4672	0.32150	0.03307	0.14093	0.23882	1.48823	6.05061	9.66264	0.68595	2.16959	14.03772	73.27687	155.70137
11	50	6850	6442	0.44330	0.02436	0.14358	0.38240	1.21800	6.76559	16.42823	0.76217	1.59808	5.93013	49.91963	205.62100
12	55	8270	7862	0.54101	0.01954	0.10976	0.49216	1.07487	5.73218	22.16040	0.83838	1.28207	2.19688	20.31753	225.93853
13	60	9100	8692	0.59813	0.01142	0.07742	0.56957	0.68538	4.40063	26.56104	0.91460	0.74938	0.35854	6.38856	232.32709
14	65	9910	9502	0.65387	0.01115	0.05643	0.62600	0.72461	3.52498	30.08602	0.99082	0.73132	0.00405	0.90647	233.23356
15	70	10540	10132	0.69722	0.00867	0.04355	0.67554	0.60694	3.32886	33.41488	1.06703	0.56881	0.16767	0.42930	233.66286
16	75	11120	10712	0.73713	0.00798	0.04163	0.71718	0.59868	3.01404	36.42892	1.14325	0.52366	0.70495	2.18157	235.84443
17	80	11720	11312	0.77842	0.00826	0.04060	0.75778	0.66061	3.14822	39.57714	1.21947	0.54172	1.71172	6.04168	241.88611
18	85	12180	11772	0.81007	0.00633	0.03647	0.79425	0.53812	2.99683	42.57397	1.29568	0.41532	2.38208	10.23448	252.12059
19	90	12560	12152	0.83622	0.00523	0.02890	0.82315	0.47069	2.52202	45.09600	1.37190	0.34309	3.11301	13.73771	265.85830
20	95	12880	12472	0.85824	0.00440	0.02408	0.84723	0.41839	2.22268	47.31868	1.44812	0.28892	3.80607	17.29769	283.15599
21	100	13240	12832	0.88302	0.00495	0.02340	0.87063	0.49546	2.28461	49.60329	1.52433	0.32503	5.86222	24.17071	307.32669
22	105	13530	13122	0.90297	0.00399	0.02236	0.89299	0.41908	2.28633	51.88962	1.60055	0.26183	6.19499	30.14302	337.46971
23	110	13780	13372	0.92018	0.00344	0.01858	0.91157	0.37848	1.99388	53.88350	1.67677	0.22572	6.78207	32.44266	369.91237
24	115	13990	13582	0.93463	0.00289	0.01583	0.92740	0.33237	1.77711	55.66061	1.75298	0.18960	7.05236	34.58608	404.49845
25	120	14110	13702	0.94288	0.00165	0.01135	0.93876	0.19818	1.32638	56.98699	1.82920	0.10834	4.88702	29.84846	434.34691
26	125	14280	13872	0.95458	0.00234	0.00998	0.94873	0.29246	1.22660	58.21360	1.90542	0.15349	8.25449	32.85379	467.20069
27	130	14430	14022	0.96491	0.00206	0.01101	0.95974	0.26837	1.40208	59.61568	1.98163	0.13543	8.56119	42.03922	509.23991
28	135	14550	14142	0.97316	0.00165	0.00929	0.96903	0.22296	1.22832	60.84400	2.05785	0.10834	7.95379	41.28745	550.52737
29	140	14670	14262	0.98142	0.00165	0.00826	0.97729	0.23121	1.13543	61.97942	2.13407	0.10834	9.14119	42.73745	593.26482
30	145	14750	14342	0.98693	0.00110	0.00688	0.98417	0.15965	0.97715	62.95658	2.21028	0.07223	6.94079	40.20495	633.46977
31	150	14820	14412	0.99174	0.00096	0.00516	0.98933	0.14451	0.76039	63.71697	2.28650	0.06320	6.86218	34.50742	667.97719
32	155	14890	14482	0.99656	0.00096	0.00482	0.99415	0.14933	0.73459	64.45156	2.36272	0.06320	7.69934	36.40381	704.38100
33	160	14940	14532	1.00000	0.00069	0.00413	0.99828	0.11010	0.64857	65.10012	2.43893	0.04514	6.13191	34.57814	738.95915
34	165	14980	14572	1.00275	0.00055	0.00310	1.00138	0.09083	0.50234	65.60246	2.51515	0.03611	5.43896	28.92718	767.88633
35	170	15040	14632	1.00688	0.00083	0.00344	1.00482	0.14038	0.57803	66.18050	2.59137	0.05417	8.99387	36.09708	803.98341
36	175	15110	14702	1.01170	0.00096	0.00447	1.00929	0.16859	0.77243	66.95293	2.66758	0.06320	11.52969	51.32391	855.30732
37	180	15120	14712	1.01239	0.00014	0.00275	1.01204	0.02477	0.48342	67.43635	2.74380	0.00903	1.80110	33.32698	888.63430
38	185	15170	14762	1.01583	0.00069	0.00206	1.01411	0.12731	0.38020	67.81654	2.82002	0.04514	9.80992	29.02754	917.66185
39	190	15170	14762	1.01583	0.00000	0.00172	1.01583	0.00000	0.31826	68.13481	2.89623	0.00000	0.00000	24.52479	942.18664
40	195	15220	14812	1.01927	0.00069	0.00172	1.01755	0.13419	0.33547	68.47027	2.97245	0.04514	11.52197	28.80492	970.99156
41	200	15230	14822	1.01996	0.00014	0.00206	1.01961	0.02753	0.40428	68.87455	3.04867	0.00903	2.48592	35.01972	1006.01128
42	205	15240	14832	1.02064	0.00014	0.00069	1.02030	0.02821	0.13935	69.01390	3.12488	0.00903	2.67433	12.90062	1018.91190
43	210	15260	14852	1.02202	0.00028	0.00103	1.02133	0.05780	0.21504	69.22894	3.20110	0.01806	5.73924	21.03391	1039.94581
44	215	15270	14862	1.02271	0.00014	0.00103	1.02236	0.02959	0.21848	69.44743	3.27732	0.00903	3.07179	22.02757	1061.97338
45	220	15310	14902	1.02546	0.00055	0.00172	1.02408	0.12111	0.37675	69.82418	3.35353	0.03611	13.12337	40.48790	1102.46128
46	225	15320	14912	1.02615	0.00014	0.00172	1.02581	0.03097	0.38020	70.20438	3.42975	0.00903	3.49678	41.55036	1144.01164
47	230	15320	14912	1.02615	0.00000	0.00034	1.02615	0.00000	0.07742	70.28179	3.50597	0.00000	0.00000	8.74194	1152.75358
48	235	15350	14942	1.02821	0.00041	0.00103	1.02718	0.09703	0.24257	70.52436	3.58218	0.02709	11.84786	29.61966	1182.37324
49	240	15370	14962	1.02959	0.00028	0.00172	1.02890	0.06606	0.40772	70.93208	3.65840	0.01806	8.37173	50.54899	1232.92223
50	300														
51	360														
52	420														
53	480														
54	540														
55	600														

		3 cells													
Flow rate, L/min		0.52													
C back, uS/cm		405													
Co, uS/cm		15370													
Mean det. time, sec		82.17													
Actual volume, ml		712.16													
Sample	Time, sec	C, uS/cm	C corr., uS/cm	F(t)	E(t)	Partial E(t)	Cum. E(t)	tE(t)	Partial tE(t)	Cum. tE(t)	θ	E(θ)	(t−τ)²E(t)	Partial (t−τ)²E(t)	Cum. (t−τ)²E(t)=σ²
1	0	405	0	0.00000	0.00000	0.00000	0.00000	0.00000	0.00000	0.00000	0.00000	0.00000	0.00000	0.00000	0.00000
2	5	405	0	0.00000	0.00000	0.00000	0.00000	0.00000	0.00000	0.00000	0.06085	0.00000	0.00000	0.00000	0.00000
3	10	405	0	0.00000	0.00000	0.00000	0.00000	0.00000	0.00000	0.00000	0.12170	0.00000	0.00000	0.00000	0.00000
4	15	405	0	0.00000	0.00000	0.00000	0.00000	0.00000	0.00000	0.00000	0.18254	0.00000	0.00000	0.00000	0.00000
5	20	405	0	0.00000	0.00000	0.00000	0.00000	0.00000	0.00000	0.00000	0.24339	0.00000	0.00000	0.00000	0.00000
6	25	408	3	0.00020	0.00004	0.00010	0.00010	0.00100	0.00251	0.00251	0.30424	0.00329	0.13105	0.32763	0.32763
7	30	425	20	0.00134	0.00023	0.00067	0.00077	0.00682	0.01955	0.02205	0.36509	0.01867	0.61842	1.87368	2.20132
8	35	444	39	0.00261	0.00025	0.00120	0.00197	0.00889	0.03926	0.06131	0.42593	0.02087	0.56504	2.95866	5.15998
9	40	674	269	0.01798	0.00307	0.00832	0.01029	0.12295	0.32960	0.39091	0.48678	0.25258	5.46686	15.07976	20.23974
10	45	957	552	0.03689	0.00378	0.01714	0.02743	0.17020	0.73288	1.12379	0.54763	0.31079	5.22614	26.73249	46.97223
11	50	2035	1630	0.10892	0.01441	0.04547	0.07290	0.72035	2.22636	3.35015	0.60848	1.18385	14.91211	50.34562	97.31785
12	55	3900	3495	0.23354	0.02492	0.09833	0.17123	1.37087	5.22803	8.57818	0.66932	2.04813	18.40298	83.28772	180.60557
13	60	5710	5305	0.35449	0.02419	0.12279	0.29402	1.45139	7.05563	15.63381	0.73017	1.98773	11.89207	75.73762	256.34319
14	65	7090	6685	0.44671	0.01844	0.10658	0.40060	1.19880	6.62546	22.25927	0.79102	1.51551	5.43869	43.32690	299.67008
15	70	8130	7725	0.51620	0.01390	0.08086	0.48146	0.97294	5.42934	27.68861	0.85187	1.14212	2.05939	18.74521	318.41530
16	75	9030	8625	0.57634	0.01203	0.06482	0.54627	0.90210	4.68760	32.37621	0.91272	0.98838	0.61876	6.69539	325.11069
17	80	9800	9395	0.62780	0.01029	0.05580	0.60207	0.82325	4.31340	36.68961	0.97356	0.84561	0.04857	1.66832	326.77901
18	85	10520	10115	0.67591	0.00962	0.04978	0.65185	0.81791	4.10291	40.79252	1.03441	0.79070	0.07693	0.31375	327.09276
19	90	11000	10595	0.70799	0.00641	0.04009	0.69195	0.57735	3.48814	44.28065	1.09526	0.52713	0.39305	1.17497	328.26773
20	95	11520	11115	0.74273	0.00695	0.03341	0.72536	0.66021	3.09389	47.37454	1.15611	0.57106	1.14353	3.84146	332.10919
21	100	11990	11585	0.77414	0.00628	0.03308	0.75844	0.62813	3.22085	50.59539	1.21695	0.51615	1.99635	7.84970	339.95889
22	105	12370	11965	0.79953	0.00508	0.02840	0.78684	0.53324	2.90344	53.49883	1.27780	0.41731	2.64641	11.60690	351.56579
23	110	12760	12355	0.82559	0.00521	0.02573	0.81256	0.57334	2.76646	56.26529	1.33865	0.42830	4.03617	16.70645	368.27224
24	115	13060	12655	0.84564	0.00401	0.02305	0.83562	0.46108	2.58603	58.85132	1.39950	0.32946	4.32069	20.89214	389.16438
25	120	13360	12955	0.86569	0.00401	0.02005	0.85566	0.48112	2.35550	61.20682	1.46034	0.32946	5.73710	25.14445	414.30883
26	125	13630	13225	0.88373	0.00361	0.01904	0.87471	0.45105	2.33044	63.53725	1.52119	0.29651	6.61857	30.88917	445.19800
27	130	13840	13435	0.89776	0.00281	0.01604	0.89075	0.36485	2.03976	65.57701	1.58204	0.23062	6.41992	32.59624	477.79424
28	135	14050	13645	0.91179	0.00281	0.01403	0.90478	0.37888	1.85934	67.43635	1.64289	0.23062	7.83239	35.63078	513.42502
29	140	14240	13835	0.92449	0.00254	0.01336	0.91814	0.35550	1.83595	69.27230	1.70374	0.20866	8.49136	40.80937	554.23439
30	145	14440	14035	0.93785	0.00267	0.01303	0.93117	0.38757	1.85767	71.12997	1.76458	0.21964	10.55077	47.60532	601.83972
31	150	14530	14125	0.94387	0.00120	0.00969	0.94086	0.18042	1.41998	72.54995	1.82543	0.09884	5.53361	40.21095	642.05067
32	155	14670	14265	0.95322	0.00187	0.00768	0.94855	0.29001	1.17608	73.72603	1.88628	0.15375	9.32369	38.64326	680.69393
33	160	14750	14345	0.95857	0.00107	0.00735	0.95590	0.17107	1.15269	74.87872	1.94713	0.08786	6.47605	40.99937	721.69330
34	165	14840	14435	0.96458	0.00120	0.00568	0.96158	0.19846	0.92382	75.80254	2.00797	0.09884	8.25175	36.81950	758.51280
35	170	14930	14525	0.97060	0.00120	0.00601	0.96759	0.20448	1.00735	76.80989	2.06882	0.09884	9.27807	43.82455	802.33735
36	175	14940	14535	0.97127	0.00013	0.00334	0.97093	0.02339	0.56966	77.37955	2.12967	0.01098	1.15162	26.07422	828.41157
37	180	15000	14595	0.97528	0.00080	0.00234	0.97327	0.14434	0.41931	77.79886	2.19052	0.06589	7.67410	22.06428	850.47586
38	185	15060	14655	0.97928	0.00080	0.00401	0.97728	0.14835	0.73171	78.53057	2.25136	0.06589	8.47860	40.38173	890.85759
39	190	15120	14715	0.98329	0.00080	0.00401	0.98129	0.15236	0.75175	79.28233	2.31221	0.06589	9.32319	44.50446	935.36204
40	195	15130	14725	0.98396	0.00013	0.00234	0.98363	0.02606	0.44604	79.72837	2.37306	0.01098	1.70131	27.56125	962.92329
41	200	15170	14765	0.98664	0.00053	0.00167	0.98530	0.10692	0.33244	80.06081	2.43391	0.04393	7.42177	22.80770	985.73099
42	205	15170	14765	0.98664	0.00000	0.00134	0.98664	0.00000	0.26729	80.32810	2.49475	0.00000	0.00000	18.55442	1004.28540
43	210	15200	14795	0.98864	0.00040	0.00100	0.98764	0.08420	0.21049	80.53859	2.55560	0.03295	6.55124	16.37811	1020.66351
44	215	15220	14815	0.98998	0.00027	0.00167	0.98931	0.05747	0.35416	80.89275	2.61645	0.02196	4.71585	28.16773	1048.83125
45	220	15270	14865	0.99332	0.00067	0.00234	0.99165	0.14701	0.51119	81.40394	2.67730	0.05491	12.69392	43.52442	1092.35566
46	225	15270	14865	0.99332	0.00000	0.00167	0.99332	0.00000	0.36752	81.77147	2.73815	0.00000	0.00000	31.73479	1124.09046
47	230	15270	14865	0.99332	0.00000	0.00000	0.99332	0.00000	0.00000	81.77147	2.79899	0.00000	0.00000	0.00000	1124.09046
48	235	15270	14865	0.99332	0.00000	0.00000	0.99332	0.00000	0.00000	81.77147	2.85984	0.00000	0.00000	0.00000	1124.09046
49	240	15320	14915	0.99666	0.00067	0.00167	0.99499	0.16037	0.40094	82.17240	2.92069	0.05491	16.64521	41.61301	1165.70347
50	300	15370	14965	1.00000	0.00006	0.02172	1.01671	0.01671	5.31240	87.48480	3.65086	0.00458	2.64221	578.62257	1744.32604
51	360														
52	420														
53	480														
54	540														
55	600														

	4 cells														
Flow rate, L/min	0.505														
C back, uS/cm	426														
Co, uS/cm	15440														
Mean det. time, sec	103.19														
Actual volume, ml	868.47														
Sample	Time, sec	C, uS/cm	C corr., uS/cm	F(t)	E(t)	Partial E(t)	Cum. E(t)	tE(t)	Partial tE(t)	Cum. tE(t)	θ	E(θ)	(t−τ)²E(t)	Partial (t−τ)²E(t)	Cum. (t−τ)²E(t)=σ²
1	0	426	0	0.00000	0.00000	0.00000	0.00000	0.00000	0.00000	0.00000	0.00000	0.00000	0.00000	0.00000	0.00000
2	5	426	0	0.00000	0.00000	0.00000	0.00000	0.00000	0.00000	0.00000	0.04846	0.00000	0.00000	0.00000	0.00000
3	10	426	0	0.00000	0.00000	0.00000	0.00000	0.00000	0.00000	0.00000	0.09691	0.00000	0.00000	0.00000	0.00000
4	15	426	0	0.00000	0.00000	0.00000	0.00000	0.00000	0.00000	0.00000	0.14537	0.00000	0.00000	0.00000	0.00000
5	20	426	0	0.00000	0.00000	0.00000	0.00000	0.00000	0.00000	0.00000	0.19383	0.00000	0.00000	0.00000	0.00000
6	25	426	0	0.00000	0.00000	0.00000	0.00000	0.00000	0.00000	0.00000	0.24228	0.00000	0.00000	0.00000	0.00000
7	30	429	3	0.00020	0.00004	0.00010	0.00010	0.00120	0.00300	0.00300	0.29074	0.00412	0.21404	0.53511	0.53511
8	35	433	7	0.00047	0.00005	0.00023	0.00033	0.00186	0.00766	0.01066	0.33920	0.00550	0.24773	1.15442	1.68953
9	40	447	21	0.00140	0.00019	0.00060	0.00093	0.00746	0.02331	0.03397	0.38765	0.01924	0.74454	2.48067	4.17020
10	45	479	53	0.00353	0.00043	0.00153	0.00246	0.01918	0.06660	0.10057	0.43611	0.04398	1.44313	5.46919	9.63939
11	50	546	120	0.00799	0.00089	0.00330	0.00576	0.04463	0.15952	0.26009	0.48457	0.09209	2.52457	9.91925	19.55864
12	55	768	342	0.02278	0.00296	0.00962	0.01539	0.16265	0.51818	0.77827	0.53302	0.30514	6.86611	23.47670	43.03534
13	60	1788	1362	0.09072	0.01359	0.04136	0.05675	0.81524	2.44472	3.22299	0.58148	1.40201	25.33962	80.51433	123.54967
14	65	3680	3254	0.21673	0.02520	0.09698	0.15372	1.63820	6.13361	9.35660	0.62994	2.60059	36.74861	155.22059	278.77025
15	70	5400	4974	0.33129	0.02291	0.12029	0.27401	1.60384	8.10510	17.46170	0.67839	2.36417	25.23169	154.95076	433.72101
16	75	6630	6204	0.41321	0.01638	0.09824	0.37225	1.22885	7.08172	24.54343	0.72685	1.69066	13.01594	95.61909	529.34010
17	80	7680	7254	0.48315	0.01399	0.07593	0.44818	1.11896	5.86952	30.41295	0.77531	1.44324	7.51862	51.33640	580.67651
18	85	8400	7974	0.53110	0.00959	0.05894	0.50713	0.81524	4.83549	35.24843	0.82376	0.98965	3.17171	26.72583	607.40234
19	90	9060	8634	0.57506	0.00879	0.04596	0.55308	0.79126	4.01625	39.26469	0.87222	0.90718	1.52841	11.75031	619.15265
20	95	9520	9094	0.60570	0.00613	0.03730	0.59038	0.58212	3.43346	42.69815	0.92068	0.63228	0.41052	4.84732	623.99996
21	100	10140	9714	0.64700	0.00826	0.03597	0.62635	0.82590	3.52005	46.21820	0.96913	0.85220	0.08378	1.23575	625.23571
22	105	10610	10184	0.67830	0.00626	0.03630	0.66265	0.65739	3.70821	49.92640	1.01759	0.64602	0.02062	0.26102	625.49673
23	110	11060	10634	0.70827	0.00599	0.03064	0.69329	0.65938	3.29193	53.21833	1.06605	0.61853	0.27840	0.74757	626.24430
24	115	11550	11124	0.74091	0.00653	0.03130	0.72459	0.75063	3.52504	56.74337	1.11450	0.67351	0.91116	2.97391	629.21821
25	120	11860	11434	0.76156	0.00413	0.02664	0.75123	0.49554	3.11543	59.85880	1.16296	0.42610	1.16758	5.19686	634.41507
26	125	12180	11754	0.78287	0.00426	0.02098	0.77221	0.53284	2.57093	62.42973	1.21142	0.43985	2.02858	7.99042	642.40548
27	130	12500	12074	0.80418	0.00426	0.02131	0.79353	0.55415	2.71746	65.14720	1.25987	0.43985	3.06506	12.73410	655.13958
28	135	12760	12334	0.82150	0.00346	0.01932	0.81284	0.46756	2.55428	67.70148	1.30833	0.35737	3.50566	16.42679	671.56637
29	140	13020	12594	0.83882	0.00346	0.01732	0.83016	0.48488	2.38111	70.08259	1.35679	0.35737	4.69414	20.49950	692.06587
30	145	13250	12824	0.85414	0.00306	0.01632	0.84648	0.44425	2.32283	72.40542	1.40524	0.31614	5.35704	25.12795	717.19382
31	150	13450	13024	0.86746	0.00266	0.01432	0.86080	0.39963	2.10970	74.51512	1.45370	0.27490	5.83893	27.98993	745.18375
32	155	13680	13254	0.88278	0.00306	0.01432	0.87512	0.47489	2.18629	76.70141	1.50216	0.31614	8.22568	35.16153	780.34528
33	160	13850	13424	0.89410	0.00226	0.01332	0.88844	0.36233	2.09305	78.79446	1.55061	0.23367	7.30984	38.83882	819.18409
34	165	14010	13584	0.90476	0.00213	0.01099	0.89943	0.35167	1.78500	80.57946	1.59907	0.21992	8.14406	38.63476	857.81885
35	170	14160	13734	0.91475	0.00200	0.01032	0.90975	0.33968	1.72839	82.30785	1.64753	0.20618	8.92016	42.66054	900.47939
36	175	14300	13874	0.92407	0.00186	0.00966	0.91941	0.32636	1.66511	83.97296	1.69598	0.19243	9.61815	46.34577	946.82516
37	180	14420	13994	0.93206	0.00160	0.00866	0.92807	0.28773	1.53523	85.50819	1.74444	0.16494	9.43206	47.62553	994.45069
38	185	14520	14094	0.93872	0.00133	0.00733	0.93539	0.24644	1.33542	86.84361	1.79290	0.13745	8.91660	45.87165	1040.32233
39	190	14640	14214	0.94672	0.00160	0.00733	0.94272	0.30372	1.37538	88.21900	1.84135	0.16494	12.04770	52.41074	1092.73307
40	195	14720	14294	0.95204	0.00107	0.00666	0.94938	0.20781	1.27881	89.49780	1.88981	0.10996	8.98360	52.57826	1145.31133
41	200	14800	14374	0.95737	0.00107	0.00533	0.95471	0.21313	1.05235	90.55015	1.93827	0.10996	9.98869	47.43074	1192.74207
42	205	14830	14404	0.95937	0.00040	0.00366	0.95837	0.08192	0.73764	91.28780	1.98672	0.04124	4.14265	35.32835	1228.07042
43	210	14910	14484	0.96470	0.00107	0.00366	0.96204	0.22379	0.76429	92.05208	2.03518	0.10996	12.15872	40.75342	1268.82384
44	215	14970	14544	0.96870	0.00080	0.00466	0.96670	0.17184	0.98908	93.04116	2.08364	0.08247	9.99274	55.37866	1324.20250
45	220	15020	14594	0.97203	0.00067	0.00366	0.97036	0.14653	0.79592	93.83709	2.13209	0.06873	9.08868	47.70355	1371.90605
46	225	15050	14624	0.97402	0.00040	0.00266	0.97303	0.08992	0.59111	94.42820	2.18055	0.04124	5.93002	37.54674	1409.45279
47	230	15130	14704	0.97935	0.00107	0.00366	0.97669	0.24510	0.83755	95.26575	2.22901	0.10996	17.13818	57.67049	1467.12329
48	235	15150	14724	0.98068	0.00027	0.00333	0.98002	0.06261	0.76928	96.03503	2.27746	0.02749	4.62906	54.41810	1521.54139
49	240	15200	14774	0.98401	0.00067	0.00233	0.98235	0.15985	0.55615	96.59118	2.32592	0.06873	12.46726	42.74079	1564.28218
50	300	15380	14954	0.99600	0.00020	0.02598	1.00833	0.05994	6.59385	103.18503	2.90740	0.02062	7.74000	606.21773	2170.49992
51	360	15440	15014	1.00000	0.00007	0.00799	1.01632	0.02398	2.51765	105.70268	3.48888	0.00687	4.39283	363.98494	2534.48486
52	420														
53	480														
54	540														
55	600														

	5 cells														
Flow rate, L/min	0.5														
C back, uS/cm	475														
Co, uS/cm	14400														
Mean det. time, sec	125.71														
Actual volume, ml	1047.57														
Sample	Time, sec	C, uS/cm	C corr., uS/cm	F(t)	E(t)	Partial E(t)	Cum. E(t)	tE(t)	Partial tE(t)	Cum. tE(t)	θ	E(θ)	(t−τ)²E(t)	Partial (t−τ)²E(t)	Cum. (t−τ)²E(t)=σ²
1	0	475	0	0.00000	0.00000	0.00000	0.00000	0.00000	0.00000	0.00000	0.10203	0.00000	0.00000	0.00000	0.00000
2	5	475	0	0.00000	0.00000	0.00000	0.00000	0.00000	0.00000	0.00000	0.07955	0.00000	0.00000	0.00000	0.00000
3	10	475	0	0.00000	0.00000	0.00000	0.00000	0.00000	0.00000	0.00000	0.11932	0.00000	0.00000	0.00000	0.00000
4	15	475	0	0.00000	0.00000	0.00000	0.00000	0.00000	0.00000	0.00000	0.15910	0.00000	0.00000	0.00000	0.00000
5	20	475	0	0.00000	0.00000	0.00000	0.00000	0.00000	0.00000	0.00000	0.19887	0.00000	0.00000	0.00000	0.00000
6	25	475	0	0.00000	0.00000	0.00000	0.00000	0.00000	0.00000	0.00000	0.23865	0.00000	0.00000	0.00000	0.00000
7	30	475	0	0.00000	0.00000	0.00000	0.00000	0.00000	0.00000	0.00000	0.27842	0.00000	0.00000	0.00000	0.00000
8	35	475	0	0.00000	0.00000	0.00000	0.00000	0.00000	0.00000	0.00000	0.31820	0.00000	0.00000	0.00000	0.00000
9	40	475	0	0.00000	0.00000	0.00000	0.00000	0.00000	0.00000	0.00000	0.35797	0.00000	0.00000	0.00000	0.00000
10	45	475	0	0.00000	0.00000	0.00000	0.00000	0.00000	0.00000	0.00000	0.39774	0.00000	0.00000	0.00000	0.00000
11	50	479	4	0.00029	0.00006	0.00014	0.00014	0.00287	0.00718	0.00718	0.43752	0.00722	0.32930	0.82324	0.82324
12	55	501	26	0.00187	0.00032	0.00093	0.00108	0.01738	0.05063	0.05781	0.47729	0.03972	1.57981	4.77276	5.59600
13	60	524	49	0.00352	0.00033	0.00162	0.00269	0.01982	0.09300	0.15081	0.51707	0.04153	1.42630	7.51526	13.11126
14	65	600	125	0.00898	0.00109	0.00355	0.00625	0.07095	0.22693	0.37774	0.55684	0.13722	4.02301	13.62328	26.73454
15	70	1115	640	0.04596	0.00740	0.02122	0.02747	0.51777	1.47181	1.84955	0.59662	0.92384	22.95565	67.44666	94.18120
16	75	1579	1104	0.07928	0.00666	0.03515	0.06262	0.49382	2.54399	4.39354	0.63639	0.83776	17.13639	100.23010	194.41131
17	80	2803	2328	0.16718	0.01758	0.06061	0.12323	1.40639	4.76553	9.15907	0.67617	2.20995	36.72957	134.66489	329.07620
18	85	4490	4015	0.28833	0.02423	0.10452	0.22776	2.05953	8.66481	17.82388	0.71594	3.04590	40.15378	192.20836	521.28456
19	90	5570	5095	0.36589	0.01551	0.09935	0.32711	1.39605	8.63896	26.46284	0.75571	1.94995	19.77921	149.83248	671.11704
20	95	6330	5855	0.42047	0.01092	0.06607	0.39318	1.03698	6.08259	32.54542	0.79549	1.37219	10.29376	75.18243	746.29946
21	100	7120	6645	0.47720	0.01135	0.05566	0.44883	1.13465	5.42908	37.97451	0.83526	1.42635	7.49338	44.48285	790.78231
22	105	7760	7285	0.52316	0.00919	0.05135	0.50018	0.96517	5.24955	43.22406	0.87504	1.15553	3.94207	28.60363	819.38594
23	110	8420	7945	0.57056	0.00948	0.04668	0.54686	1.04273	5.01975	48.24381	0.91481	1.19164	2.33919	15.70314	835.08909
24	115	8940	8465	0.60790	0.00747	0.04237	0.58923	0.85889	4.75404	52.99785	0.95459	0.93887	0.85648	7.98917	843.07826
25	120	9390	8915	0.64022	0.00646	0.03483	0.62406	0.77558	4.08618	57.08402	0.99436	0.81248	0.21064	2.66781	845.74607
26	125	9810	9335	0.67038	0.00603	0.03124	0.65530	0.75404	3.82406	60.90808	1.03414	0.75832	0.00303	0.53417	846.28024
27	130	10180	9705	0.69695	0.00531	0.02837	0.68366	0.69084	3.61221	64.52029	1.07391	0.66804	0.09786	0.25222	846.53246
28	135	10520	10045	0.72136	0.00488	0.02549	0.70916	0.65925	3.37522	67.89551	1.11368	0.61387	0.42156	1.29854	847.83100
29	140	10850	10375	0.74506	0.00474	0.02406	0.73321	0.66355	3.30700	71.20251	1.15346	0.59582	0.96802	3.47396	851.30495
30	145	11160	10685	0.76732	0.00445	0.02298	0.75619	0.64560	3.27289	74.47540	1.19323	0.55971	1.65697	6.56249	857.86744
31	150	11390	10915	0.78384	0.00330	0.01939	0.77558	0.49551	2.85278	77.32819	1.23301	0.41527	1.94922	9.01548	866.88292
32	155	11640	11165	0.80180	0.00359	0.01724	0.79282	0.55655	2.63016	79.95835	1.27278	0.45138	3.08070	12.57479	879.45772
33	160	11870	11395	0.81831	0.00330	0.01724	0.81005	0.52855	2.71275	82.67110	1.31256	0.41527	3.88444	17.41284	896.87055
34	165	12090	11615	0.83411	0.00316	0.01616	0.82621	0.52136	2.62478	85.29587	1.35233	0.39721	4.87807	21.90627	918.77682
35	170	12270	11795	0.84704	0.00259	0.01436	0.84057	0.43950	2.40215	87.69803	1.39211	0.32499	5.07157	24.87410	943.65092
36	175	12400	11925	0.85637	0.00187	0.01113	0.85171	0.32675	1.91562	89.61364	1.43188	0.23472	4.53646	24.02007	967.67099
37	180	12560	12085	0.86786	0.00230	0.01041	0.86212	0.41364	1.85099	91.46463	1.47166	0.28888	6.77351	28.27492	995.94591
38	185	12730	12255	0.88007	0.00244	0.01185	0.87397	0.45171	2.16338	93.62801	1.51143	0.30694	8.58350	38.39251	1034.33842
39	190	12880	12405	0.89084	0.00215	0.01149	0.88546	0.40934	2.15260	95.78061	1.55120	0.27083	8.90490	43.72100	1078.05942
40	195	13020	12545	0.90090	0.00201	0.01041	0.89587	0.39210	2.00359	97.78420	1.59098	0.25277	9.65426	46.39791	1124.45733
41	200	13140	12665	0.90952	0.00172	0.00934	0.90521	0.34470	1.84201	99.62621	1.63075	0.21666	9.51242	47.91669	1172.37402
42	205	13220	12745	0.91526	0.00115	0.00718	0.91239	0.23555	1.45063	101.07684	1.67053	0.14444	7.22395	41.84092	1214.21493
43	210	13340	12865	0.92388	0.00172	0.00718	0.91957	0.36194	1.49372	102.57056	1.71030	0.21666	12.24561	48.67391	1262.88884
44	215	13440	12965	0.93106	0.00144	0.00790	0.92747	0.30880	1.67684	104.24740	1.75008	0.18055	11.45123	59.24211	1322.13095
45	220	13450	12975	0.93178	0.00014	0.00395	0.93142	0.03160	0.85099	105.09838	1.78985	0.01806	1.27696	31.82047	1353.95143
46	225	13580	13105	0.94111	0.00187	0.00503	0.93645	0.42011	1.12926	106.22765	1.82963	0.23472	18.40771	49.21167	1403.16309
47	230	13650	13175	0.94614	0.00101	0.00718	0.94363	0.23124	1.62837	107.85601	1.86940	0.12639	10.93524	73.35736	1476.52045
48	235	13720	13245	0.95117	0.00101	0.00503	0.94865	0.23627	1.16876	109.02478	1.90917	0.12639	12.00890	57.36034	1533.88079
49	240	13830	13355	0.95907	0.00158	0.00646	0.95512	0.37917	1.53860	110.56338	2.38647	0.19861	20.63731	81.61553	1615.49632
50	300	14180	13705	0.98420	0.00042	0.05996	1.01508	0.12567	15.14542	125.70880	2.86376	0.05266	12.72543	1000.88225	2616.37857
51	360	14310													
52	420	14350													
53	480	14380													
54	540	14400													
55	600														

	6 cells														
Flow rate, L/min	0.5														
C back, uS/cm	512														
Co, uS/cm	14400														
Mean det. time, sec	140.59														
Actual volume, ml	1171.56														
Sample	Time, sec	C, uS/cm	C corr., uS/cm	F(t)	E(t)	Partial E(t)	Cum. E(t)	tE(t)	Partial tE(t)	Cum. tE(t)	θ	E(θ)	(t−τ)*E(t)	Partial (t−τ)*E(t)	Cum. (t−τ)*E(t)=σ²
1	0	512	0	0.00000	0.00000	0.00000	0.00000	0.00000	0.00000	0.00000	0.00000	0.00000	0.00000	0.00000	0.00000
2	5	512	0	0.00000	0.00000	0.00000	0.00000	0.00000	0.00000	0.00000	0.03557	0.00000	0.00000	0.00000	0.00000
3	10	512	0	0.00000	0.00000	0.00000	0.00000	0.00000	0.00000	0.00000	0.07113	0.00000	0.00000	0.00000	0.00000
4	15	512	0	0.00000	0.00000	0.00000	0.00000	0.00000	0.00000	0.00000	0.10670	0.00000	0.00000	0.00000	0.00000
5	20	512	0	0.00000	0.00000	0.00000	0.00000	0.00000	0.00000	0.00000	0.14226	0.00000	0.00000	0.00000	0.00000
6	25	512	0	0.00000	0.00000	0.00000	0.00000	0.00000	0.00000	0.00000	0.17783	0.00000	0.00000	0.00000	0.00000
7	30	512	0	0.00000	0.00000	0.00000	0.00000	0.00000	0.00000	0.00000	0.21339	0.00000	0.00000	0.00000	0.00000
8	35	512	0	0.00000	0.00000	0.00000	0.00000	0.00000	0.00000	0.00000	0.24896	0.00000	0.00000	0.00000	0.00000
9	40	512	0	0.00000	0.00000	0.00000	0.00000	0.00000	0.00000	0.00000	0.28452	0.00000	0.00000	0.00000	0.00000
10	45	515	3	0.00022	0.00004	0.00011	0.00011	0.00194	0.00486	0.00486	0.32009	0.00607	0.39474	0.98686	0.98686
11	50	540	28	0.00202	0.00036	0.00101	0.00112	0.01800	0.04986	0.05472	0.35565	0.05061	2.95439	8.37282	9.35968
12	55	664	152	0.01094	0.00179	0.00536	0.00648	0.09821	0.29054	0.34526	0.39122	0.25105	13.08077	40.08789	49.44757
13	60	714	202	0.01454	0.00072	0.00626	0.01274	0.04320	0.35354	0.69880	0.42678	0.10123	4.67623	44.39251	93.84008
14	65	801	289	0.02081	0.00125	0.00493	0.01768	0.08144	0.31160	1.01040	0.46235	0.17614	7.15830	29.58635	123.42642
15	70	898	386	0.02779	0.00140	0.00662	0.02430	0.09778	0.44805	1.45845	0.49791	0.19639	6.96015	35.29613	158.72255
16	75	967	455	0.03276	0.00099	0.00598	0.03028	0.07452	0.43077	1.88922	0.53348	0.13970	4.27447	28.08654	186.80909
17	80	1205	693	0.04990	0.00343	0.01105	0.04133	0.27419	0.87180	2.76102	0.56904	0.48185	12.58155	42.14005	228.94914
18	85	2402	1890	0.13609	0.01724	0.05166	0.09299	1.46522	4.34854	7.10956	0.60461	2.42343	53.26472	164.61567	393.56480
19	90	4050	3538	0.25475	0.02373	0.10243	0.19542	2.13594	9.00292	16.11247	0.64017	3.33652	60.73442	284.99785	678.56266
20	95	5140	4628	0.33324	0.01570	0.09857	0.29399	1.49122	9.06790	25.18037	0.67574	2.20680	32.62191	233.39085	911.95350
21	100	6040	5528	0.39804	0.01296	0.07164	0.36564	1.29608	6.96825	32.14862	0.71130	1.82213	21.35102	134.93234	1046.88584
22	105	6650	6138	0.44196	0.00878	0.05436	0.42000	0.92238	5.54615	37.69477	0.74687	1.23500	11.12542	81.19111	1128.07694
23	110	7250	6738	0.48517	0.00864	0.04356	0.46357	0.95046	4.68210	42.37687	0.78243	1.21475	8.08409	48.02378	1176.10072
24	115	7760	7248	0.52189	0.00734	0.03996	0.50353	0.84461	4.48769	46.86456	0.81800	1.03254	4.80859	32.23171	1208.33243
25	120	8150	7638	0.54997	0.00562	0.03240	0.53593	0.67396	3.79644	50.66100	0.85356	0.78959	2.38048	17.97269	1226.30512
26	125	8540	8028	0.57805	0.00562	0.02808	0.56401	0.70204	3.44002	54.10102	0.88913	0.78959	1.36462	9.36274	1235.66786
27	130	8980	8468	0.60974	0.00634	0.02988	0.59389	0.82373	3.81444	57.91547	0.92469	0.89082	0.71029	5.18726	1240.85513
28	135	9330	8818	0.63494	0.00504	0.02844	0.62234	0.68044	3.76044	61.67591	0.96026	0.70861	0.15736	2.16913	1243.02426
29	140	9740	9228	0.66446	0.00590	0.02736	0.64970	0.82661	3.76764	65.44355	0.99582	0.83008	0.00204	0.39850	1243.42276
30	145	10040	9528	0.68606	0.00432	0.02556	0.67526	0.62644	3.63263	69.07618	1.03139	0.60738	0.08411	0.21538	1243.63814
31	150	10370	9858	0.70982	0.00475	0.02268	0.69794	0.71285	3.34821	72.42440	1.06695	0.66811	0.42103	1.26285	1244.90099
32	155	10660	10148	0.73070	0.00418	0.02232	0.72026	0.64732	3.40042	75.82481	1.10252	0.58713	0.86749	3.22128	1248.12228
33	160	10880	10368	0.74654	0.00317	0.01836	0.73862	0.50691	2.88558	78.71040	1.13808	0.44541	1.19391	5.15351	1253.27578
34	165	11100	10588	0.76238	0.00317	0.01584	0.75446	0.52275	2.57416	81.28456	1.17365	0.44541	1.88815	7.70515	1260.98093
35	170	11320	10808	0.77823	0.00317	0.01584	0.77031	0.53859	2.65337	83.93793	1.20921	0.44541	2.74079	11.57233	1272.55326
36	175	11560	11048	0.79551	0.00346	0.01656	0.78687	0.60484	2.85858	86.79651	1.24478	0.48590	4.09291	17.08425	1289.63751
37	180	11750	11238	0.80919	0.00274	0.01548	0.80235	0.49251	2.74338	89.53989	1.28034	0.38467	4.25021	20.85781	1310.49532
38	185	11910	11398	0.82071	0.00230	0.01260	0.81495	0.42627	2.29695	91.83684	1.31591	0.32393	4.54485	21.98766	1332.48298
39	190	12090	11578	0.83367	0.00259	0.01224	0.82719	0.49251	2.29695	94.13378	1.35147	0.36443	6.32900	27.18464	1359.66762
40	195	12230	11718	0.84375	0.00202	0.01152	0.83871	0.39315	2.21414	96.34793	1.38704	0.28344	5.96918	30.74547	1390.41308
41	200	12420	11908	0.85743	0.00274	0.01188	0.85059	0.54724	2.35095	98.69888	1.42260	0.38467	9.65826	39.06859	1429.48167
42	205	12540	12028	0.86607	0.00173	0.01116	0.86175	0.35426	2.25374	100.95262	1.45817	0.24295	7.16987	42.07031	1471.55198
43	210	12650	12138	0.87399	0.00158	0.00828	0.87003	0.33266	1.71731	102.66993	1.49373	0.22270	7.63234	37.00551	1508.55749
44	215	12760	12248	0.88191	0.00158	0.00792	0.87795	0.34058	1.68311	104.35304	1.52930	0.22270	8.77150	41.00961	1549.56710
45	220	12890	12378	0.89127	0.00187	0.00864	0.88659	0.41187	1.88112	106.23416	1.56486	0.26320	11.80622	51.44430	1601.01140
46	225	13010	12498	0.89991	0.00173	0.00900	0.89559	0.38882	2.00173	108.23589	1.60043	0.24295	12.31358	60.29950	1661.31090
47	230	13110	12598	0.90711	0.00144	0.00792	0.90351	0.33122	1.80012	110.03600	1.63599	0.20246	11.51294	59.56631	1720.87721
48	235	13230	12718	0.91575	0.00173	0.00792	0.91143	0.40611	1.84332	111.87932	1.67156	0.24295	15.40388	67.29204	1788.16925
49	240	13310	12798	0.92151	0.00115	0.00720	0.91863	0.27650	1.70651	113.58583	1.70712	0.16197	11.38575	66.97407	1855.14332
50	300	14020	13508	0.97264	0.00085	0.06012	0.97876	0.25562	15.96342	129.54925	2.13390	0.11979	21.65269	991.15324	2846.29656
51	360	14280	13768	0.99136	0.00031	0.03492	1.01368	0.11233	11.03831	140.58756	2.56068	0.04387	15.02121	1100.21692	3946.51348
52	420	14340	13828	0.99568	0.00007	0.01152	1.02520	0.03024	4.27707	144.86463	2.98746	0.01012	5.62149	619.28110	4565.79458
53	480	14380	13868	0.99856	0.00005	0.00360	1.02880	0.02304	1.59850	146.46313	3.41424	0.00675	5.52999	334.54461	4900.33919
54	540	14400													
55	600														

	7 cells														
Flow rate, L/min	0.49														
C back, uS/cm	470														
Co, uS/cm	11590														
Mean det. time, sec	163.47														
Actual volume, ml	1335.00														
Sample	Time, sec	C, uS/cm	C corr., uS/cm	F(t)	E(t)	Partial E(t)	Cum. E(t)	tE(t)	Partial tE(t)	Cum. tE(t)	θ	E(θ)	(t−τ)*E(t)	Partial (t−τ)*E(t)	Cum. (t−τ)*E(t)=σ²
1	0	470	0	0.00000	0.00000	0.00000	0.00000	0.00000	0.00000	0.00000	0.00000	0.00000	0.00000	0.00000	0.00000
2	5	470	0	0.00000	0.00000	0.00000	0.00000	0.00000	0.00000	0.00000	0.03059	0.00000	0.00000	0.00000	0.00000
3	10	470	0	0.00000	0.00000	0.00000	0.00000	0.00000	0.00000	0.00000	0.06117	0.00000	0.00000	0.00000	0.00000
4	15	470	0	0.00000	0.00000	0.00000	0.00000	0.00000	0.00000	0.00000	0.09176	0.00000	0.00000	0.00000	0.00000
5	20	470	0	0.00000	0.00000	0.00000	0.00000	0.00000	0.00000	0.00000	0.12235	0.00000	0.00000	0.00000	0.00000
6	25	470	0	0.00000	0.00000	0.00000	0.00000	0.00000	0.00000	0.00000	0.15293	0.00000	0.00000	0.00000	0.00000
7	30	470	0	0.00000	0.00000	0.00000	0.00000	0.00000	0.00000	0.00000	0.18352	0.00000	0.00000	0.00000	0.00000
8	35	470	0	0.00000	0.00000	0.00000	0.00000	0.00000	0.00000	0.00000	0.21411	0.00000	0.00000	0.00000	0.00000
9	40	470	0	0.00000	0.00000	0.00000	0.00000	0.00000	0.00000	0.00000	0.24469	0.00000	0.00000	0.00000	0.00000
10	45	480	10	0.00090	0.00018	0.00045	0.00045	0.00809	0.02023	0.02023	0.27528	0.02940	2.52428	6.31070	6.31070
11	50	484	14	0.00126	0.00007	0.00063	0.00108	0.00360	0.02923	0.04946	0.30587	0.01176	0.92628	8.62641	14.93711
12	55	488	18	0.00162	0.00007	0.00036	0.00144	0.00396	0.01888	0.06835	0.33645	0.01176	0.84645	4.43182	19.36893
13	60	491	21	0.00189	0.00005	0.00031	0.00175	0.00324	0.01799	0.08633	0.36704	0.00882	0.57766	3.56026	22.92919
14	65	498	28	0.00252	0.00013	0.00045	0.00220	0.00818	0.02855	0.11488	0.39763	0.02058	1.22075	4.49601	27.42521
15	70	520	50	0.00450	0.00040	0.00130	0.00351	0.02770	0.08970	0.20459	0.42821	0.06468	3.45690	11.69412	39.11933
16	75	527	57	0.00513	0.00013	0.00130	0.00481	0.00944	0.09285	0.29744	0.45880	0.02058	0.98539	11.10574	50.22507
17	80	560	90	0.00809	0.00059	0.00180	0.00661	0.04748	0.14231	0.43975	0.48939	0.09702	4.13518	12.80142	63.02649
18	85	633	163	0.01466	0.00131	0.00477	0.01138	0.11160	0.39771	0.83746	0.51997	0.21463	8.08442	30.54900	93.57549
19	90	848	378	0.03399	0.00387	0.01295	0.02433	0.34802	1.14906	1.98651	0.55056	0.63212	20.87262	72.39260	165.96809
20	95	1052	582	0.05234	0.00367	0.01884	0.04317	0.34856	1.74146	3.72797	0.58115	0.59978	17.20080	95.18356	261.15165
21	100	1331	861	0.07743	0.00502	0.02172	0.06488	0.50180	2.12590	5.85387	0.61174	0.82029	20.21429	93.53774	354.68939
22	105	1778	1308	0.11763	0.00804	0.03264	0.09753	0.84415	3.36488	9.21875	0.64232	1.31422	27.48466	119.24738	473.93677
23	110	2724	2254	0.20270	0.01701	0.06263	0.16016	1.87158	6.78934	16.00809	0.67291	2.78133	48.64379	190.32111	664.25788
24	115	3820	3350	0.30126	0.01971	0.09182	0.25198	2.26691	10.34622	26.35432	0.70350	3.22235	46.30965	237.38359	901.64147
25	120	4550	4080	0.36691	0.01313	0.08210	0.33408	1.57554	9.60612	35.96043	0.73408	2.14627	24.80938	177.79756	1079.43903
26	125	5100	4630	0.41637	0.00989	0.05755	0.39164	1.23651	7.03013	42.99056	0.76467	1.61705	14.63927	98.62160	1178.06063
27	130	5600	5130	0.46133	0.00899	0.04721	0.43885	1.16906	6.01394	49.00450	0.79526	1.47005	10.07376	61.78257	1239.84320
28	135	6110	5640	0.50719	0.00917	0.04541	0.48426	1.23831	6.01844	55.02293	0.82584	1.49945	7.43452	43.77070	1283.61390
29	140	6560	6090	0.54766	0.00809	0.04317	0.52743	1.13309	5.92851	60.95144	0.85643	1.32304	4.45803	29.73136	1313.34526
30	145	6930	6460	0.58094	0.00665	0.03687	0.56430	0.96493	5.24505	66.19649	0.88702	1.08784	2.27004	16.82017	1330.16542
31	150	7290	6820	0.61331	0.00647	0.03282	0.59712	0.97122	4.84038	71.03687	0.91760	1.05844	1.17470	8.61184	1338.77727
32	155	7660	7190	0.64658	0.00665	0.03282	0.62995	1.03147	5.00674	76.04362	0.94819	1.08784	0.47735	4.13011	1342.90738
33	160	7880	7410	0.66637	0.00396	0.02653	0.65647	0.63309	4.16142	80.20504	0.97878	0.64682	0.04763	1.31244	1344.21982
34	165	8150	7680	0.69065	0.00486	0.02203	0.67851	0.80126	3.58588	83.79092	1.00936	0.79383	0.01138	0.14751	1344.36733
35	170	8360	7890	0.70953	0.00378	0.02158	0.70009	0.64209	3.60836	87.39928	1.03995	0.61742	0.16108	0.43115	1344.79847
36	175	8600	8130	0.73112	0.00432	0.02023	0.72032	0.75540	3.49371	90.89299	1.07054	0.70562	0.57390	1.83746	1346.63594
37	180	8790	8320	0.74820	0.00342	0.01933	0.73966	0.61511	3.42626	94.31924	1.10112	0.55862	0.93380	3.76926	1350.40520
38	185	9020	8550	0.76888	0.00414	0.01888	0.75854	0.76529	3.45099	97.77023	1.13171	0.67622	1.91763	7.12857	1357.53377
39	190	9150	8680	0.78058	0.00234	0.01619	0.77473	0.44424	3.02383	100.79406	1.16230	0.38221	1.64574	8.90843	1366.44220
40	195	9320	8850	0.79586	0.00306	0.01349	0.78822	0.59622	2.60117	103.39523	1.19288	0.49982	3.03975	11.71373	1378.15593
41	200	9510	9040	0.81295	0.00342	0.01619	0.80441	0.68345	3.19919	106.59442	1.22347	0.55862	4.56028	19.00008	1397.15602
42	205	9640	9170	0.82464	0.00234	0.01439	0.81879	0.47932	2.90692	109.50135	1.25406	0.38221	4.03278	21.48266	1418.63867
43	210	9780	9310	0.83723	0.00252	0.01214	0.83094	0.52878	2.52023	112.02158	1.28464	0.41161	5.45168	23.71114	1442.34981
44	215	9900	9430	0.84802	0.00216	0.01169	0.84263	0.46403	2.48201	114.50360	1.31523	0.35281	5.73108	27.95689	1470.30670
45	220	9990	9520	0.85612	0.00162	0.00944	0.85207	0.35612	2.05036	116.55396	1.34582	0.26461	5.17291	27.25996	1497.56667
46	225	10100	9630	0.86601	0.00198	0.00899	0.86106	0.44514	2.00315	118.55710	1.37640	0.32341	7.49031	31.65804	1529.22471
47	230	10200	9730	0.87500	0.00180	0.00944	0.87050	0.41367	2.14703	120.70414	1.40699	0.29401	7.96100	38.62828	1567.85299
48	235	10270	9800	0.88129	0.00126	0.00764	0.87815	0.29586	1.77383	122.47797	1.43758	0.20581	6.44179	36.00699	1603.85998
49	240	10380	9910	0.89119	0.00198	0.00809	0.88624	0.47482	1.92671	124.40468	1.46816	0.32341	11.58745	45.07310	1648.93308
50	300	11120	10650	0.95773	0.00111	0.09263	0.97887	0.33273	24.22662	148.63129	1.83521	0.18131	20.67452	967.85921	2616.79229
51	360	11420	10950	0.98471	0.00045	0.04676	1.02563	0.16187	14.83813	163.46942	2.20225	0.07350	17.36703	1141.24652	3758.03882
52	420	11530	11060	0.99460	0.00016	0.01644	1.04406	0.06924	6.93345	170.40288	2.56929	0.02695	10.84963	846.49969	4604.53851
53	480	11560	11090	0.99730	0.00004	0.00629	1.05036	0.02158	2.72482	173.12770	2.93633	0.00735	4.50502	460.63944	5065.17795
54	540	11580	11110	0.99910	0.00003	0.00225	1.05261	0.01619	1.13309	174.26079	3.30337	0.00490	4.24986	262.64630	5327.82424
55	600	11590	11120	1.00000	0.00001	0.00135	1.05396	0.00899	0.75540	175.01619	3.67041	0.00245	2.85610	213.17873	5541.00297

	8 cells														
Flow rate, L/min	0.49														
C back, uS/cm	393														
Co, uS/cm	14200														
Mean det. time, sec	177.53														
Actual volume, ml	1449.83														
Sample	Time, sec	C, uS/cm	C corr., uS/cm	F(t)	E(t)	Partial E(t)	Cum. E(t)	tE(t)	Partial tE(t)	Cum. tE(t)	θ	E(θ)	(t−τ)²E(t)	Partial (t−τ)²E(t)	Cum. (t−τ)²E(t)=σ²
1	0	393	0	0.00000	0.00000	0.00000	0.00000	0.00000	0.00000	0.00000	0.00000	0.00000	0.00000	0.00000	
2	5	393	0	0.00000	0.00000	0.00000	0.00000	0.00000	0.00000	0.00000	0.02816	0.00000	0.00000	0.00000	0.00000
3	10	393	0	0.00000	0.00000	0.00000	0.00000	0.00000	0.00000	0.00000	0.05633	0.00000	0.00000	0.00000	0.00000
4	15	393	0	0.00000	0.00000	0.00000	0.00000	0.00000	0.00000	0.00000	0.08449	0.00000	0.00000	0.00000	0.00000
5	20	393	0	0.00000	0.00000	0.00000	0.00000	0.00000	0.00000	0.00000	0.11266	0.00000	0.00000	0.00000	0.00000
6	25	393	0	0.00000	0.00000	0.00000	0.00000	0.00000	0.00000	0.00000	0.14082	0.00000	0.00000	0.00000	0.00000
7	30	393	0	0.00000	0.00000	0.00000	0.00000	0.00000	0.00000	0.00000	0.16899	0.00000	0.00000	0.00000	0.00000
8	35	393	0	0.00000	0.00000	0.00000	0.00000	0.00000	0.00000	0.00000	0.19715	0.00000	0.00000	0.00000	0.00000
9	40	393	0	0.00000	0.00000	0.00000	0.00000	0.00000	0.00000	0.00000	0.22531	0.00000	0.00000	0.00000	0.00000
10	45	393	0	0.00000	0.00000	0.00000	0.00000	0.00000	0.00000	0.00000	0.25348	0.00000	0.00000	0.00000	0.00000
11	50	393	0	0.00000	0.00000	0.00000	0.00000	0.00000	0.00000	0.00000	0.28164	0.00000	0.00000	0.00000	0.00000
12	55	393	0	0.00000	0.00000	0.00000	0.00000	0.00000	0.00000	0.00000	0.30981	0.00000	0.00000	0.00000	0.00000
13	60	393	0	0.00000	0.00000	0.00000	0.00000	0.00000	0.00000	0.00000	0.33797	0.00000	0.00000	0.00000	0.00000
14	65	393	0	0.00000	0.00000	0.00000	0.00000	0.00000	0.00000	0.00000	0.36613	0.00000	0.00000	0.00000	0.00000
15	70	395	2	0.00014	0.00003	0.00007	0.00007	0.00203	0.00507	0.00507	0.39430	0.00514	0.33498	0.83746	0.83746
16	75	396	3	0.00022	0.00001	0.00011	0.00018	0.00109	0.00779	0.01286	0.42246	0.00257	0.15228	1.21815	2.05560
17	80	399	6	0.00043	0.00004	0.00014	0.00033	0.00348	0.01141	0.02426	0.45063	0.00771	0.41336	1.41410	3.46970
18	85	404	11	0.00080	0.00007	0.00029	0.00062	0.00616	0.02408	0.04835	0.47879	0.01286	0.62011	2.58368	6.05338
19	90	415	22	0.00159	0.00016	0.00058	0.00120	0.01434	0.05124	0.09959	0.50696	0.02829	1.22079	4.60224	10.65562
20	95	438	45	0.00326	0.00033	0.00123	0.00243	0.03165	0.11498	0.21457	0.53512	0.05915	2.26926	8.72512	19.38074
21	100	458	65	0.00471	0.00029	0.00156	0.00398	0.02897	0.15155	0.36612	0.56328	0.05143	1.74142	10.02670	29.40744
22	105	525	132	0.00956	0.00097	0.00315	0.00713	0.10190	0.32719	0.69331	0.59145	0.17230	5.10556	17.11745	46.52489
23	110	660	267	0.01934	0.00196	0.00732	0.01445	0.21511	0.79253	1.48584	0.61961	0.34717	8.91787	35.05858	81.58347
24	115	1165	772	0.05591	0.00732	0.02318	0.03763	0.84124	2.64087	4.12671	0.64778	1.29866	28.60238	93.80063	175.38409
25	120	2091	1698	0.12298	0.01341	0.05182	0.08945	1.60962	6.12715	10.25386	0.67594	2.38130	44.39499	182.49344	357.87754
26	125	3250	2857	0.20692	0.01679	0.07551	0.16495	2.09857	9.27048	19.52434	0.70411	2.98048	46.32686	226.80463	584.68217
27	130	4340	3947	0.28587	0.01579	0.08144	0.24640	2.05258	10.37789	29.90222	0.73227	2.80304	35.66951	204.99092	789.67309
28	135	5260	4867	0.35250	0.01333	0.07279	0.31919	1.79909	9.62917	39.53140	0.76043	2.36587	24.10539	149.43725	939.11034
29	140	5920	5527	0.40030	0.00956	0.05722	0.37640	1.33845	7.84385	47.37524	0.78860	1.69725	13.46596	93.92837	1033.03870
30	145	6430	6037	0.43724	0.00739	0.04237	0.41877	1.07120	6.02412	53.39936	0.81676	1.31151	7.81763	53.20898	1086.24768
31	150	6970	6577	0.47635	0.00782	0.03802	0.45680	1.17332	5.61128	59.01065	0.84493	1.38866	5.92849	34.36532	1120.61300
32	155	7310	6917	0.50098	0.00493	0.03187	0.48867	0.76338	4.84175	63.85239	0.87309	0.87434	2.50001	21.07125	1141.68425
33	160	7870	7477	0.54154	0.00811	0.03259	0.52126	1.29789	5.15318	69.00558	0.90125	1.44009	2.49284	12.48212	1154.16637
34	165	8380	7987	0.57847	0.00739	0.03875	0.56001	1.21895	6.29210	75.29768	0.92942	1.31151	1.15990	9.13184	1163.29821
35	170	8600	8207	0.59441	0.00319	0.02644	0.58644	0.54175	4.40175	79.69943	0.95758	0.56575	0.18071	3.35151	1166.64972
36	175	8970	8577	0.62121	0.00536	0.02137	0.60781	0.93793	3.69921	83.39864	0.98575	0.95149	0.03431	0.53754	1167.18726
37	180	9290	8897	0.64438	0.00464	0.02499	0.63279	0.83436	4.43072	87.82936	1.01391	0.82291	0.02827	0.15647	1167.34373
38	185	9600	9207	0.66684	0.00449	0.02281	0.65561	0.83074	4.16274	91.99211	1.04208	0.79720	0.25056	0.69708	1168.04080
39	190	9880	9487	0.68712	0.00406	0.02137	0.67698	0.77062	4.00340	95.99551	1.07024	0.72005	0.63067	2.20308	1170.24388
40	195	10170	9777	0.70812	0.00420	0.02064	0.69762	0.81915	3.97443	99.96994	1.09840	0.74576	1.28204	4.78179	1175.02567
41	200	10440	10047	0.72767	0.00391	0.02028	0.71790	0.78221	4.00340	103.97335	1.12657	0.69433	1.97466	8.14175	1183.16742
42	205	10700	10307	0.74651	0.00377	0.01919	0.73709	0.77207	3.88571	107.85906	1.15473	0.66862	2.84193	12.04147	1195.20889
43	210	10930	10537	0.76316	0.00333	0.01774	0.75483	0.69965	3.67929	111.53835	1.18290	0.59147	3.51250	15.88609	1211.09498
44	215	11120	10727	0.77692	0.00275	0.01521	0.77004	0.59173	3.22843	114.76678	1.21106	0.48860	3.86408	18.44146	1229.53644
45	220	11340	10947	0.79286	0.00319	0.01485	0.78489	0.70109	3.23206	117.99884	1.23923	0.56575	5.74795	24.03008	1253.56652
46	225	11500	11107	0.80445	0.00232	0.01376	0.79865	0.52147	3.05642	121.05526	1.26739	0.41146	5.22258	27.42632	1280.99283
47	230	11680	11287	0.81748	0.00261	0.01231	0.81097	0.59970	2.80293	123.85819	1.29555	0.46289	7.17830	31.00218	1311.99501
48	235	11850	11457	0.82980	0.00246	0.01267	0.82364	0.57869	2.94597	126.80416	1.32372	0.43717	8.13314	38.27860	1350.27361
49	240	11960	11567	0.83776	0.00159	0.01014	0.83378	0.38241	2.40277	129.20692	1.35188	0.28288	6.21818	35.87830	1386.15191
50	300	13290	12897	0.93409	0.00161	0.09597	0.92975	0.48164	25.92163	155.12856	1.68985	0.28502	24.08013	908.94917	2295.10108
51	360	13900	13507	0.97827	0.00074	0.07025	1.00000	0.26508	22.40168	177.53024	2.02782	0.13072	24.51665	1457.90328	3753.00435
52	420	14190	13797	0.99928	0.00035	0.03259	1.03259	0.14703	12.36329	189.89353	2.36579	0.06215	20.58082	1352.92389	5105.92824
53	480	14200	13807	1.00000	0.00001	0.01086	1.04346	0.00579	4.58463	194.47816	2.70376	0.00214	1.10437	650.55549	5756.48373
54	540														
55	600														

Table 8. Parameters for 1-cell through 8-cell reactor with horizontal slots and Q=1.0 L min^{-1}

Flow Area, m²	5.05E-04									
Electrode Area, m²	1.02E-02									
Max. Reactor Vol., m³	1.54E-03									
Max. Cell Vol., m³	1.54E-04									
	No of Cells	Potential, V	Current, A	ΔCurrent, A	Current density, A/m²	Max. Reactor Vol., m³	Actual Reactor Vol., m³	Avg. Cell Vol, m³	Dead Vol, m³	L, m
	0	-	-	-	-	-	1.93E-04	-	-	0.38
	1	-	-	-	-	4.62E-04	2.90E-04	9.67E-05	1.72E-04	0.57
	2	-	-	-	-	6.16E-04	3.87E-04	9.67E-05	2.29E-04	0.77
	3	-	-	-	-	7.70E-04	4.84E-04	9.67E-05	2.86E-04	0.96
	4	-	-	-	-	9.24E-04	5.80E-04	9.67E-05	3.44E-04	1.15
	5	-	-	-	-	1.08E-03	6.77E-04	9.67E-05	4.01E-04	1.34
	6	-	-	-	-	1.23E-03	7.74E-04	9.67E-05	4.58E-04	1.53
	7	-	-	-	-	1.39E-03	8.71E-04	9.67E-05	5.15E-04	1.72
	8	-	-	-	-	1.54E-03	9.67E-04	9.67E-05	5.73E-04	1.92
Avg. Current density, A/m²	-									
Avg. Cell Vol, m³	9.67E-05									
Avg. Cell τ, m³	5.8									
Reactor L, m	1.53									
Mean Fluid Velocity, m/s	3.23E-02									
Effective Electrode Area, m³	9.67E-03									

Table 9. Parameters for 1-cell through 8-cell reactor with horizontal slots and Q=0.5 L min^{-1}

Flow Area, m²	5.05E-04									
Electrode Area, m²	1.02E-02									
Max. Reactor Vol., m³	1.54E-03									
Max. Cell Vol., m³	1.54E-04									
	No of Cells	Potential, V	Current, A	ΔCurrent, A	Current density, A/m²	Max. Reactor Vol., m³	Actual Reactor Vol., m³	Avg. Cell Vol, m³	Dead Vol, m³	L, m
	0	-	-	-	-	-	1.89E-04	-	-	0.37
	1	-	-	-	-	4.62E-04	2.84E-04	9.47E-05	1.78E-04	0.56
	2	-	-	-	-	6.16E-04	3.79E-04	9.47E-05	2.37E-04	0.75
	3	-	-	-	-	7.70E-04	4.73E-04	9.47E-05	2.97E-04	0.94
	4	-	-	-	-	9.24E-04	5.68E-04	9.47E-05	3.56E-04	1.12
	5	-	-	-	-	1.08E-03	6.63E-04	9.47E-05	4.15E-04	1.31
	6	-	-	-	-	1.23E-03	7.57E-04	9.47E-05	4.75E-04	1.50
	7	-	-	-	-	1.39E-03	8.52E-04	9.47E-05	5.34E-04	1.69
	8	-	-	-	-	1.54E-03	9.47E-04	9.47E-05	5.93E-04	1.87
Avg. Current density, A/m²	-									
Avg. Cell Vol, m³	9.47E-05									
Avg. Cell τ, m³	11.4									
Reactor L, m	1.50									
Mean Fluid Velocity, m/s	1.58E-02									
Effective Electrode Area, m³	9.47E-03									

Table 10. Parameters for 1-cell through 8-cell reactor with vertical slots and Q=1.0 L min^{-1}

Flow Area, m^2	5.05E-04									
Electrode Area, m^2	1.02E-02									
Max. Reactor Vol., m^3	1.54E-03									
Max. Cell Vol., m^3	1.54E-04									
	No of Cells	Potential, V	Current, A	ΔCurrent, A	Current density, A/m^2	Max. Reactor Vol., m^3	Actual Reactor Vol., m^3	Avg. Cell Vol, m^3	Dead Vol. m^3	L, m
	0	0.0	0.0	0.0	0.0	-	3.11E-04	-	-	0.62
	1	30.7	1.3	1.3	92.7	4.62E-04	4.57E-04	1.52E-04	5.40E-06	0.90
	2	32.8	2.6	1.3	92.7	6.16E-04	5.98E-04	1.50E-04	1.80E-05	1.18
	3	34.0	4.0	1.4	99.8	7.70E-04	7.40E-04	1.48E-04	2.96E-05	1.47
	4	33.7	5.4	1.4	99.8	9.24E-04	8.65E-04	1.44E-04	5.90E-05	1.71
	5	33.4	6.7	1.3	92.7	1.08E-03	1.01E-03	1.45E-04	6.60E-05	2.00
	6	33.4	8.0	1.3	92.7	1.23E-03	1.15E-03	1.43E-04	8.64E-05	2.27
	7	34.0	9.3	1.3	92.7	1.39E-03	1.32E-03	1.47E-04	6.73E-05	2.61
	8	34.0	10.8	1.5	106.9	1.54E-03	1.43E-03	1.43E-04	1.07E-04	2.84
Avg. Current density, A/m^2	96.2									
Avg. Cell Vol, m^3	1.46E-04									
Avg. Cell τ, m^3	8.7									
Reactor L, m	2.22									
Mean Fluid Velocity, m/s	3.23E-02									
Effective Electrode Area, m^3	1.40E-02									

Table 11. Parameters for 1-cell through 8-cell reactor with vertical slots and Q=0.5 L min^{-1}

Flow Area, m^2	5.05E-04									
Electrode Area, m^2	1.02E-02									
Max. Reactor Vol., m^3	1.54E-03									
Max. Cell Vol., m^3	1.54E-04									
	No of Cells	Potential, V	Current, A	ΔCurrent, A	Current density, A/m^2	Max. Reactor Vol., m^3	Actual Reactor Vol., m^3	Avg. Cell Vol, m^3	Dead Vol. m^3	L, m
	0	-	-	-	-	-	2.87E-04	-	-	0.57
	1	-	-	-	-	4.62E-04	4.33E-04	1.44E-04	2.91E-05	0.86
	2	-	-	-	-	6.16E-04	5.69E-04	1.42E-04	4.75E-05	1.13
	3	-	-	-	-	7.70E-04	7.12E-04	1.42E-04	5.78E-05	1.41
	4	-	-	-	-	9.24E-04	8.68E-04	1.45E-04	5.55E-05	1.72
	5	-	-	-	-	1.08E-03	1.05E-03	1.50E-04	3.04E-05	2.07
	6	-	-	-	-	1.23E-03	1.17E-03	1.46E-04	6.04E-05	2.32
	7	-	-	-	-	1.39E-03	1.34E-03	1.48E-04	5.10E-05	2.64
	8	-	-	-	-	1.54E-03	1.49E-03	1.49E-04	5.02E-05	2.95
Avg. Current density, A/m^2	-									
Avg. Cell Vol, m^3	1.46E-04									
Avg. Cell τ, m^3	17.5									
Reactor L, m	2.38									
Mean Fluid Velocity, m/s	1.66E-02									
Effective Electrode Area, m^3	1.50E-02									

Table 12. DataFit results for the non- linear regression of the dispersion model

Equation:

1: Dispersion

Fit Information | Data Table | Model Plot | Residual Scatter | Residual Probability | Evaluate

DataFit version 9.0.59
Results from project "C:\Users\GR\Dropbox\Thesis\Regression.dft"
Equation ID: Dispersion
Model Definition:
Y = (4*Sqr(1+(4*k/15.13)*x)*Exp(15.13/2))/((1+Sqr(1+(4*k/15.13)*x))^2*Exp(Sqr(1+(4*k/15.13)*x)*(15.13/2))-(1-Sqr(1+(4*k/15.13)*x))^2*Exp(-Sqr(1+(4*k/15.13)*x)*(15.13/2)))

Number of observations = 9
Number of missing observations = 0
Solver type: Nonlinear
Nonlinear iteration limit = 250
Diverging nonlinear iteration limit =10
Number of nonlinear iterations performed = 20
Residual tolerance = 0.0000000001
Sum of Residuals = -3.14205563902896E-02
Average Residual = -3.49117293225439E-03
Residual Sum of Squares (Absolute) = 2.37532752281539E-02
Residual Sum of Squares (Relative) = 2.37532752281539E-02
Standard Error of the Estimate = 5.44899936090953E-02
Coefficient of Multiple Determination (R^2) = 0.9742291709
Proportion of Variance Explained = 97.42291709%
Adjusted coefficient of multiple determination (Ra^2) = 0.9710078172
Durbin-Watson statistic = 0.903650266449748

Regression Variable Results

Variable	Value	Standard Error	t-ratio	Prob(t)
k	4.40802719622408E-02	3.06478675221694E-03	14.38281862	0.0

68% Confidence Intervals

Variable	Value	68% (+/-)	Lower Limit	Upper Limit
k	4.40802719622408E-02	3.2492869147004E-03	4.08309850475404E-02	4.73295588769412E-02

90% Confidence Intervals

Variable	Value	90% (+/-)	Lower Limit	Upper Limit
k	4.40802719622408E-02	5.6989709657474E-03	3.83813009964934E-02	4.97792429279882E-02

95% Confidence Intervals

Variable	Value	95% (+/-)	Lower Limit	Upper Limit
k	4.40802719622408E-02	7.06739825061226E-03	3.70128737116285E-02	5.11476702128531E-02

99% Confidence Intervals

Variable	Value	99% (+/-)	Lower Limit	Upper Limit
k	4.40802719622408E-02	1.02835854683887E-02	3.37966864938521E-02	5.43638574306295E-02

Variance Analysis

Source	DF	Sum of Squares	Mean Square	F Ratio	Prob(F)
Regression	1	0.897958444771846	0.897958444771846	302.4285068	0
Error	8	2.37532752281539E-02	2.96915940351924E-03		
Total	9	0.92171172			

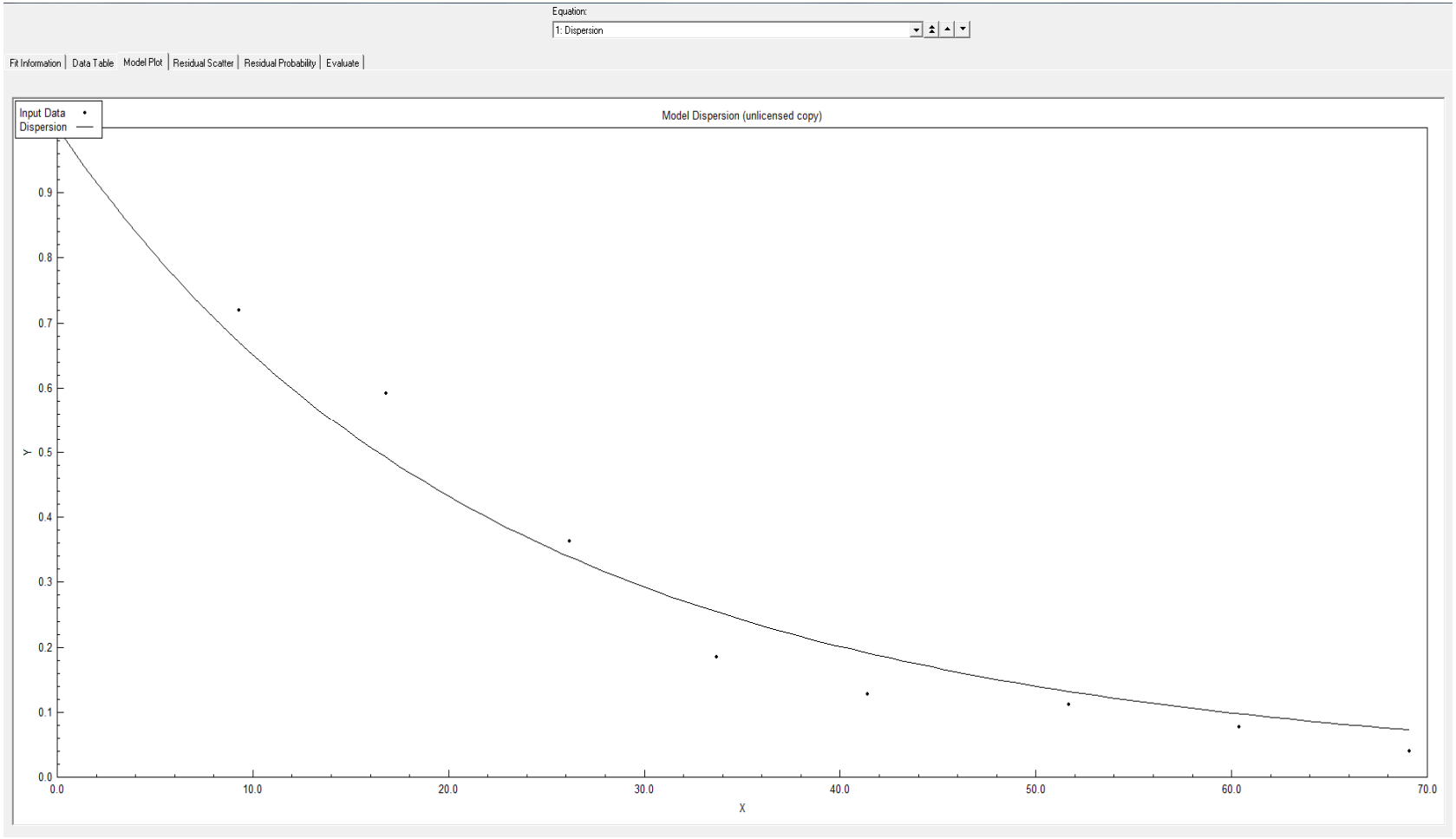

Figure 30. DataFit plot for the non-linear regression of the dispersion model.

Table 13. DataFit results for the non-linear regression of the TIS model

Equation:

2: TIS

Fit Information | Data Table | Model Plot | Residual Scatter | Residual Probability | Evaluate

DataFit version 9.0.59
Results from project "C:\Users\GR\Dropbox\Thesis\Regression.dft"
Equation ID: TIS
Model Definition:
Y = 1/(1+(k*x/8))^8

Number of observations = 9
Number of missing observations = 0
Solver type: Nonlinear
Nonlinear iteration limit = 250
Diverging nonlinear iteration limit =10
Number of nonlinear iterations performed = 14
Residual tolerance = 0.0000000001
Sum of Residuals = -3.48806773481883E-02
Average Residual = -3.87563081646536E-03
Residual Sum of Squares (Absolute) = 2.45249501752101E-02
Residual Sum of Squares (Relative) = 2.45249501752101E-02
Standard Error of the Estimate = 5.53680302331703E-02
Coefficient of Multiple Determination (R^2) = 0.9733919515
Proportion of Variance Explained = 97.33919515%
Adjusted coefficient of multiple determination (Ra^2) = 0.9700659454
Durbin-Watson statistic = 0.886283844150925

Regression Variable Results

Variable	Value	Standard Error	t-ratio	Prob(t)
k	4.43101271188328E-02	3.15166197590698E-03	14.05928918	0.0

68% Confidence Intervals

Variable	Value	68% (+/-)	Lower Limit	Upper Limit
k	4.43101271188328E-02	3.34139202685658E-03	4.09687350919762E-02	4.76515191456894E-02

90% Confidence Intervals

Variable	Value	90% (+/-)	Lower Limit	Upper Limit
k	4.43101271188328E-02	5.86051544419903E-03	3.84496116746337E-02	5.01706425630318E-02

95% Confidence Intervals

Variable	Value	95% (+/-)	Lower Limit	Upper Limit
k	4.43101271188328E-02	7.2677325164415E-03	3.70423946023913E-02	5.15778596352743E-02

99% Confidence Intervals

Variable	Value	99% (+/-)	Lower Limit	Upper Limit
k	4.43101271188328E-02	1.05750865939583E-02	3.37350405248745E-02	5.48852137127911E-02

Variance Analysis

Source	DF	Sum of Squares	Mean Square	F Ratio	Prob(F)
Regression	1	0.89718676982479	0.89718676982479	292.6609068	0
Error	8	2.45249501752101E-02	3.06561877190126E-03		
Total	9	0.92171172			

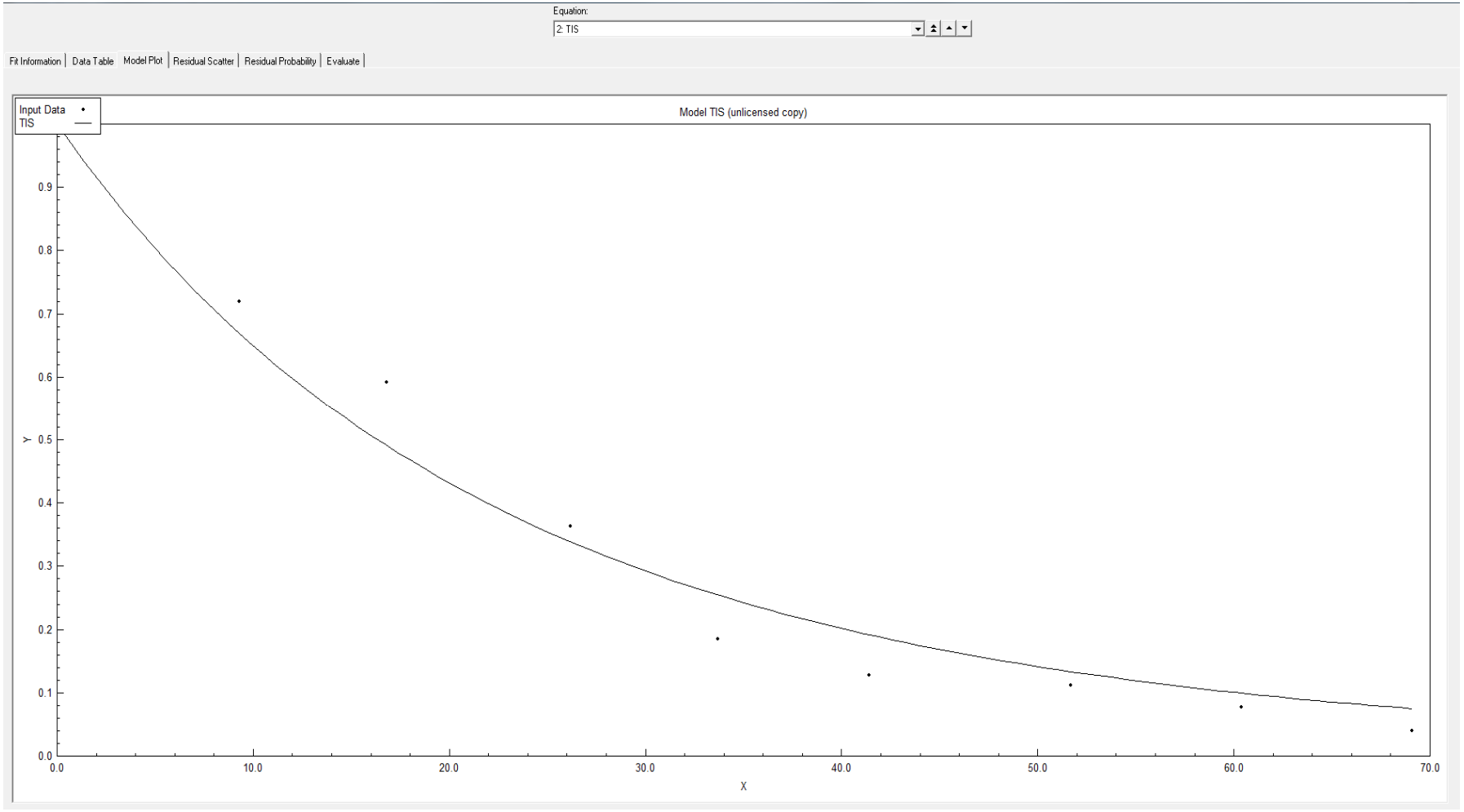

Figure 31. DataFit plot for the non-linear regression of the TIS model.

Vita

Guillermo José Rincón was born in Maracaibo, Venezuela in 1976. He graduated from La Universidad del Zulia with a bachelor's degree in Chemical Engineering in July of 2000. Worked as an infrastructure engineer for Petroleos de Venezuela, PDVSA, from October of 2000 until February of 2002 when was fired by the regime of President Dictator Hugo Chavez for joining a national strike seeking anticipated presidential elections. In the following years, Guillermo joined the team of Aeropostal Alas de Venezuela as an instructor in the area of hazardous materials.

Victim of political persecution, Guillermo left his country and relocated to the United States in 2007, and in 2009 was admitted to the doctoral program in engineering and applied sciences at the University of New Orleans.